The interaction between Sir3 and Sir4 is dispensable for silent chromatin spreading in budding yeast

Rosalind J. Gerson

Thesis Submitted to the
Faculty of Graduate and Postdoctoral Studies
In Partial Fulfillment of the Requirements
For the M.Sc. Degree in Biochemistry

Department of Biochemistry, Microbiology, and Immunology
Faculty of Medicine
University of Ottawa

Abstract

In *Saccharomyces cerevisiae*, telomeric and *HM* silencing requires the histone deacetylase Sir2 and the chromatin binding proteins Sir3 and Sir4, which interact to form the SIR complex. Silent chromatin formation begins with a nucleation step, followed by spreading of Sir proteins along chromatin. Overexpression of Sir3 extends silent chromatin domains, however the role of Sir protein interactions within silent chromatin extensions remains unknown. Here, we generated the Sir3 mutant, Sir3-4A, which cannot interact with Sir4 but is capable of forming silent chromatin extensions when overexpressed. Within extended silent domains, Sir2 and Sir4 enrichments are similar whether Sir3 or Sir3-4A is overexpressed, suggesting that silent chromatin extensions require Sir4 but not the interaction between Sir3 and Sir4. Tethering Sir3-4A at an *HMR* silencer cannot nucleate silencing in the absence of Sir3, suggesting that in addition to Sir3 recruitment, the Sir3-Sir4 interaction has at least one other function during silent chromatin nucleation.

Acknowledgements

I would like to thank my supervisor, Dr. Adam Rudner, for his exceptional mentoring and guidance. Adam's patience and understanding, knowledge and expertise, and enthusiasm for research have helped create a wonderful learning environment that I have been fortunate to be a part of.

I would also like to thank all of the members of my lab for their help and support: Carole Doré, Katherine Harding, Erin Kennedy, Noel Lianga, Elizabeth Williams, Michelle Parsons, Michael Dysart, Rea Konci, Sophie Pilon, Elise Ferguson, Alick Wang, Camille Fortinez, Jean-Sébastien Deneault, and Alexandra Weirich. Thanks especially to Carole Doré, who made contributions to this thesis, and to Katherine Harding for her collaborations as well as to Erin Kennedy, Elizabeth Williams and Noel Lianga for their advice and mentoring throughout my studies.

Thank you to the members of my Thesis Advisory Committee, Dr. Jean-François Couture and Dr. Alexandre Blais, for their advice and guidance, to the members of the Blais lab, especially Dr. Alexandre Blais, Imane Chakroun, Yubing Liu, and Ellias Horner, for their qPCR expertise, to Dr. David Bickel, Dr. Mayer Alvo, Marta Padilla, and Hilary Phenix for helpful discussions about statistical analysis, and to the Gottschling and Gartenberg labs, who provided strains and plasmids I used in my research.

Thanks also to the Canadian Institutes of Health Research, Natural Science and Engineering Research Council of Canada, Government of Ontario, and University of Ottawa for funding my research.

Finally, a big thank you to my family and friends for their support and encouragement throughout my studies.

Table of Contents

List of Abbreviations

2μ - 2 micron plasmid
AAA+ - ATPases Associated with various cellular Activities protein domain
Abf1 - ARS-Binding Factor (protein)
ac - acetyl
ACS - ARS-consensus sequence
ACT1 - actin (gene)
ADP - adenosine diphosphate
AMP - ampicillin
ANOVA - analysis of variance (statistical test)
Ard1 - arrest defective 1 (protein)
Asf2 - anti-silencing factor 2 (protein)
ATP - adenosine triphosphate
BAH - bromo adjacent homology domain
bp - base pairs
Bz - benzamidine
CC - coiled coil
Cdc13 - cell division cycle 13 (protein)
Cdc14 - cell division cycle 14 (protein)
Cdk1 - cyclin dependent kinase 1 (protein)
CEN - centromeric plasmid
ChIP - chromatin immunoprecipitation
DMSO - dimethyl sulfoxide
DNA - deoxyribonucleic acid
dNTP - deoxyribonucleotide
Dot1 - disruptor of telomeric silencing
Dot1L - Dot1-like H3K79 methyltransferase
DTT - dithiothreitol
ECL - enhanced chemiluminescence
EDTA - ethylene diamine tetraacetic acid
EGTA - ethylene glycol tetraacetic acid
Esa1 - essential *SAS* family acetyltransferase 1 (protein)
Esc1 - establishes silent chromatin 1 (protein)
FOA - 5-fluoroorotic acid
GFP - green fluorescent protein
GST - glutathione S-transferase
H2A - histone H2A
H2B - histone H2B
H3 - histone H3
H4 - histone H4
HAT - histone acetyltransferase
HCl - hydrochloric acid
HDAC - histone deacetylase
HDM - histone demethylase
HEPES - (4-(2-hydroxyethyl)-1-piperazineethanesulfonic acid
His - histidine
HM - hidden *MAT*
HML - hidden *MAT* left
HMR - hidden *MAT* right
HMT - histone methyltransferase
HO - homothallic switching endonuclease
Hos3 - Hda one similar 3 (protein)
HP1 - heterochromatin protein 1
HRP - horseradish peroxidase
Htz1 - yeast homologue of H2A.Z
HYG - hygromycin B
IP - immunoprecipitation
IPTG - isopropyl β-D-1-thiogalactopyranoside
KAN - kanamycin
Kbp - kilobasepairs
KlURA3 - *Kluveromyces lactis URA3*
KOH - potassium hydroxide
LB - luria bertani medium
LBPC - leupeptin bestatin pepstatin A-chymostatin cocktail
Leu - leucine
LiCl - lithium chloride
MAT - mating type locus
Me -methyl
$Mg(OAc)_2$ - magnesium acetate
Mps3 - MonoPolar Spindle Protein 3
NaCl - sodium chloride
NAD - nicotanmide adenine dinucleotide
NaOAc - sodium acetate
NAT - nourseothricin
NatA - N-terminal acetyltransferase protein complex
$NaVO_4$ - sodium vanadate
Net1 - nucleolar silencing establishing factor and telophase regulator 1 (protein)

NP-40 - nonyl phenoxypolyethoxyethanol
Nup170 - nuclear pore 170 (protein)
***O*-AAR** - 2'-*O*-acetyl-ADP-Ribose
Orc1 - origin recognition protein1
PAD - partitioning and anchoring domain
PAGE - polyacrylamide gel electrophoresis
PAU - seripauperin genes
PBS - phosphate buffered saline
PCR - polymerase chain reaction
PDB - protein data bank
PEV - position effect variegation
PIC - pre-initiation complex
PMSF - phenylmethylsulfonyl fluoride
Ppr1 - pyrimidine pathway regulation 1 (protein)
qPCR - quantitative PCR
Rap1 - repressor activator protein1
rDNA - ribosomal DNA
RENT - regulator of nucleolar silencing and telophase (protein complex)
Rif1,2 - Rap1-interacting factor 1, 2 (proteins)
RNA - ribonucleic acid
RNAi - RNA-interference
Sas2 - something about silencing 2 (protein)
SC - synthetic complete media
SDS - sodium dodecyl sulfate
SGD - Saccharomyces genome database
SID - Sir2 interacting domain
Sir1-4 - Silent Information Regulator 1-4 (proteins)
SIRT1-7 - sirtuin 1-7 (proteins)
Stn1 - suppressor of cdc thirteen 1 (protein)
STR - sub-telomeric repeat
Swi6 - Switching deficient protein 6 (an *S. pombe* homologue of HP1)
Tbf1 -TTAGGG repeat-binding factor 1 (protein)
TE - Tris-EDTA
TEL - telomere
Ten1 - telomeric pathways with Stn1 (protein)
Tip60 - HIV-1 Tat interactive protein 60
Tlc1 - Telomerase Component Protein 1
TPE - telomere position effect
Trp - tryptophan
TRP1 - tryptophan requiring 1 (gene)
Ura - Uracil
URA3 - uracil requiring 3 (gene)
wH - winged helix domain
YEp13 - yeast episomal vector with *LEU2* marker (plasmid)
yKu - yeast KU protein

List of Figures

List of Tables

Chapter 1 – Introduction

1.1 General Introduction to Heterochromatin

1.1.1 Historical overview of heterochromatin research

In eukaryotes, DNA is packaged along with nucleosomes and other structural and regulatory proteins into chromatin. Chromatin was first described in cytological observations by Walter Flemming in the 1880s (Olins et al., 2003), and was further classified as either diffuse euchromatin or dark-staining, condensed heterochromatin by Emil Heitz in 1928 (Yasuhara et al., 2006). Heitz proposed that heterochromatin consisted of genetic material that was not expressed, an idea which was confirmed in the following decades with the discovery of position effect variegation (PEV), the variegated silencing effect on euchromatic genes translocated to an area of the genome located close to a region of heterochromatin (Muller et al., 1930, Demerec et al., 1940, Cohen et al., 1962). In the 1970s through work by Roger Kornberg and others, chromatin was found to consist of repeating nucleosomes, each comprising eight histones and wrapped with approximately 146 DNA base pairs (Thomas et al., 1975). Around the same time, chemical modifications to histone tails were identified and their role in chromatin regulation became an area of investigation (Mersfelder et al., 2006). The past few decades of research have provided much insight into the mechanisms underlying the formation and regulation of heterochromatin, which will be discussed in more detail below.

1.1.2 Characteristics of Heterochromatin and Mechanisms of Silencing

Heterochromatin is generally found at repetitive DNA elements near centromeres and telomeres, but may also occur in other regions of the genome. Generally, heterochromatin that is maintained consistently throughout an organism's life cycle is termed constitutive heterochromatin, while heterochromatin that forms to silence genes for only a portion of a life cycle is termed facultative (Oberdoerffer et al., 2007). While facultative heterochromatin can be transcribed more readily than constitutive heterochromatin, transcription is possible and sometimes even necessary for silencing within regions of constitutive heterochromatin (Trojer et al., 2007). Mechanisms for heterochromatin formation often involve changes in histone post-translational modifications and binding of silencing proteins (Grewal et al., 2003), repositioning of nucleosomes (Jiang et al., 2009), the substitution of canonical histones with histone variants (Kamakaka et al., 2005), and, in some species, DNA methylation (Newell-Price et al., 2000), or the use of noncoding RNAs or RNA-interference (RNAi) (Verdel et al., 2005).

1.1.2.1 Histone Modifications

The basic unit of chromatin packaging is the nucleosome, a histone octamer, comprising an H3-H4 tetramer and two H2A-H2B dimers. All four types of histones share a similar core histone fold, but are highly different in the sequences of their N-terminal tails (Ramakrishnan et al., 1997). Heterochromatin is often characterized by altered post-translational histone modifications such as acetylation, methylation, phosphorylation, ubiquitylation, ADP-ribosylation, and sumoylation. Although these modifications primarily occur along histone tails, numerous modifications within histone cores have also been identified (Mersfelder et al., 2006). Tables 1 and 2 provide a summary of key histone lysine

residues that are acetylated or methylated in *Saccharomyces cerevisiae* (budding yeast) and vertebrates.

Table 1. Key acetylated residues within histone tails in vertebrates and yeast

	Vertebrates	***S. cerevisiae***
H2A	K5, 9	K4, 7
H2B	K5, 12, 15, 20	K6, 11, 16, 17, 21, 22
H3	K9, K14, K18, K23	K9, K14, K18, K23
H4	K5, K8, K12, K16	K5, K8, K12, K16

(Adapted from Roth et al 2001)

Table2. Key lysine residues that are methylated in vertebrates and yeast. Marks of active transcription are italicized, while silencing marks are highlighted in bold font.

	Vertebrates	***S. cerevisiae***
H3	*K4*, **K9, K27***, K36, K79*	*K4, K36, K79*
H4	**K20**	**K20**

(Adapted from: Bottomley et al., 2004; Kato et al., 2010; Edwards et al., 2011; Klose et al., 2007)

Some histone modifications are known to recruit or repel chromatin-binding proteins that play an important role in heterochromatin formation. In mammals, the repressive histone mark H3K9me3 recruits Heterochromatin Protein 1 (HP1), which plays an important role in silent chromatin formation (Bannister et al., 2011, Mersfelder et al., 2006). In budding yeast, methylation of H3K79 reduces the affinity of the silencing protein Sir3 (Silent Information Regulator 3) for the nucleosome (Armache et al., 2011). Histone modifications have also been proposed to alter chromatin condensation, leading to changes in transcriptional activity (Roth et al., 2001; Bannister et al., 2011).

Often, the presence of a particular histone modification recruits enzymes that make additional modifications – a phenomenon known as histone cross-talk (Bannister et al., 2011, Mersfelder et al., 2006). A well-known example is the ubiquitination of H2BK123, which promotes methylation of H3K4 and K79 (Nguyen et al., 2011; Sun et al., 2002).

1.1.2.2 Differences in the Heterochromatin of Yeast and Vertebrates

In most eukaryotes, the underlying principles of silent chromatin formation and regulation are the same: a complex of chromatin-binding proteins and histone modifying enzymes is recruited to a region of chromatin, and this complex makes modifications to adjacent nucleosomes, facilitating the recruitment of additional chromatin-binding and histone modifying enzymes. In this manner, silent chromatin is able to spread, sometimes many kilobases, from a site of nucleation. Spreading is limited by other chromatin-binding and histone-modifying proteins, which act within euchromatic regions to block the formation of heterochromatin, thus creating a boundary between heterochromatin and euchromatin (Grewal et al., 2003).

In both yeast and vertebrates, regions of euchromatin and heterochromatin are defined by many of the same histone posttranslational modifications; one notable exception is the repressive histone methylation of H3K9 and H3K27, which occurs in vertebrates but not in *Saccharomyces cerevisiae* (Klose, et al., 2007, Table 2). Many histone modifying enzymes are also conserved across evolution, these include the yeast histone acetyltransferase Esa1 (conserved as human Tip60), the NAD-dependent histone deacetylase Sir2 (SIRT 1-7), and the histone lysine methyltransferase Dot1 (Dot1L) (Blander et al., 2004; Torres-Machorro et at 2014; Mersfelder et al., 2006). Unlike vertebrates, budding yeast do not contain centromeric heterochromatin (Grunstein et al., 2013).

The greatest difference between budding yeast and vertebrate heterochromatin lies in the chromatin-binding proteins that mediate heterochromatin formation. In the fission yeast *Schizosaccharomyces pombe* and in vertebrates, heterochromatin formation requires deacetylation of H3K9 and H3K14, followed by methylation of H3K9. The H3K9me3 mark is recognized by HP1, which contains both an H3K9me3-binding chromodomain as well as a

chromoshadow domain capable of homodimerization (Grewal et al., 2002). Recent work demonstrates that, upon interaction of HP1 with the nucleosome, the chromodomain forms a second dimerization domain, allowing HP1 to multimerize and spread along the chromatin (Canzio et al., 2011; Canzio et al., 2013). In budding yeast, telomeric and *HM* loci silencing depends on the Silent Information Regulator (SIR) protein complex composed of Sir2, Sir3, and Sir4 dimers, which are recruited to the chromatin through interactions with proteins bound to specific DNA sequences termed silencer elements. Sir2, an NAD-dependent histone deacetylase, removes the acetyl group from H4K16 and several other residues. Interactions of Sir3 and Sir4 with each other and with histones allow propagation of SIR complexes along the chromatin (Rusche et al., 2003). The mechanism for Sir-mediated silencing will be discussed in more detail in section 1.2.

Unlike Sir3 and Sir4, Sir2 is conserved in the fission yeast *Schizosaccharomyces pombe* and in higher eukaryotes. In fission yeast, Sir2 deacetylates a number of histone residues including H4K16 and H3K9, and is required for silent chromatin formation in a number of genomic regions (Shankaranarayana et al., 2003; Alper et al., 2013; Buscaino et al., 2013). The human sirtuins, SIRT1-7, are homologues of Sir2 and play a role in heterochromatin formation as well as in a number of other biological processes (Vassilopulos et al., 2013).

1.1.3 Biological Significance of Heterochromatin

The biological roles of heterochromatin can be grouped into three major categories: (1) maintenance of chromosome stability, (2) regulation of cell identity and development, and (3) regulation of phenotypic diversity.

In fission yeast and higher eukaryotes, centromeric heterochromatin plays an important structural role during mitosis. Heterochromatin protein HP1 (or the HP1 homologue Swi6 in fission yeast) interacts directly with a component of the Cohesin complex, targeting Cohesin to centromeres. This recruitment is essential for the maintenance of chromosome cohesion during mitosis, and defects in centromeric heterochromatin often result in lagging chromosomes and aneuploidy (Bernard et al., 2001; Nonaka et al., 2002; Gartenberg et al., 2009). The heterochromatin structure also maintains the stability of rDNA repeats, a function that is conserved from budding yeast to higher eukaryotes and has important implications in replicative life span and ageing (Salvi et al., 2013; Oberdoerffer et al., 2007a).

By regulating gene expression, heterochromatin plays an important role in determining cell identity. In budding yeast and other single celled organisms, silent chromatin forms at specific loci in order to regulate a cell's mating type (Rusche et al., 2003). In multicellular organisms, heterochromatin plays an essential role in embryonic development and stem-cell differentiation (Li et al., 2002; Stancheva et al., 2011; Fadloun et al., 2013; Meshorer et al., 2006). Heterochromatin misregulation is implicated in several genetic disorders and multiple types of cancers (Wutz et al., 2011; Marks et al., 2001; Ropero et al., 2007, Zhu et al., 2011).

Telomeric silent chromatin is also important for maintaining phenotypic diversity within a population of single-celled organisms. In budding yeast, a number of genes involved in cell-wall integrity are located near telomeres. Expression of these genes is regulated by telomeric silent chromatin in response to changing environmental stimuli (Stone et al., 1996; Ai et al., 2002, Ray et al., 2003; Halme et al., 2004), which may improve survival under different environmental conditions. The malaria parasite, *Plasmodium falciparum*, uses

similar silent chromatin structures to vary the expression of telomeric antigen genes in order to evade host immune systems (Varunan et al., 2013, Freitas-Junior et al., 2005, Mancio-Silva et al., 2008), and in the pathogenic yeast species *Candida glabrata*, telomeric heterochromatin regulates the expression of cell adhesion genes that influence pathogenicity (Martinez-Jimenez et al., 2013).

1.2 Silent Chromatin in Saccharomyces cerevisiae

1.2.1 Saccharomyces cerevisiae as a model organism

The budding yeast, *Saccharomyces cerevisiae*, serves as an excellent model organism for the study of silent chromatin regulation. Budding yeast is easy and inexpensive to work with, and its short doubling time of approximately 90 minutes allows cultures to be grown rapidly. Budding yeast cells spend part of their life cycle in a haploid state; most laboratory yeast strains are therefore maintained as haploids in order to simplify genetic manipulation (Herskowitz et al., 1988). The relatively small *S. cerevisiae* genome contains about 6000 genes and has been studied extensively, with genome sequence, gene information, and curated databases of high throughput genomic and proteomic data easily accessible through an online database (Saccharomyces Genome Database). Yeast can readily be made competent for DNA transformation, and genes can be efficiently deleted or mutated through homologous recombination of transformed PCR products (Amberg et al., 2006; Gietz et al., 2007; Longtine et al., 1998; Lundblad et al., 2001). Decades of previous research have fine-tuned a wide range of biochemical and genetic techniques for the study of chromatin biology in *S. cerevisiae* (Amberg et al., 2005). Past research with *S. cerevisiae* also provides a

substantial body of knowledge of budding yeast chromatin biology, which supports deeper and more complex investigations into the current questions of this field.

1.2.2 Structure and Function of the HM loci, Telomeres, and rDNA repeats

Silent chromatin forms at three locations within the *S. cerevisiae* genome: at telomeres, *HM* loci, and rDNA repeats. Telomeric and *HM* silencing requires the SIR complex, formed from the Silent Information Regulator proteins Sir2, Sir3, and Sir4 (Figure 1A) (Rusche et al., 2003). At rDNA repeats, silencing is mediated by the RENT complex, which contains Sir2, as well as the mitotic exit protein phosphatase Cdc14, and the nucleolar protein Net1 which interacts with Sir2 and Cdc14 and recruits Sir2 to the rDNA (Figure 1B) (Shou et al., 1999; Straight et al., 1999; Tanny et al., 2004; Cubizolles et al 2006).

1.2.2.1 The HM loci

Budding yeast, like vertebrates, have a sexual cycle and as haploids exist as one of two possible mating types: a, or alpha. All mating type information is contained in a set of two genes (either *a1* and *a2*, or *α1* and *α2*) found in the *MAT* locus on chromosome III. This locus is flanked on either side by the silent *HM* loci, each of which is separated from the *MAT* locus by approximately 100 kilobases. To the right of the *MAT* locus is *HMR*, which typically contains a-cell mating type genes; *HML*, found to the left of the *MAT* locus, contains alpha-cell mating type genes (Figure 2A) (Coic et al., 2006). The *HMRa* and *HMLα* loci are normally kept silent by the Sir proteins, allowing a cell's mating type to be determined only by the genes present at the *MAT* locus. In the wild, genetic recombination mediated by the *HO* endonuclease allows mating-type switching, which likely increases the chance of successful mating and may confer an evolutionary advantage (Kostriken et al.,

A

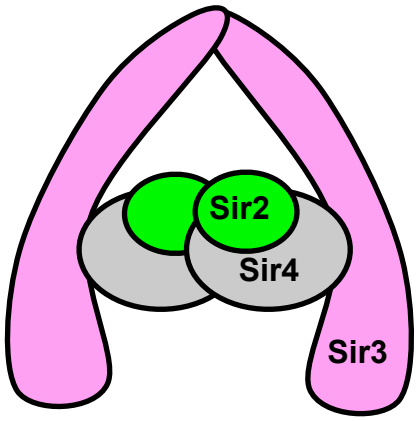

B

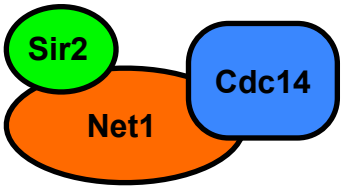

Figure 1. Silencing Protein Complexes in *Saccharomyces cerevisiae*. (A) The SIR complex is thought to be composed of two dimers of Sir2, Sir3, and Sir4. Sir4 interacts directly with Sir2 and Sir3, and both Sir3 and Sir4 bind chromatin. Sir2 is an NAD-dependent histone deacetylase. All three Sir proteins are required for telomeric and *HM* silencing. **(B)** The RENT complex is composed of Cdc14, Sir2, and Net1. Figures adapted from Moazed et al., 2001 and Liou et al., 2005.

A

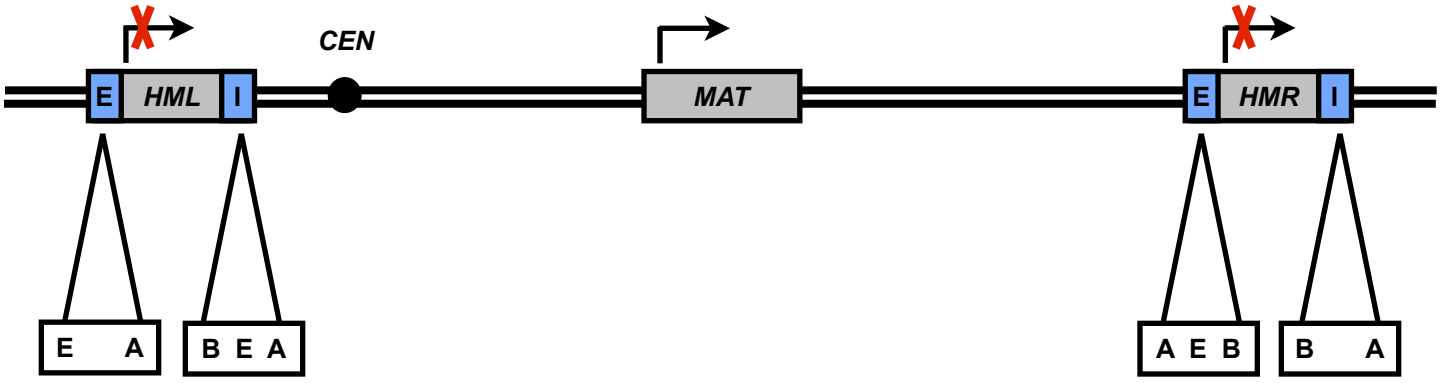
CEN
E
HML
I
MAT
E
HMR
I
E A
B E A
A E B
B A

B

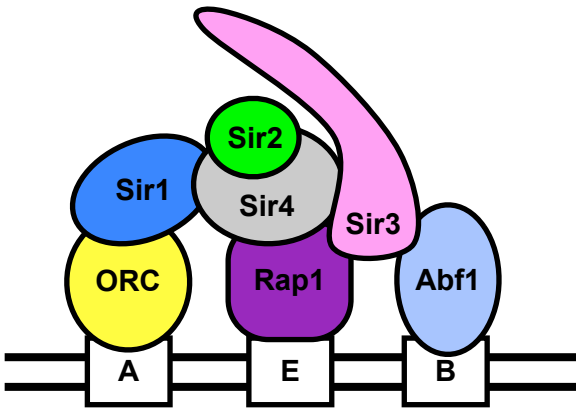
Sir2
Sir1
Sir4
Sir3
ORC
Rap1
Abf1
A
E
B

C

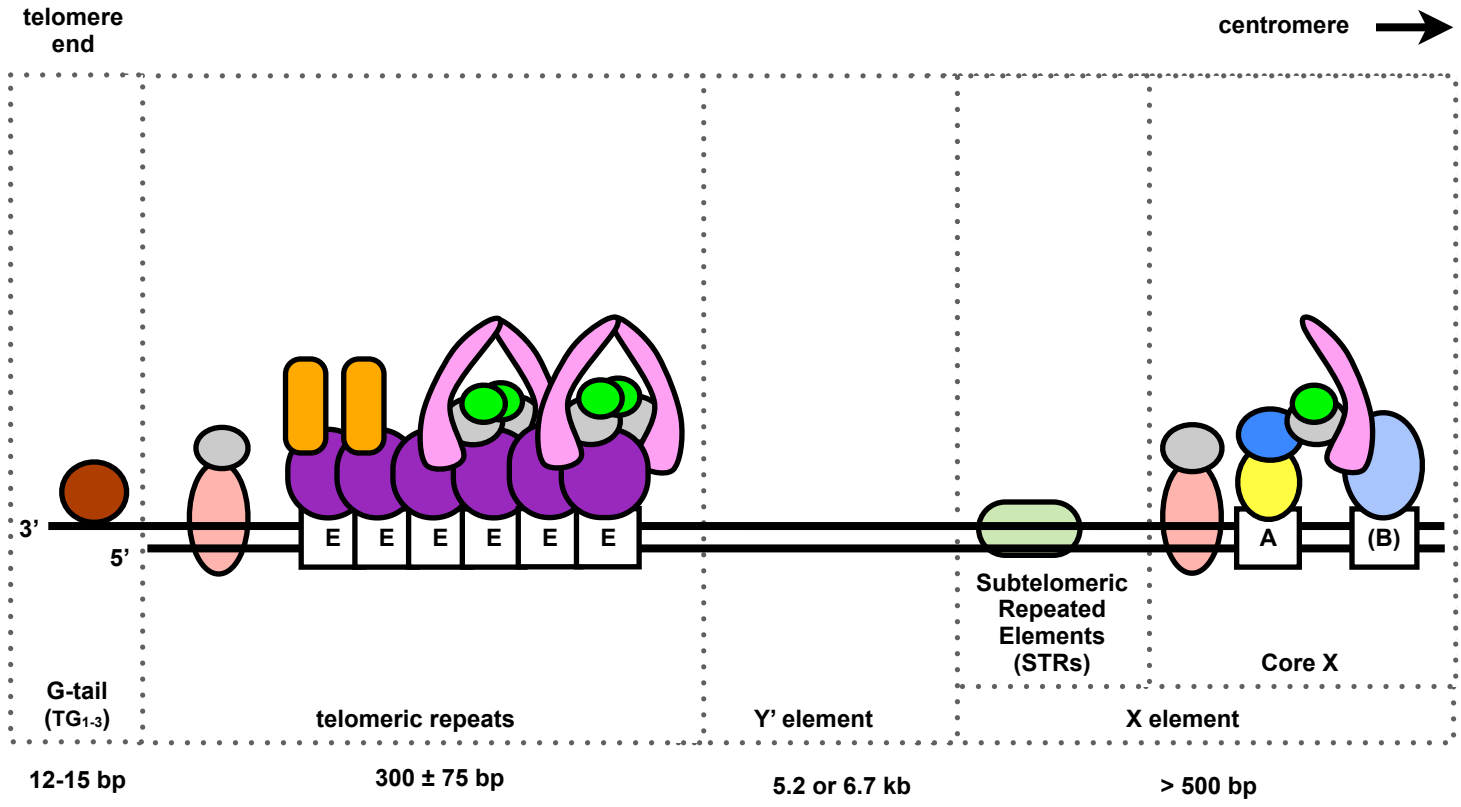
telomere end
centromere
3'
5'
E
E
E
E
E
E
A
(B)
Subtelomeric Repeated Elements (STRs)
Core X
G-tail (TG1-3)
telomeric repeats
Y' element
X element
12-15 bp
300 ± 75 bp
5.2 or 6.7 kb
> 500 bp

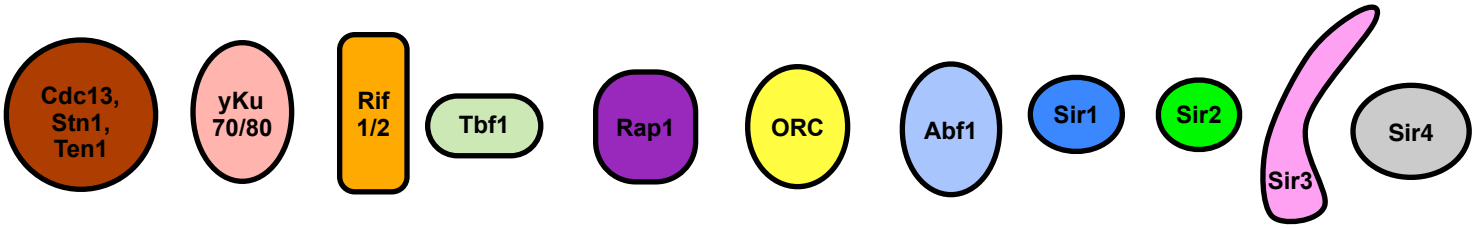
Cdc13, Stn1, Ten1
yKu 70/80
Rif 1/2
Tbf1
Rap1
ORC
Abf1
Sir1
Sir2
Sir3
Sir4

D

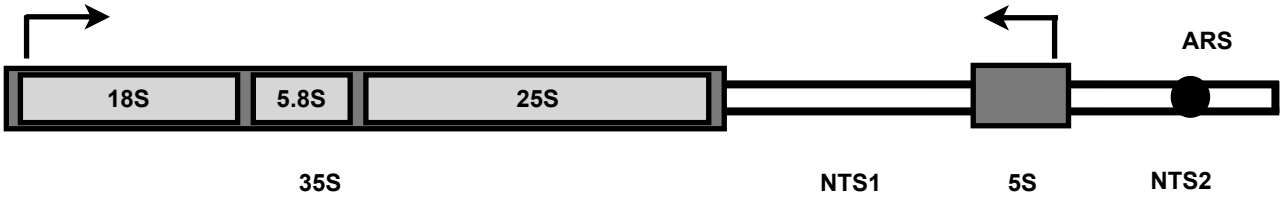
ARS
18S
5.8S
25S
35S
NTS1
5S
NTS2

Figure 2. Structure of silent chromatin domains in *Saccharomyces cerevisiae*. (A) Structure of the *HM* loci. The transcriptionally active *MAT* locus found on chromosome III contains the either the *a1/a2* or *α1/α2* genes, which control mating-type information. The silenced *HML* locus contains the *α1/α2* genes and is located approximately 100 kb upstream of the *MAT* locus, while the silenced *HMR* locus, which contains the *a1/a2* genes is about 100 kb downstream of *MAT*. Both *HML* and *HMR* are flanked by the E (essential) and I (important) silencers, which contain two or three of the following DNA consensus sequences or protosilencers: A (ORC complex binding sequence), E (Rap1 binding sequence), B (Abf1 binding sequence). Figure adapted from Rusche et al., 2003, not to scale. **(B)** Recruitment of the Sir proteins to the *HMR-E* silencer. Chromatin binding proteins ORC (protein complex), Rap1, and Abf1 respectively bind the A, E, and B DNA consensus sequences. These proteins then recruit the Sir proteins to initiate silencing. Figure adapted from: Rusche et al., 2003; Bose et al., 2004; Sampath et al., 2009. **(C)** Structure of the *S. cerevisiae* telomere. All *S. cerevisiae* telomeres contain a G-tail, telomeric repeats, and a Core X element. Some telomeres also contain a Y' element, and/or sub-telomeric repeated X elements. Numerous Rap1 binding sites (E) are located within the telomeric repeats. The Core X element contains an ORC binding sequence and sometimes also an Abf1 binding sequence. Looping of the telomere end may allow interaction of the Sir proteins recruited to the telomeric repeats with those at the Core X element. Figure adapted from Wellinger et al., 2012, not to scale. **(D)** Structure of an rDNA repeat. Figure adapted from Rusche et al., 2003, not to scale. 35S, 18S, 5.8S, 25S, 5S – sequences for ribosomal subunits. NTS – non transcribed spacer. ARS – autonomously replicating sequence.

1983). Similar heterothallism is found in most fungal species (Lee et al., 2003). In most laboratory strains, the *HO* endonuclease gene is deleted in order to prevent unwanted mating-type switching (Grunstein et al., 2013).

Flanking both *HMR* and *HML* are the E and I silencer elements, DNA regions that contain two or three proto-silencer sequences capable of recruiting proteins required for the nucleation of silent chromatin (Bi et al., 1999; Rusche et al., 2003) (Figure 2A). At *HMR*, the E (essential) silencer element is required for silencing, while the I (important) element is not; at *HML* silencing can be mediated by either the E or I element alone (Rivier et al., 1999; Mahoney et al., 1989). Three protosilencers form the silencer elements: the ACS (A) sequence, which recruits the Origin Recognition Protein Complex (ORC), the RAP1 (E) sequence, which recruits the Repressor Activator protein Rap1, and the ABF1 (B) sequence, which recruits ARS-Binding Factor protein Abf1 (Bi et al., 1999; Rusche et al., 2003). These chromatin-binding proteins then recruit the Sir proteins as follows: Orc1 interacts with Sir1 (which in turn recruits Sir4), Rap1 binds Sir3 and Sir4, and Abf1 interacts with Sir3 (Figures 2A,B) (Bose et al., 2004; Luo et al., 2002; Sampath et al., 2009). Multiple protosilencers work redundantly to recruit silencing nucleation proteins; mutation of one protosilencer within a silencer element weakens but does not necessarily abolish *HM* silencing (Sussell et al., 1991). However, no single protosilencer is capable of initiating silencing on its own (Zhang et al., 2012). Strains with a weakened *HMR-E* silencer are commonly used to assess *HM* silencing defects as they are more sensitive to perturbations of silent chromatin structure (Sussell et al., 1991; Zhang et al., 2012).

1.2.2.2 The Telomeres

Budding yeast telomeres are usually found around the nuclear periphery, tethered to the nuclear membrane (Taddei et al., 2004). Telomeres contain several types of repetitive DNA sequences and a number of chromatin binding proteins. The telomere structure can be divided into several regions (Figure 2C). At the end of the telomere is the G-tail, a short 3' overhang consisting of TG_{1-3} repeats that is important for telomere stability and is recognized by telomerase for telomere elongation (Greider et al., 1989). The telomere-capping proteins Cdc13, Stn1, and Ten1 form a complex and bind in this region, helping to protect the telomere ends (Grandin et al., 1997; Hughes et al., 2000; Wellinger et al., 2012).

Adjacent to the G-tail are telomeric repeats, which are usually around 300 base pairs in length and contain repetitive tracts of $TG_{2-3}(TG)_{1-6}$ (Forstermann et al., 2000). These repeats form the consensus sites for the binding of Rap1 and therefore serves as a site for silent chromatin nucleation (Wahlin et al., 2000; Luo et al., 2002; Sampath et al., 2009). The interaction between Sir4 and Rap1 is facilitated by Nup170, a nuclear pore complex protein that interacts with Sir4 and is required for silencing (Van de Vosse et al., 2013). Rap1 also interacts with Rif1 and Rif2, proteins that play a role in telomere protection and capping, and, through their competition with Sir3 and Sir4 for Rap1, have a negative impact on silencing (Moretti et al., 1994; Buck et al., 1995; Shi et al., 2013). The Ku complex, composed of proteins yKu70 and yKu80 binds both at telomeric repeats as well as within the Core X element. This protein is required for telomeric silencing (Boulton et al., 1998; Laroche et al., 1998; Mishra et al., 1999) and is involved in recruitment of Sir4, the anchoring of telomeres to the nuclear membrane, and prevention of unwanted recombination of telomere ends (Taddei et al., 2004; Marvin et al., 2009).

On the centromere-proximal side of the telomeric repeats are the sub-telomeric elements. All budding yeast telomeres include a Core X element, which is approximately 500 bp in length and contains consensus binding sequences for the ORC complex and sometimes Abf1, allowing recruitment of Sir proteins, loss of H4K16ac and H3K79me, and silencing of this region (Pryde et al., 1999; Zhu et al., 2009; Takahashi et al., 2011). Some telomeres also contain sub-telomeric repetitive elements (STRs) as part of the X element; these are situated between the telomeric repeats and the Core X region and contain the bound transcription factor Tbf1, which plays a role in telomerase recruitment (Pryde et al., 1999; Arneric et al., 2007). Translocation of an X element to a euchromatic region is not sufficient to initiate silencing of this region (Pryde et al., 1999), suggesting that X elements work in conjunction with telomeric repeats to nucleate silencing. Telomere ends may form loops, allowing Sir proteins recruited at the Core X to interact with those bound at the sub-telomeric repeats (Zhu et al., 2009).

Unlike X elements, Y' elements are found only in a subset of budding yeast telomeres. These sequences are located between the telomeric repeats and the X elements, and do not contain sequences responsible for nucleating silent chromatin. Y' elements are transcriptionally active, and have high levels of H3K79 methylation and H4K16 acetylation (Pryde et al., 1999; Zhu et al., 2009; Takahashi et al., 2011).

Since yeast telomeres may or may not contain Y' and STR elements, four types of yeast telomeres exist (summarized in Table 3); telomere structure has been shown to influence the patterns of Sir3 binding and spreading (Radman-Livaja et al., 2011). The overexpression of Sir3, which has been shown to extend silent chromatin regions (Renauld et al., 1993) has a much more pronounced effect at some telomeres than at others (Pryde et al., 1999). Some studies of telomeric silencing employ synthetic telomeres, in which a native Y'

element is deleted (Renauld et al., 1993). Along at least one telomere, *TELV-R*, silent chromatin spreading induced by Sir3 overexpression is similar whether the Y' element is present or absent (Renauld et al., 1993).

Table 3. Four different combinations of sub-telomeric elements in *S. cerevisiae*

Sub-telomeric Elements	***S. cerevisiae* telomere**
Core X only	1R, 6R
Core X + STR	1L, 2R, 3L, 3R, 4L, 7L, 9R, 10R, 11L, 11R, 13R, 14R, 15L
Core X + Y'	5L, 16R
Core X + STR + Y'	2L, 4R, 5R, 6L, 7R, 8L, 8R, 9L, 10L, 12L, 12R, 13L, 14L, 15R,16L

Adapted from Radman-Livaja et al., 2011

Telomeres and *HM* loci form clusters at the nuclear envelope, producing distinct foci observable by fluorescence microscopy (Gotta et al., 1996). Tethering of telomeres to the nuclear envelope is mediated by at least two distinct mechanisms. The first involves the interaction of the Ku protein complex with Sir4 and telomerase subunits such as Tlc1 (Taddei et al., 2004; Schober et al., 2009), and also requires the integral nuclear membrane protein Mps3 (Schober et al., 2009; Bupp et al., 2007). In a separate pathway, telomeres are anchored through interactions of Sir4 with the inner nuclear membrane protein Esc1 (Taddei et al., 2004). Nuclear pore complex proteins, such as Nup170p, also play a role in telomere anchoring (Van de Vosse et al., 2013). Telomere clustering and localization to the nuclear periphery thought to help sequester and concentrate Sir proteins at the telomeres, enhancing telomeric silencing while preventing ectopic localization of the Sir proteins to other genomic loci (Taddei et al., 2009). However, peripheral localization to the nuclear envelope is not required for the silencing of *HMR* (Gartenberg et al., 2004) or for silencing of specific telomeres (Mondoux et al., 2007). Interestingly, Sir3 overexpression induces telomere

hyperclustering away from the nuclear envelope (Ruault et al., 2011), suggesting that telomere clustering occurs independently of peripheral anchoring. Both telomere clustering and localization to the nuclear envelope can occur independently of silencing (Taddei et al., 2004; Ruault et al., 2011).

In single-celled organisms, telomeric heterochromatin may function to generate phenotypic diversity. A number of *S. cerevisiae* genes are located near sub-telomeric regions and may be regulated by telomeric heterochromatin. The Seripauperins (*PAU*) are a family of 24 genes that encode serine-poor cell-wall mannoproteins that play a role in modifying cell-wall properties in response to stress (Luo et al., 2008). Many *PAU* genes are located near telomeres and serve as sites of Sir3 recruitment (Radman-Livaja et al., 2011). Under normal conditions, *PAU* genes are maintained in a silenced state. However, expression of *PAU5* can be induced by low-temperature or low-oxygen stress (Luo et al., 2008), and rapamycin stress promotes Sir3 phosphorylation and dissociation of Sir3 from the telomeric *PAU3* gene, resulting in increased expression of *PAU3* (Ai et al., 2002). It has been proposed that stress-induced changes in the affinity of Sir proteins for telomeres regulates expression of the *PAU* genes, allowing budding yeast to adapt their cell-wall properties in order to survive changing environmental conditions (Ai et al., 2002). Another set of telomeric budding yeast genes, the *FLO* genes, play a role in cell adhesion and are silenced by histone deacetylases (Halme et al., 2004). In the pathogenic yeast species *Candida glabrata,* these genes are conserved as the *EPA* genes, most of which are also located near telomeres. Regulation of the many *EPA* genes by homologues of the Sir proteins produces a variegated population, which is thought to improve pathogenicity of the species (Martinez-Jiminez et al., 2012; Gallegos-Garcia et al., 2012). The genome of the malaria parasite, *Plasmodium falciparum,* contains approximately sixty different *var* genes, which encode different variants of a cell membrane

protein. The *var* genes are located near telomeres and are regulated by *P. falciparum* homologues of Sir2 and Orc1/Sir3. Expression of *var* genes is mutually exclusive such that only one *var* gene is expressed at any time, and a single *P. falciparum* cell can switch its expression from one *var* gene to another, a property that may to help this organism evade recognition by the host immune system (Varunan et al., 2013; Freitas-Junior et al., 2005; Mancio-Silva et al., 2008).

1.2.2.3 The rDNA repeats

The rDNA repeats, located within the nucleolus, contain highly repetitive sequences encoding the ribosomal RNA that makes up 18S, 5.8S, 25S, and 5S ribosomal subunits. Each rDNA segment spans 9.1 kb and is repeated 100 to 200 times (Figure 2D). Silencing of rDNA depends on Cdc14, Net1, Sir2, and the N-terminal tails of histones H3 and H4 (Rusche et al., 2003; Goetze et al., 2010). Although rDNA silencing does not require Sir3 and Sir4, both of these proteins are recruited to rDNA repeats at low levels (Rusche et al., 2003; Goetze et al., 2010; Hoppe et al., 2002). The binding of Sir3 to the rDNA repeats depends on the catalytic activity of Sir2, and localization of Sir3 to the nucleolus and rDNA repeats appears to increase in cells lacking Sir4 (Gotta et al., 1997; Hoppe et al., 2002).

1.2.3 Structure and Function of the Sir Proteins

1.2.3.1 Sir3

Sir3 contains an N-terminal bromo-adjacent homology (BAH) domain, an ATPases Associated with various cellular Activities (AAA+) domain, and a C-terminal winged-helix (wh) domain (Figure 3A) (Oppikofer et al., 2013b). Sir3 is a paralogue of the chromatin-binding origin recognition complex protein Orc1; Sir3 arose from Orc1 through a whole-genome duplication event during the evolution of *S. cerevisiae*, and the two proteins share highly similar N-terminal regions (Bell et al., 1995; Hickman et al., 2011). Although a member of the AAA+ ATPase protein family, Sir3 lacks ATPase activity (Ehrentraut et al., 2011).

The first 214 amino acids of Sir3 constitute the BAH domain, which is essential for silencing (Gotta et al., 1998). This region plays an important role in nucleosome binding (Armache et al., 2011) and is the region of Sir3 that bears closest homology to Orc1 (Oppikofer et al., 2013a). Indeed, replacement of the Sir3 BAH domain with that of Orc1 produces a protein chimera capable of mediating silencing (Bell et al., 1995). Upon translation of the Sir3 protein, the N-terminal methionine is cleaved, and the subsequent alanine residue is acetylated by the NatA acetyltransferase complex (Wang et al., 2004). This acetylation is essential for silencing and acts by stabilizing the interaction of a surface loop on Sir3 BAH with histones H2B and H4 (Arnaudo et al., 2013; Yang et al., 2013). Interaction of the Sir3 BAH domain with the nucleosome is sensitive to H3K79 methylation and H4K16 acetylation; both histone marks reduce the affinity of Sir3 BAH for the nucleosome (Onishi et al., 2007).

A

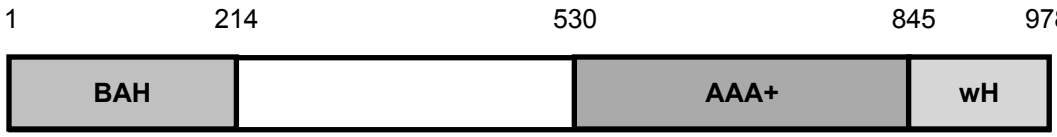

B

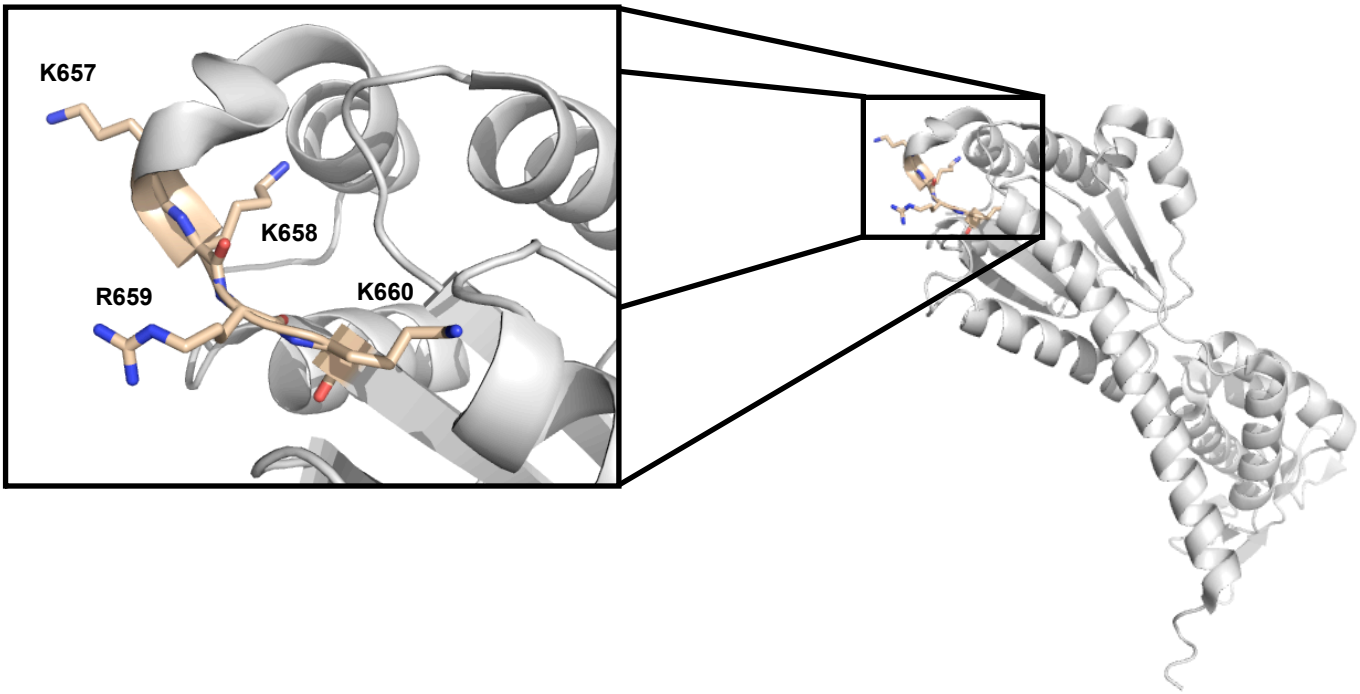

Figure 3. Domains and Structural Elements of the Silencing Protein Sir3. (A) Structural domains of the Sir3 protein. Sir3 contains an N-terminal BAH (Bromo Adjacent Homology) domain, a catalytically inactive AAA+ (ATPases Associated with various cellular Activities) domain, and a C-terminal wH (Winged Helix) domain. Figure adapted from Oppikofer et al., 2013a. **(B)** Crystal structure of the Sir3 AAA+ domain and Sir4 binding site (PDB ID 3TE6, Ehrentraut et al., 2011). Inset, the Sir4 binding site of Sir3. Residues involved in Sir4 binding are coloured beige. Figure was generated using Pymol Molecular Graphics Software Version 1.3 (Shrödinger, LLC, http://www.pymol.org/).

A recent study found that binding of the Sir3 BAH domain to the nucleosome induces a conformational change in the H4 tail, causing it to associate closely with nucleosomal DNA; this may play an important role in chromatin condensation and silencing (Wang et al., 2013). The stability of silent chromatin may be regulated by Sir3 phosphorylation, and several Sir3 phosphorylation sites are located in a region between the BAH domain and the AAA+ domain (Stone et al., 1996; Ai et al., 2002; Ray et al., 2003).

At the C-terminus of Sir3 is a 138-amino acid winged helix (wH) domain, which is required for silencing and has been shown to mediate Sir3 homodimerization (Oppikofer et al., 2013b). The wH domain cannot interact with DNA, chromatin, or other silencing proteins such as Sir4 (Oppikofer et al., 2013b); thus, a Sir3 truncation containing only the wH domain is not able to rescue the silencing defect of strains lacking full-length Sir3 (Park et al., 1999). However, when tethered to a silencer, Sir3-wH domain can nucleate silent chromatin spreading in the presence of wild type Sir3 (Park et al., 1998; Liaw et al., 2006). Thus, Sir3 homodimerization likely plays an important role in silent chromatin nucleation. Although no interaction between the Sir3 wH domain and chromatin has been identified, the presence of this domain improves both the affinity of the Sir3 AAA+ domain and that of the entire SIR complex for chromatin, suggesting that Sir3 homodimerization also plays an important role in stabilizing interactions between chromatin and the SIR complex (Oppikofer et al., 2013b). Abrogation of Sir3 dimerization does not completely block recruitment of Sir4 to the *HML-E* silencer, but prevents Sir4 spreading along *TELVI-R* (Oppikofer et al., 2013b). Although an early study identified a putative second dimerization interface between the Sir3 C-terminus and the internal AAA+ domain (King et al., 2006), no interaction of these two regions could be identified by the more recent work of Oppikofer et al. (2013b). Indeed, replacement of the C-terminal winged helix domain with a similar-sized bacterial protein

capable of dimerization produced a Sir3 fusion protein with the ability to silence, suggesting that the essential role of the Sir3 wH domain in silencing results exclusively from its ability to homodimerize (Oppikofer et al., 2013b).

Proteins containing an AAA+ domain are normally capable of hydrolysing ATP and undergoing conformational changes (Hanson et al., 2005). Although the Sir3 contains a region bearing sequence similarity to functional AAA+ domains, several structural features of the Sir3 AAA+ domain prevent the binding of ATP, rendering Sir3 AAA+ catalytically inactive (Bell et al., 1995; Ehrentraut et al., 2011). The Sir3 AAA+ domain also appears unable to bind 2'-*O*-acetyl-ADP-Ribose (*O*-AAR), a metabolic byproduct of the Sir2 deacetylation reaction (Ehrentraut et al., 2011). Like the BAH domain, the Sir3 AAA+ domain interacts with the nucleosomes. The ability of the AAA+ domain to bind nucleosomes is substantially reduced in the presence of H3K79 methylation (Hecht et al., 1995; Altaf et al., 2007; Ehrentraut et al., 2011). The Sir3 AAA+ domain may also interact with the N-terminal tails of H3 and H4 (Hecht et al., 1995), however the nature of this interaction is not well understood. The AAA+ domain of Sir3 contains a surface loop comprising lysine and arginine residues K657, K658 R659 and K660 (Figure 3B), which are implicated in the Sir3-Sir4 interaction. Mutation of at least two of these residues to alanine prevents recruitment of Sir3 to the chromatin, and disrupts the Sir3-Sir4 interaction in yeast-two-hybrid and *in vitro* assays (Ehrentraut et al., 2011). However, this study did not directly test whether mutation of these residues prevented the Sir3-Sir4 interaction *in vivo*, nor did the study demonstrate whether this exposed loop of Sir3 interacted directly with the known binding site for Sir3 on Sir4. The residues K657 and R659 are predicted to project outward from the loop while K658 and K660 project inward (Figure 3B), suggesting that disruption of the surface loop structure may block the interaction of Sir3 and Sir4. Sir3 also interacts

with Rap1; this interaction is mediated by a region of Sir3 on the N-terminal side of the AAA+ domain (Chen et al., 2011).

1.2.3.2 Sir4

Sir4, the largest of the Sir proteins, interacts with both Sir2 and Sir3 and therefore acts as the scaffolding subunit of the SIR complex (Figure 1A). Sir4 contains several important protein interaction domains (Figure 4A), especially within the C-terminal portion of the protein, which is essential for silencing (Murphy et al., 2003). The C-terminal 76 amino acids of Sir4 (1282-1358) form an alpha helix that homodimerizes to generate a C-terminal coiled-coil (Chang et al., 2003) (Figure 4B). The residues M1307, E1310, and I1311 project from the Sir4 coiled-coil dimer (Figure 4B), forming the only known binding site on Sir4 for Sir3; mutation of these residues abolishes or greatly reduces *HM* and telomeric silencing (Chang et al., 2003; Rudner et al., 2005). Overexpression of either full-length Sir4 or a Sir4 C-terminal fragment exerts a dominant negative effect on silencing by preventing interaction of Sir3 with a functional SIR complex (Gotta et al., 1998). The C-terminal half of Sir4 also plays an important role in interactions with other silencing proteins including Rap1 (Moretti et al., 2001), Ku70, and Ku80 (Taddei et al., 2004; Roy et al., 2004). The interaction between Sir4 and Sir2 is required for silencing and is mediated by Sir4 residues 737-893, which form the Sir2 Interaction Domain (SID) (Hsu et al., 2013). As well as serving to recruit Sir2 to the nucleosome, the interaction of Sir4 with Sir2 stabilizes Sir2 tertiary structure and enhances Sir2 catalytic activity toward H4K16ac (Hsu et al., 2013). Between the SID domain and the C-terminal coiled coil of Sir4 lies the PAD (Partitioning and Anchoring) domain, which plays an important role in the anchoring of silent chromatin to the

A

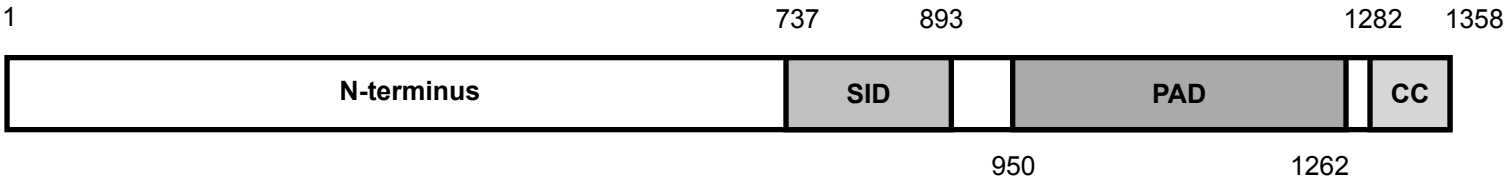
1
737
893
1282
1358
N-terminus
SID
PAD
CC
950
1262

B

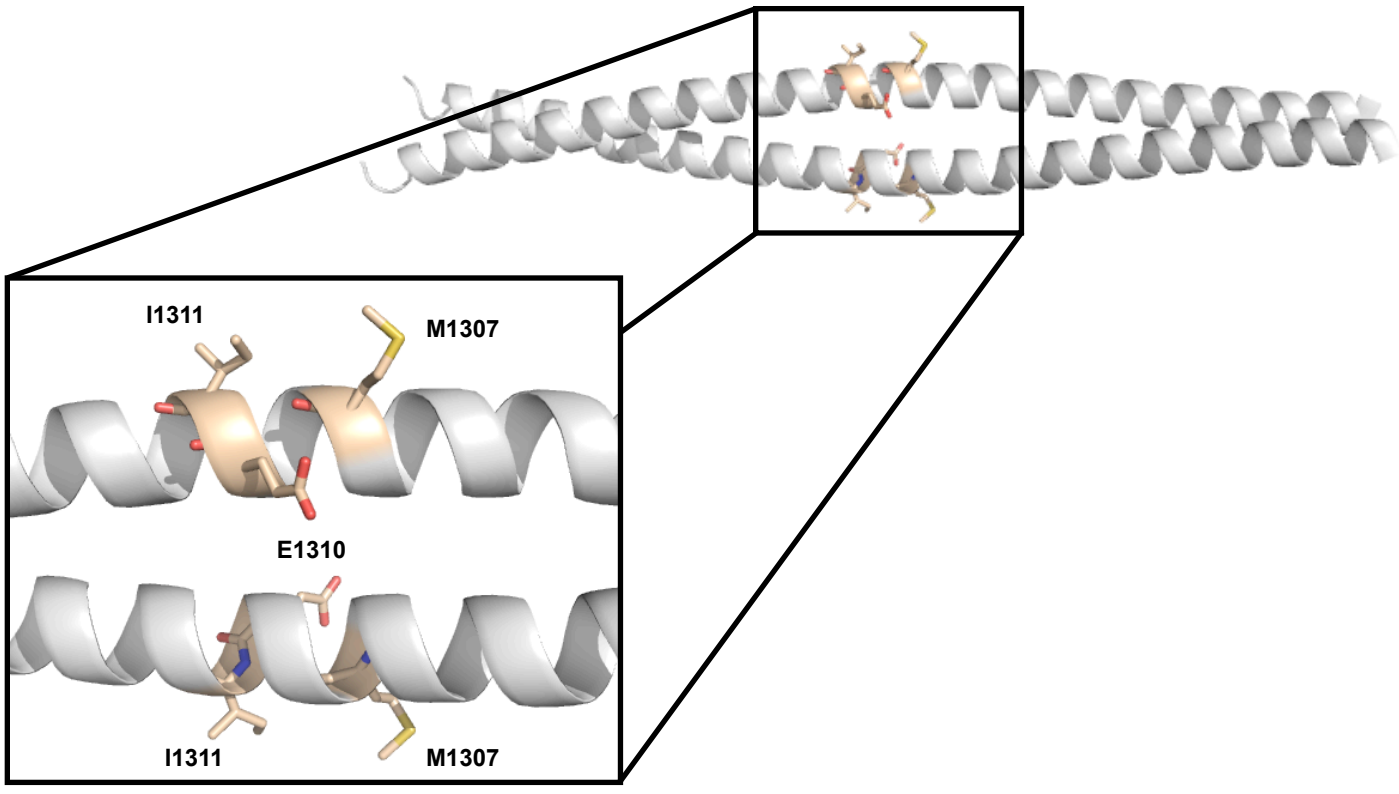
I1311
M1307
E1310
I1311
M1307

Figure 4. Domains and Structural Elements of the Silencing Protein Sir4.
(A) Structural domains of the Sir4 protein. Sir4 contains a chromatin binding N-terminal region, a Sir2 Interacting Doman (SID), a Positioning and Anchoring (PAD) domain, and a C-terminal Coiled-Coil (CC) domain. Figure adapted from Oppikofer et al., 2013a. **(B)** Crystal structure of the Sir4 Coiled-Coil domain and Sir3 binding site (PDB ID 1PL5, Chang et al., 2003). Inset, the Sir3 binding site of Sir4. Residues involved in Sir3 binding are coloured beige. Figure was generated using Pymol Molecular Graphics Software Version 1.3 (Shrödinger, LLC, http://www.pymol.org/).

nuclear envelope through interactions with the Ku proteins and with Esc1 (Taddei et al., 2004). No interactions between the Sir4 coiled-coil and chromatin have been detected (Martino et al., 2009).

The Sir4 N-terminus interacts with several proteins including Ku80 and Sir1 (Kueng et al., 2012). The initial 271 amino acids of Sir4 also interact with chromatin, and bind DNA nonspecifically. Overexpression of the $Sir4^{1-271}$ N-terminal fragment displaces SIR complexes from chromatin, disrupting silencing (Martino et al., 2009). Although an early study suggested that Sir4 may interact with H3 and H4 tails (Hecht et al., 1995), possible Sir4-nucleosome interactions have not been well characterized. Unlike the C-terminus of Sir4, which is essential for silencing, the N-terminal 746 residues of Sir4 are dispensable for Sir complex formation, tethering of silent chromatin to the nuclear periphery, and for silencing at the *HM* loci when all silencers are intact (Kueng et al., 2012). However, loss of this N-terminal fragment prevents silencing at telomeres or at *HM* loci with weakened silencers, suggesting that the DNA-binding ability of the Sir4 N-terminus is required for the SIR complex-chromatin interaction in the absence of strong recruitment factors (Kueng et al., 2012). The phosphorylation of several residues within the Sir4 N-terminus may alter telomeric silencing, suggesting a regulatory role for the Sir4 N-terminus in silencing (Kueng et al., 2012).

Asf2 (Anti Silencing Factor 2) is a Sir4 paralogue that arose from a whole-genome duplication event during the evolution of *S. cerevisiae* (Hickman et al., 2011). Asf2 bears close sequence homology to Sir4, especially in a C-terminal region that is predicted to dimerize and form a coiled-coil (Isabelle Callebaut, Université Pierre et Marie Curie, France, unpublished work, 2014). Asf2 is not required for telomeric or *HM* silencing, however, like Sir4, overexpression of Asf2 disrupts silencing (Le et al., 1997). Unpublished work from our

lab shows that Asf2 interacts with Sir3 through conserved residues in its putative coiled-coil domain (Williams and Rudner, 2014), and that overexpression of Asf2 disrupts the interaction between Sir3 and Sir4 (Rudner, 2003).

1.2.3.3 Sir2

Sir2 is a Class III histone deacetylase (HDAC) bearing close homology to the human Sirtuins SIRT1-7 (Delcuve et al. 2012, Vassilopoulos et al., 2011). Sir2 requires nicotinamide adenine dinucleotide (NAD+) for deacetylase activity, and produces nicotinamide and *O*-AAR as byproducts of the deacetylation reaction (Jackson et al., 2002). The role of *O*-AAR in silent chromatin spreading is disputed (Oppikofer et al., 2013a) and will be discussed further in section 1.2.4. Sir2 contains an N-terminal helical domain that interacts with Sir4 and a C-terminal catalytic domain that contains binding sites for the acetyl-lysine substrate, as well as for NAD+, nicotinamide, and *O*-AAR (Figure 5A,B, Hsu et al., 2013). Catalytic activity of Sir2 is required for both SIR complex spreading and for the clustering of telomeres near the nuclear periphery (Hoppe et al., 2002).

A

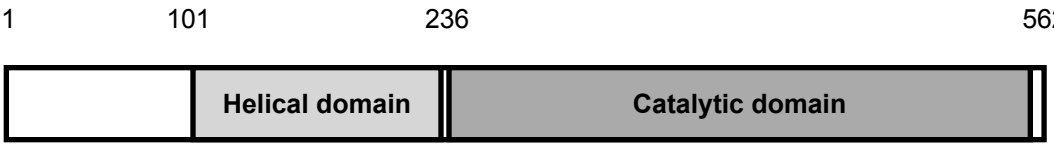

B

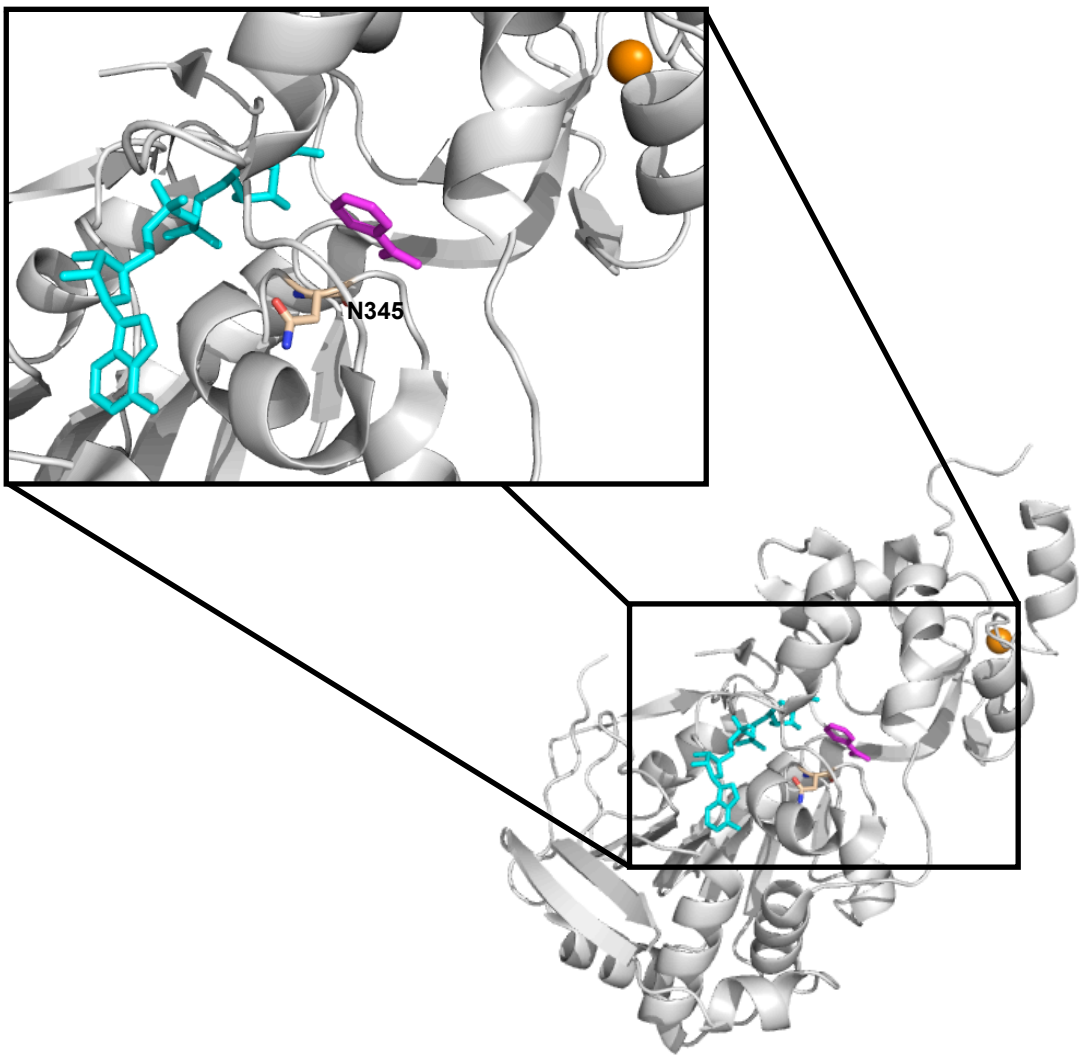

Figure 5. Domains and Structural Elements of the Silencing Protein Sir2. (A) Structural domains of the Sir2 protein. Sir2 contains an N-terminal helical domain and a C-terminal catalytic domain. Figure adapted from Oppikofer et al., 2013a. **(B)** Crystal structure of Sir2 (PDB ID 2HJH, Hall et al., 2008). Inset, the catalytic site of Sir2. N345, a key catalytic residue, is coloured beige. Nicotinamide is magenta and an acetyl-ribosyl-ADP reaction intermediate is coloured cyan. A Zn atom is displayed as an orange sphere. Figure was generated using Pymol Molecular Graphics Software Version 1.3 (Shrödinger, LLC, http://www.pymol.org/).

1.2.4 Silent Chromatin Nucleation and Spreading

1.2.4.1 Silent Chromatin Nucleation

Silent chromatin formation occurs in two steps: an initial step of nucleation, and a subsequent step of spreading (Grunstein et al., 2013). While interaction of Sir2 or Sir3 with the *HM* silencers requires Sir4, Sir4 can bind to the silencers independently of Sir2 and Sir3 (Hoppe et al., 2002; Rusche et al., 2002). Several studies identified a Sir4/Sir2 subcomplex that contains little or no bound Sir3 (Moazed et al., 1997; Ghidhelli et al., 2001; Hoppe et al., 2002), while others have been able to isolate a soluble SIR complex from cells (Rudner et al., 2005). Although active chromatin marks such as H4K16ac and H3K79me decrease the affinity of Sir3 for the nucleosome (Carmen et al., 2002; Johnson et al., 2009; Oppikofer et al., 2011; Altaf et al., 2007; Onishi et al., 2007; Armache et al., 2011) the Sir4/Sir2 subcomplex shows a high *in vitro* affinity for nucleosomes containing the H4K16ac mark (Oppikofer et al., 2011). These findings suggest that silent chromatin nucleation begins with the binding of a Sir4/Sir2 subcomplex to silencer elements (Figure 6A,B). This recruitment occurs through interactions of Sir4 with nucleation proteins Rap1 and Sir1 (Chang et al., 2003; Luo et al., 2002; Bose et al., 2004) and may be facilitated by the high affinity of the Sir4/Sir2 subcomplex for H4K16ac (Oppikofer et al., 2011).

Recruitment of Sir4/Sir2 to the silencer is followed by the binding of Sir3. Mutation of the Sir3 binding site on Sir4 prevents recruitment of Sir3 to the silencers, suggesting that Sir3 recruitment requires the Sir3-Sir4 interaction (Rudner et al., 2005). The deacetylation of H4K16ac by Sir2 is also required for the binding of Sir3 to the nucleosome (Carmen et al., 2002; Onishi et al., 2007). Interestingly, Sir3, the Sir4/Sir2 subcomplex, and the H3K79 methyltransferase Dot1 all show high affinity for the H4 tail. Altaf et al. (2007) propose a model in which Sir3 and Dot1 compete for binding to the H4 tail. While Sir3 can only bind

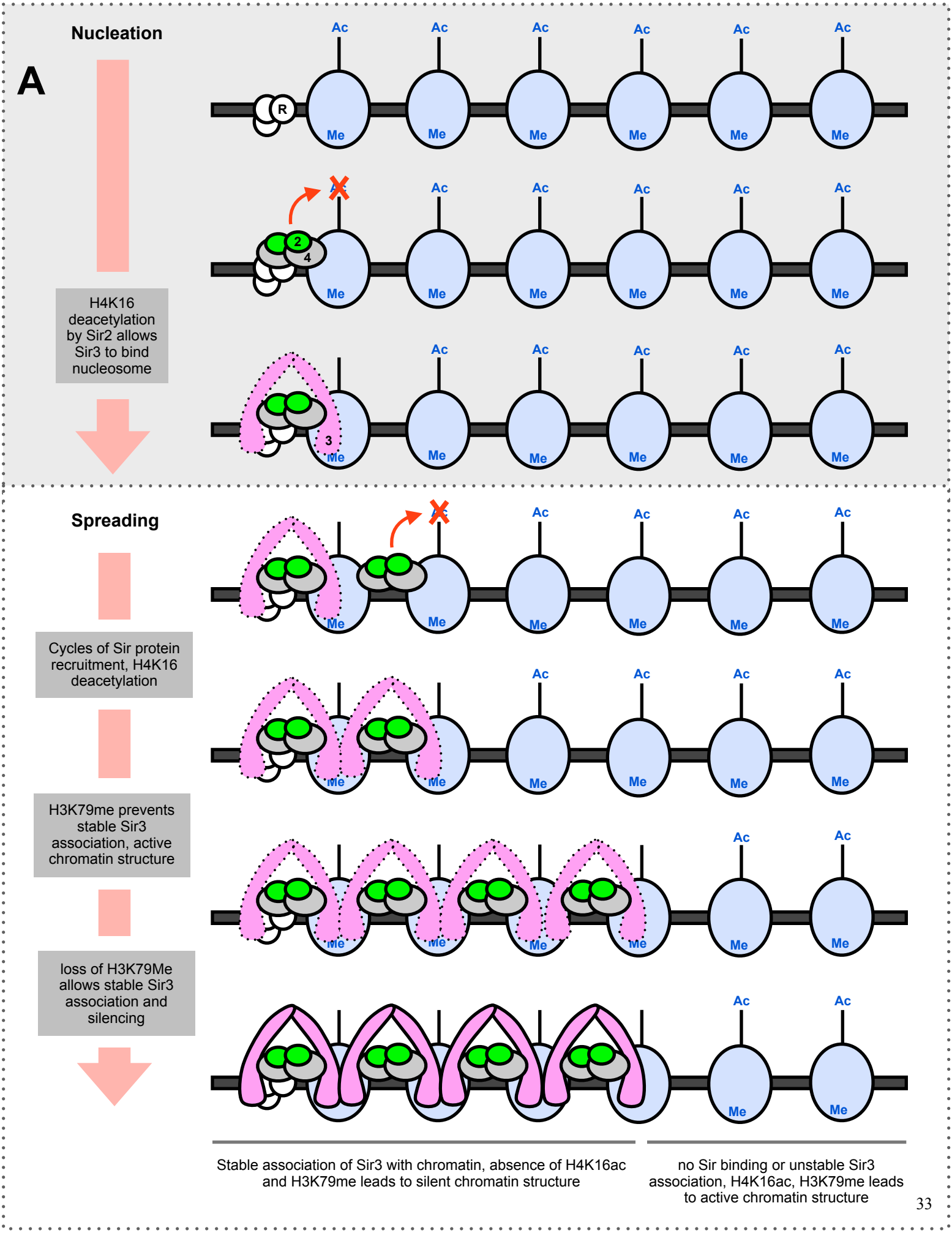
A
Nucleation
R
Ac
Me
H4K16 deacetylation by Sir2 allows Sir3 to bind nucleosome
2
4
3
Spreading
Cycles of Sir protein recruitment, H4K16 deacetylation
H3K79me prevents stable Sir3 association, active chromatin structure
loss of H3K79Me allows stable Sir3 association and silencing
Stable association of Sir3 with chromatin, absence of H4K16ac and H3K79me leads to silent chromatin structure
no Sir binding or unstable Sir3 association, H4K16ac, H3K79me leads to active chromatin structure

B

Nucleation

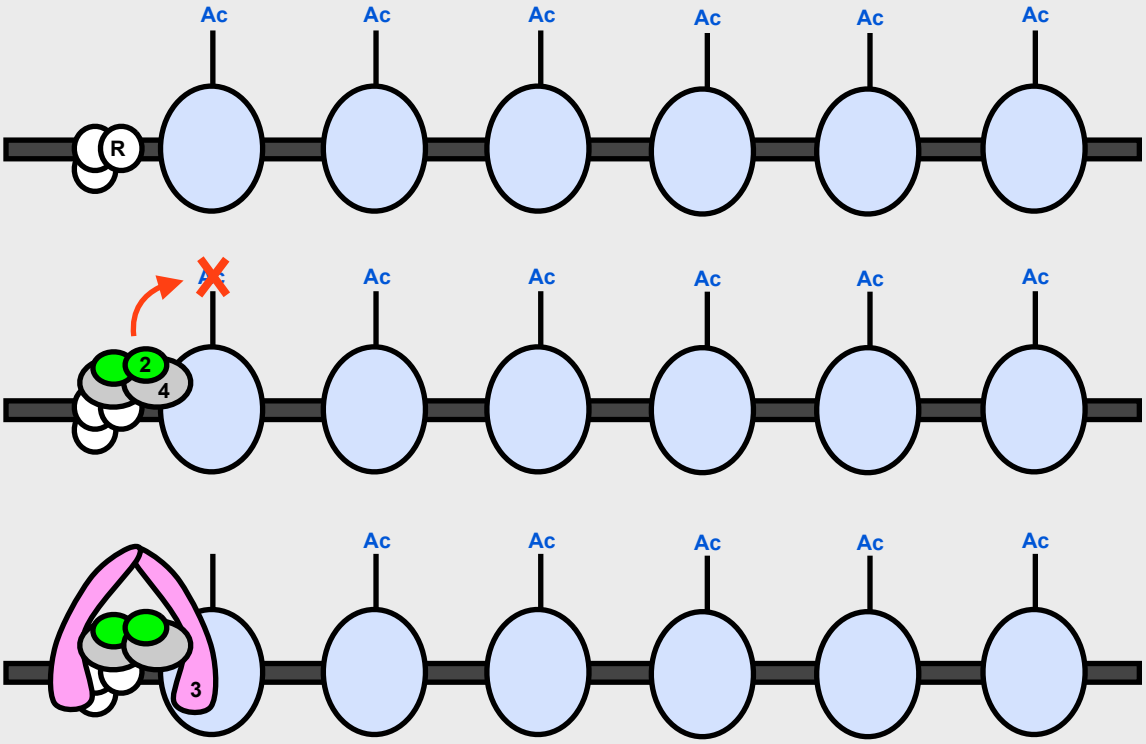

H4K16 deacetylation by Sir2 allows Sir3 to bind nucleosome

Spreading

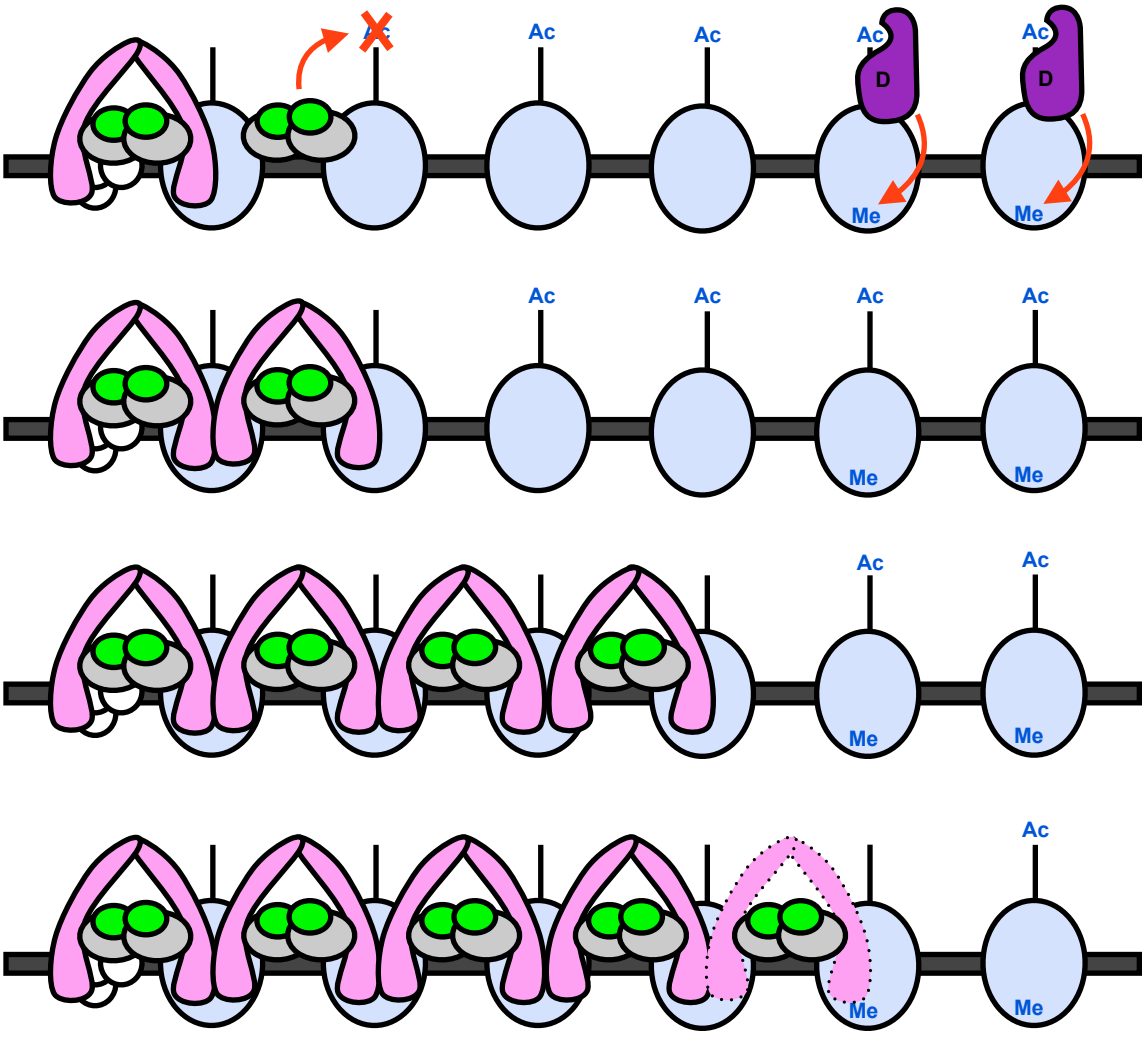

Dot1 competes with Sir3 or Sir4/ Sir2 for H4 tails

Cycles of Sir protein recruitment, H4K16 deacetylation

Stable association of Sir3 with chromatin, absence of H4K16ac and H3K79me leads to silent chromatin structure

no Sir binding or unstable Sir3 association, H4K16ac, H3K79me leads to active chromatin structure

Figure 6. Silent Chromatin Nucleation and Spreading. Models for silent chromatin nucleation and spreading. R – Recruitment proteins, Ac – H4K16ac, Me – H3K79me, D – Dot1, 2 – Sir2, 3 – Sir3, 4 – Sir4. H4K16 acetylation and H3K79 methylation are mediated by Sas2 and Dot1 respectively. Recruitment begins with binding of a Sir4/Sir2 subcomplex to silencer elements and an H4K16-acetylated nucleosome. Deacetylation of H4K16 by Sir2 allows binding of Sir3. Spreading occurs through iterative rounds of Sir protein recruitment and H4K16 deacetylation and is driven by Sir3-Sir3 multimerization, which may be mediated by two separate domains on Sir3. In **(A)**, the dotted outline of Sir3 indicates that Sir3 may bind unstably to H3K79 methylated nucleosomes; this binding may be sufficient for Sir protein spreading but not silencing (as suggested by Kitada et al., 2012, see section 1.2.4.4). In this model, loss of H3K79 methylation occurs as a later step in silent chromatin formation, allowing strong Sir protein binding and silencing. In **(B)**, Sir binding begins before nucleosomes have been H3K79 methylated by Dot1. Dot1 competes with Sir3 or Sir4/Sir2 for H4 tails. Dot1 binds Sir protein-free nucleosomes, methylating H3K79 and preventing stable Sir complex spreading. Sir3 (dotted outline) may still bind H3K79 methylated nucleosomes, but this binding would be insufficient for silencing.

to the deacetylated H4 tail, Dot1 may be able to interact with the H4 tail in either its acetylated or deacetylated form; thus, H4K16 acetylation favors Dot1 binding. In an alternative model proposed by Oppikofer et al (2013a), Dot1 competes with Sir4/Sir2 rather than Sir3 for H4K16-acetylated histone tails. Based on this model, H4K16-acetylated nucleosomes may: (1) recruit Sir4/Sir2, allowing H4K16 deacetylation and Sir3 binding, which would prevent H3K79 methylation by Dot1, or (2) recruit Dot1, leading to H3K79 methylation, which would prevent stable Sir3 association and silencing (Figure 6B). However, whether loss of H3K79 methylation is a cause or an effect of SIR complex spreading remains unknown (Figures 6A,B).

The deacetylation of H4K16 by Sir2 produces *O*-AAR, a byproduct that may play an important role in silent chromatin formation. Incubation of *O*-AAR with purified Sir proteins increased the affinity of Sir3 for the Sir complex (Liou et al., 2005) and improved the nucleosome-binding ability of the Sir complex *in vitro* (Martino et al., 2009). These findings suggest that *O*-AAR may cause a conformational change in the SIR complex, increasing its nucleosome affinity and ability to form silent chromatin. However, simultaneous deletion or mutation of the H4K16 acetyltransferases Sas2 and Esa1 partially rescues telomeric Sir3 binding in a Sir2 delete background (Suka et al., 2002), and in a strain expressing Sir2, mutation of the Sir2 substrates H3K9, H3K14, and H4K16 to arginine does not abolish Sir protein spreading or silencing (Yang et al., 2006; Yang et al., 2008) suggesting that active deacetylation of these three residues is not absolutely required for silent chromatin formation. Finally, in a strain lacking all NAD-dependent HDACs, tethering Sir3 to the NAD-independent HDAC Hos3 is sufficient to mediate H4K16 deacetylation and silencing at telomeres and at the *HM* loci (Chou et al., 2008), showing that any requirement for *O*-AAR in silencing can be bypassed in the absence of Sir2. Thus, the requirement for *O*-AAR

in silencing remains unclear. If *O*-AAR plays a role in silent chromatin spreading, its effects would have to be mediated through Sir2, and not by Sir3 as previously proposed.

1.2.4.2 Silent Chromatin Spreading

Silent chromatin spreading is thought to occur through iterative cycles of Sir protein recruitment and H4K16 deacetylation (Figure 6A,B). Silencing requires both H4K16 deacetylation and loss of H3K79 methylation, as well as the removal of several other marks of active transcription such as H3K56 acetylation (Oppikofer et al., 2011). While H4K16ac and H3K56ac are removed by known deacetylases, the mechanism by which H3K79 methylation is lost is poorly understood. This histone mark may be removed over multiple cell-cycles as histones bearing methylated H3K79 are replaced by their unmethylated counterparts (Katan-Khaykovich et al., 2005), however, this process occurs more slowly than the rate at which silent chromatin is established (Osborne et al., 2009; Oppikofer et al., 2013a). Alternatively, an unknown histone demethylase may actively remove the H3K79 methyl mark.

Multimerization of Sir3 is thought to drive silent chromatin spreading (Figure 6A,B) (Oppikofer et al., 2013a; Grunstein et al., 2013). Sir3 is known to dimerize (Oppikofer et al., 2013b) and has been shown to polymerize *in vitro*, forming long filaments when incubated with the other Sir proteins, NAD+, and nucleosomal arrays (Liou et al., 2005; Onishi et al., 2007). A recent study using *in vitro* nucleosomal arrays (Swygert et al., 2014) found that two Sir3 monomers bound to each nucleosome, supporting a model in which Sir3 multimerization is mediated through Sir3-Sir3 and Sir3-nucleosome interactions. Work from our lab (Harding, 2014) suggests that multimerization of Sir3 may be made possible by a second Sir3 dimerization domain located near the N-terminus of Sir3 (Figure 6A,B).

The mechanism for transcriptional inactivation by silent chromatin is poorly understood. Several studies show that the pre-initiation complex (PIC) consisting of RNA polymerase and transcription factors is absent from the promoters of silenced genes within the *HM* loci or near *TELVII-L* (Chen et al., 2005; Kitada et al., 2012), indicating that silent chromatin may block transcription initiation prior to PIC formation. However, other studies found significant enrichment of the PIC at the *HM* loci, but did not detect factors required for transcription elongation in these regions, suggesting that silent chromatin blocks transcriptional elongation at a step downstream of PIC binding (Sekinger et al., 2001, Gao et al., 2008). Sir protein spreading and loss of active chromatin marks is thought to generate higher-order chromatin structures (Georgel et al., 2001; Thurtle et al., 2014); these structures may exert steric effects that block specific steps of transcription initiation or elongation (Gottschling et al., 1992; Loo et al., 1994).

1.2.4.3 Establishment of Heterochromatin-Euchromatin Boundaries

Silent chromatin spreading is limited by histone modifiers that confer marks of transcriptional activation. These include the H4K16 acetyltransferase Sas2, and the H3K79 methyltransferase Dot1. Deletion of Sas2 causes Sir proteins to spread farther along a telomere, silencing certain sub-telomeric genes normally expressed in wild type cells (Suka et al., 2002). This ectopic spreading of the Sir proteins and their concomitant depletion from silent regions, combined with the loss of high-affinity interactions between Sir4/Sir2 and H4K16-acetylated nucleosomes, is likely the cause for *HML* and telomeric silencing defects observed in strains lacking Sas2 (Oppikofer et al., 2011). Both overexpression and deletion of Dot1 cause severe defects in telomeric, *HM*, and rDNA silencing (Singer et al., 1998; Ng et al., 2002; van Leeuwen et al., 2002). Overexpression of Dot1 causes the hypermethylation

of chromatin that would normally be silenced, preventing Sir complex binding, while deletion of Dot1 is thought to allow Sir protein spreading into euchromatic regions, diluting their enrichment at telomeres, rDNA, and *HM* loci (van Leeuwen et al., 2002). Dot1 and Sas2 therefore serve an important role in the establishment of boundaries between regions of euchromatin and heterochromatin. The histone variant Htz1 (a homologue of the vertebrate H2A.Z) also plays an important role in heterochromatin boundary formation. Htz1 is required for transcriptional activation of genes in regions flanking telomeric and *HM* silent chromatin, and is thought to prevent spreading of the Sir proteins into euchromatic regions (Hild et al., 2003; Meneghini et al., 2003).

1.2.4.4 Sir protein spreading is not sufficient for silencing

Most laboratory *Saccharomyces cerevisiae* strains contain a mutated, nonfunctional form of the *URA3* gene, which encodes an enzyme essential for the synthesis of uracil. The compound 5-Fluoroorotic acid (FOA) is toxic to cells with an intact uracil biosynthesis pathway, thus strains expressing a wild type *URA3* gene are inviable on media containing FOA. In a commonly used silencing assay, a functional *URA3* reporter gene is inserted within a region of silent chromatin, and silencing is assessed by monitoring viability on FOA media (Boeke et al., 1984). A recent study used the principle of FOA selection to enrich for cell populations with either a transcriptionally activated or silenced telomeric *URA3* gene, by growing cells in media lacking uracil or containing FOA (Kitada et al., 2012). The authors found that Sir3 enrichment, as well as H4K16 and H3K56 acetylation were not significantly different between active and silenced telomeres. However, H3K79 dimethylation was noticeably higher at active telomeres and could induce transcriptional activation in an *in vitro* assay. This study suggests that Sir protein spreading and H4K16 deacetylation are necessary

but not sufficient for silencing, a hypothesis that is supported by several earlier studies. Deletion of the N-terminal H3 tail blocks telomeric and *HM* silencing, even though Sir3 enrichment increases and H4K16ac decreases at telomeres and overall levels of H3K79me are maintained (Sperling et al., 2009; Thompson et al., 1994; Altaf et al., 2007). Likewise, mutation of H3K56 to arginine or glutamine does not alter enrichment of Sir2, Sir3, Sir4, Rap1, H4K16ac, or H3 along *TELVI-R* yet is detrimental to silencing (Xu et al., 2007). A mutation blocking the catalytic activity of Sir2 abolishes both Sir protein spreading and silencing, only the first of which can be rescued by mutation of H3K9, H3K14, and H4K16 to arginine (Yang et al., 2006). In another study, heat-shock-induced transcriptional activation of an *HSP82* gene placed at the *HMR* locus did not significantly alter levels of acetylated H4 in this region (Sekinger et al., 2001). More recently, Sir3 enrichment has been detected at a number of transcriptionally active, euchromatic genes (Radman-Livaja et al., 2011). Taken together, these studies suggest that the formation of silent chromatin not only requires Sir protein spreading and H4K16 deacetylation, but also depends on the loss of other key active chromatin marks such as dimethylated H3K79.

1.2.4.5 Role of the Sir3-Sir4 interaction in silent chromatin spreading

The Sir3-Sir4 interaction is required for the recruitment of Sir3 to the silencer during silent chromatin nucleation (Rudner et al., 2005), however the role of this interaction in silent chromatin spreading is unknown. Overexpressing Sir3 improves silencing and can cause silent chromatin domains to extend several kilobases along certain telomeres (Renauld et al., 1993). Analysis of these extended chromatin domains by Chromatin Immunoprecipitation (ChIP) at native telomeres *V-R* and *VI-R* revealed that Sir3 enrichment remained high up to 20 kb from the site of silent chromatin nucleation, while levels of Sir4 and Sir2 dropped

rapidly with increasing distance from the silencer element (Strahl-Bolsinger et al., 1997). These findings indicated that substoichiometric amounts of Sir4 and Sir2 may be sufficient for extensions of silent chromatin domains, suggesting that silent chromatin spreading may be able to occur at least partially independently of Sir4. Interestingly, an N-terminal $Sir3^{BAH}$ fragment fused to LexA to facilitate dimerization is sufficient for *HM* silencing when Sir1 is overexpressed, even though the Sir3 BAH domain does not interact with Sir4 (Connelly et al., 2006). A slightly longer $Sir3^{1-503}$ fragment, also incapable of interacting with Sir4, can extend telomeric silencing when overexpressed in the presence of endogenous, wild-type Sir3 (Gotta et al., 1998). Furthermore, overexpression of Sir3 in a *sir4-I1311N* strain allows Sir3 to spread at the *HML* locus, although this spreading is only sufficient for silencing when H4K16 is mutated to arginine (Wang et al., 2013). These findings suggest that unlike nucleation, silent chromatin may be able to spread in the absence of stoichiometric levels of Sir4, or independently of the Sir3-Sir4 interaction.

1.3 Hypothesis and Objectives

1.3.1 General Hypothesis

An intact SIR complex is essential for the initial binding of the Sir proteins to the silencer elements during silent chromatin nucleation (Hoppe et al., 2002; Rudner et al., 2005; Ehrentraut et al., 2011). During nucleation, the Sir3-Sir4 interaction is required for recruitment Sir3 to the silencer (Rudner et al., 2005), however it is unknown whether this interaction plays any additional roles in silencing initiation.

In the silent chromatin spreading that follows nucleation, the role of Sir protein interactions is poorly understood. When overexpressed, full-length Sir3 or a Sir3 fragment that does not bind Sir4 can mediate extension of silent chromatin regions, and within these

silent chromatin extensions, levels of Sir4 and Sir2 enrichment appear to be quite low relative to that of Sir3 (Renauld et al., 1993; Gotta et al., 1998; Strahl-Bolsinger et al., 1997). Thus, silent chromatin may be able to spread in the absence of Sir4 or independently of the Sir3-Sir4 interaction. In my Master's research, I investigated the role of the Sir3-Sir4 interaction in silent chromatin nucleation and spreading.

1.3.2 Specific Hypothesis

I hypothesize that while the Sir3-Sir4 interaction is required for the nucleation of silent chromatin, this interaction is dispensable for silent chromatin spreading. I also propose that during silent chromatin nucleation, the Sir3-Sir4 interaction has an additional function beyond the recruitment of Sir3.

1.3.3 Statement of Objectives

1. To further characterize the Sir3-Sir4 binding interface
2. To assess whether a Sir3 mutant that cannot bind Sir4 can mediate silent chromatin spreading
3. To characterize Sir3-Sir4 interaction independent Sir protein spreading and histone modification at active and silenced telomeres
4. To determine whether the Sir3-Sir4 interaction plays additional roles in silent chromatin nucleation aside from the recruitment of Sir3

Chapter 2 – Materials and Methods

2.1 Strains and Plasmids

Lists of strains and plasmids used in this study can be found in Tables S1.1 and S1.2. All strains originate from a W303 background (*leu2-3,112 trp1-1 can1-100 ura3-1 ade2-1 his3-11,15*) except for the following: ADR 3684-3689, 6213, 7092, 7097, 7098, 7101, 7325, and 7327; these strains were a gift from the Gottschling Lab and were constructed from YPH250 strains (Renauld et al., 1993). Strains ADR 5010 and 5012, and plasmids pAR 787, 788, and 790 were gifts from the Gartenberg Lab. All other strains and plasmids were generated in the Rudner Lab.

Plasmid amplification was achieved by transformation into chemically competent DH5α *E. coli* as described (Green et al., 2012) followed by overnight growth in LB media (1% Bacto Tryptone, 0.5% yeast extract, 1% NaCl) and plasmid preparation by alkaline lysis (Bio Basic EZ-10 Spin Column Mini-preps Kit). Yeast strains were grown at 30°C in either YPD-2% glucose supplemented with 0.2% Adenine and 0.2% Tryptophan (Sigma) or in synthetic media containing 2% glucose, yeast nitrogen base (Difco), and specified amino acids and nitrogenous bases (Sigma). FOA agar media contained 5-fluorootic acid (Toronto Research Chemicals) at a concentration of 1g/L and an extra 25 mg/L uracil, while FOA liquid media contained 10 mg/L FOA. Yeast DNA transformations were performed as described (Amberg et al., 2005; Amberg et al., 2006; Gietz et al., 2007)

Restriction digest, PCR, and other DNA manipulations were performed using standard methods (Green et al., 2012). PCR primer sequences are available upon request. Genes were deleted by homologous recombination of transformed, PCR-amplified auxotrophic markers (Longtine et al., 1998), and deletions were screened by auxotrophy,

PCR, and western blotting. Standard cloning methods (Green et al., 2012) were used to construct all plasmids generated in this study, except for those carrying the *sir3-2A, 3A,* and *4A* mutants, whose construction is described below.

sir3-2A, *3A*, and *4A* mutations were generated by site-directed mutagenesis of a single-stranded plasmid template carrying wild type Sir3 (pJB16), using oligos containing the *sir3-2A*, *3A*, and *4A* mutations (Table S1.3) (Kunkel, 1985). Sir3 mutagenesis was accompanied by insertion of a cryptic PstI restriction site, allowing mutants to be screened by restriction digest. The pJB16-derived *sir3* mutant plasmids were transformed into chemically competent DH5α *E. coli*; bacterial cultures were grown overnight at 37°C in LB media and plasmids were isolated by alkaline lysis miniprep. Isolates were screened for successful incorporation of *sir3-2A, 3A,* and *4A* mutations by digestion with Pst1 (New England Biolabs). Plasmids containing the mutations were digested with NdeI and SalI or NotI and SalI (New England Biolabs) to generate *sir3* gene fragments containing the mutations. Smaller *SIR3* fragments that included the region to be mutated were cut away from *CEN* plasmids and YEP13-derived *2μ* plasmids containing a *LEU2* auxotrophic marker and wild type *SIR3* or *SIR3-FLAG* genes. Digested plasmids and fragments were then co-transformed into the wild type yeast strain ADR4006 which was plated on synthetic media lacking leucine, allowing generation of *CEN* or *2μ sir3-2A*,*3A,* and *4A* plasmids by *in vivo* gap-repair and homologous recombination (Lundblad et al., 2001). Plasmids were rescued from yeast transformants by mechanical disruption with glass beads (0.5μm Biospec beads, Biospec mini beadbeater) in Lithium-Chloride buffer (2.5M LiCl, 50mM Tris-HCl pH 8.0, 4% Triton-X-100, 62.5mM Na_2EDTA) and 1:1 phenol-chloroform. Plasmids were transformed into chemically competent DH5α, and were isolated by alkaline lysis miniprep of bacterial cultures grown overnight in LB media at 37°C. Plasmids were screened for *sir3*

mutation by restriction digest with PstI, and expression of Sir3 or Sir3-FLAG was confirmed by Western blot.

2.2 Polyacrylamide Gel Electrophoresis and Western Blotting

Western samples were collected by measuring 600-nm absorbances (Ultrospec 2100 Pro) of log-phase cultures and harvesting approximately $3x10^7$ cells per sample. Samples were frozen immediately in liquid nitrogen, and stored at -80°C. Samples were prepared for Western blotting by mechanical disruption with glass beads as described above, in 250µL 1X sample buffer (2% SDS, 10% glycerol, 80 mM Tris-HCl pH 6.8, 0.02% bromophenol blue, 10mM EDTA, and, added just before use: 1mM PMSF), followed by centrifugation at 15 000 rpm at 4°C for 5 minutes (Eppindorf centrifuge 5415R).

A 15µL aliquot of each sample was loaded into a 12.5% polyacrylamide gel, and polyacrylamide gel electrophoresis (PAGE) was performed at 200V and 25mA per gel in Tris-SDS running buffer as described (Anderson et al., 1973; Green et al., 2012). Proteins were transferred to a nitrocellulose membrane by wet transfer (transfer buffer: 20mM Tris base, 150mM glycine, 20% methanol) at 60V and 600mA for 1.5 hours. Membranes were then blocked twice for 15 minutes in blocking solution (4% milk, 20mM Tris-HCl pH7.5, 150mM NaCl, 0.1% Tween-20, 5% glycerol), and washed with TBS-T (20mM Tris-HCl pH 7.5, 150mM NaCl, 0.1% Tween-20). Sir2, Sir3, Sir4, Asf2, and Cdk1 blots were incubated at 4°C overnight with the appropriate polyclonal rabbit primary antibodies (Rudner Lab), which were diluted in primary antibody solution (4% milk, 5% glycerol, 20mM Tris-HCl pH 7.5, 150mM NaCl, 0.1% Tween-20, 0.02% sodium azide) as follows: Sir2 – 1:2500, Sir3 – 1:1000, Sir4 – 1:1000, Asf2 – 1:1000, Cdk1 – 1:1000. Following primary antibody incubation, blots were incubated for one hour at room temperature with Horse Radish

Peroxidase (HRP)-Linked anti-rabbit secondary antibody (Amersham) which was diluted 1:5000 in blocking solution. FLAG blots were incubated for 1 to 2 hours at room temperature or at 4°C overnight with HRP-linked anti-FLAG M2 antibody (Sigma), diluted 1:5000 in primary antibody solution. Western Blots were visualized by incubation for 1-2 minutes in Western-Lightning-Plus ECL Reagent (Perkin Elmer) followed by film exposure (Hyblot-CL autoradiography film) for 1-40 minutes.

2.3 Co-Immunoprecipitation

Yeast cultures were grown at 30°C overnight until log phase. Cultures were harvested by centrifugation at 2000g for 2 minutes (Thermo Scientific Sorvall Centrifuge T1); a set of samples containing $30x10^7$ cells were taken from each culture, frozen in liquid nitrogen and stored at -80°C, and were later analyzed by Western Blotting as described above. The remainder of the cultures were collected in 200-400µL pellets which were frozen immediately in liquid nitrogen and stored at -80°C. Sample lysates were prepared on ice by addition of 350µL lysis buffer (75mM HEPES pH 8.5, 15mM $Mg(OAc)_2$, 7.5% glycerol, 7.5mM EGTA pH 8.0, 0.075mM EDTA pH 8.0, 0.3% NP-40, 450mM NaOAc, and, added just before use: 1mM DTT, 1mM LBPC, 1mM benzamidine, 1mM $NaVO_4$, 1mM PMSF), followed by rapid thawing and mechanical disruption with glass beads (0.5 µm Biospec beads, Biospec Mini Beadbeater). Lysates were collected by centrifugation at 4°C and 3000 rpm for 1 minute (Thermo Scientific Sorvall centrifuge Rc 6 Plus), and precipitate was removed by a second centrifugation at 15 000 rpm for 5 minutes (Eppindorf centrifuge 5415R). Input samples were taken by 1:1 dilution in 2X sample buffer. Protein concentrations of lysates were determined by Bradford Assay (BioRad) and normalized to equal concentrations. Sir3 and Sir4 immunoprecipitations were performed by incubation of

lysates with 1µL polyclonal Sir3 or Sir4 antibody (Rudner Lab) at 4°C for 30 minutes, followed by addition of 15µL Protein A Dynabeads (Life Technologies) and end-over-end rotation during a two hour incubation at 4°C. Anti-FLAG immunoprecipitations were performed by incubation of lysates with 50µL of anti FLAG-M2-conjugated protein A sepharose beads (Sigma) for two hours at 4°C with end-over-end rotation. Following immunoprecipitation, the beads were washed in lysis buffer, resuspended in 1.5x sample buffer, and heated to 65°C to release immunoprecipitated proteins. Input sample concentrations were normalized based on the lysate concentrations determined by the Bradford assay, and input and immunoprecipitate samples were analyzed by polyacrylamide gel electrophoresis and Western blotting.

2.4 *In vitro* GST pull-down assay

Plasmids containing His-tagged *SIR3* fragments or *GST-SIR4* fragments (Table 2) were transformed into *Rosetta E. Coli* and cultured overnight at 25°C in 2XYT media (1.6% Bacto Tryptone, 1% Bacto yeast extract, 0.5% NaCl, 10µg/mL chloramphenicol, plus 100µg/mL ampicillin or 100µg/mL kanamycin depending on plasmid resistance marker). Cultures were diluted into 0.5L 2XYT media the following day and grown to an OD of 1.0. Expression of the *SIR3* and *SIR4* fragments was induced by a 3-hour incubation with 0.5mM of IPTG (Fischer) as described (Buchberger et al., 2008). Cultures were harvested and stored at -80°C in W1 Buffer (1X PBS, 1mM EDTA, 1mM EGTA) or lysis buffer (50mM Tris pH 8.0, 500mM NaCl, 10mM imidazole, 10% glycerol, 5mM BME, and, added just before use: 1mM PMSF).

Pellets were lysed by thawing, incubation on ice for 20 minutes with 200µg/mL lysozyme, and sonication (4 x 30 seconds, with 0.5% NP-40 during final sonication). Lysates

were centrifuged for 20 minutes at 40 000g (Thermo Scientific Sorvall centrifuge Rc 6 Plus) and filtered through a 0.45 micron filter. His-tagged Sir3$^{464-978}$ was purified by His-column chromatography by incubation for 2 hours with NiNTA resin (Qiagen), followed by washing with lysis buffer containing 0.1% NP-40, and elution with lysis buffer containing 0.1% NP-40 and 20mM imidazole. Eluted Sir3 fragments were concentrated by overnight dialysis at 4°C, with three changes of dialysis buffer (20mM HEPES pH 7.5, 500mM NaCl, 1mM DTT, 1mM EDTA, 10% glycerol). Concentrations of purified protein fragments were determined by PAGE and Coomassie staining using BSA standards. Lysates from GST-Sir4$^{1267-1358}$ were incubated with rehydrated glutathione-agarose beads (Sigma) as described (Moazed et al., 1997). Equal amounts (2ug) of each purified Sir3 fragment were added to separate 105mg aliquots of GST-Sir4$^{1267-1358}$-bound beads; beads were washed and proteins eluted as described (Moazed et al., 1997). Elutates were analyzed by SDS-PAGE and Coomassie staining.

2.5 Silencing Assays

For qualitative silencing assays, cultures were grown to saturation at 25 or 30°C in 5mL minimal media for two days. Ten-fold serial dilutions were spotted on selective media and grown at 30°C for two or three days. Silencing of a *TRP1* reporter gene was assessed by lack of growth on –TRP media, and silencing of a *URA3* reporter gene was assessed by lack of growth on –URA media and growth on media containing 5-fluorootic acid (FOA), a compound that is toxic to cells with an intact uracil biosynthesis pathway (Boeke et al., 1984).

2.6 Selection for transcriptional activation or silencing of *TELV-R URA3*

To select for transcriptional silencing of *TELV-R URA3*, strains overexpressing *SIR3* or *sir3-4A* from *2μ LEU* plasmids were grown at 30°C for three days on SC –LEU +1g/L FOA agar media. This was followed by growth at 30°C for two days in 10mL SC –LEU + 10mg/L FOA liquid media. To select for activation of *TELV-R URA3*, strains overexpressing *SIR3* or *sir3-4A* from *2μ LEU* plasmids were grown at 30°C for three days on SC –LEU –URA agar media, followed by growth at 30°C for two days in 10mL SC –LEU –URA media. Control strains lacking a Sir protein or expressing endogenous levels of Sir3 were grown at 30°C for three days on –LEU agar media, and then grown at 30°C for two days in 10 mL –LEU liquid media. The 10-mL cultures were then diluted into 100 mL of the same type of media and grown to log phase before being harvested for chromatin immunoprecipitation.

2.7 Chromatin Immunoprecipitation

100 mL yeast cultures were grown at 30°C until log phase. Cultures were fixed in 1% formaldehyde for 15 minutes at room temperature, followed by quenching with 125mM glycine for 5 minutes. Cultures were then harvested by centrifugation (2000 g for 2 minutes, Thermo Scientific Sorvall Centrifuge T1), and washed once with TBS (20mM Tris-HCl pH 7.5, 150mM NaCl). Pellets of 30-50x10^7 cells were frozen in liquid nitrogen and stored at -80°C.

Sample lysates were prepared on ice by addition of 300μL ChIP lysis buffer (50mM HEPES-KOH pH 7.6, 500mM NaCl, 1mM EDTA, 1% Triton X-100, 0.1% SDS, and, added just before use, 0.1% sodium deoxycholate, 1mM PMSF, 1mM LBPC, 1mM benzamidine) and samples were lysed by mechanical disruption with 0.5μm glass beads (Biospec, Biospec mini beadbeater) for 2 x 20 seconds separated by a 5 minute incubation on ice. Lysates were

separated from beads by centrifugation at 3000 rpm for 1 minute at 4°C (Thermo Scientific Sorvall centrifuge Rc 6 Plus), identical lysates were combined, and additional ChIP lysis buffer was added to increase all lysate volumes to 1mL. Each 1-mL lysate sample was sonicated at 4°C (Covaris S220 Ultrasonicator) in order to shear DNA to an average size of 500 bp. Lysates were then centrifuged at 15 000 rpm and 4°C for 5 minutes (Eppindorf centrifuge 5415R) and precipitate was discarded. From each lysate, a 50µL input-1 sample was added to 200 µL of 50/10 TE + 1% SDS (50 mM Tris pH 8.0, 10mM EDTA, 1% SDS). Input samples were heated to 95°C for one hour to reverse crosslinks, while the remaining lysates were frozen in liquid nitrogen and stored at -80°C.

Following crosslink reversal, each input-1 sample was purified by incubation with 20 µg RNAse A at 55°C for 1 hour, incubation with 50µg/mL proteinase K at 55°C for two hours, and two extractions in an equal volume of 1:1 phenol-chloroform followed by one extraction with chloroform. Input-1 samples were then precipitated with 1mL 100% ethanol, 0.3M NaOAc pH 5.2, and 10µg glycogen and resuspended in 50µL 10/1 TE (10 mM Tris pH 8.0, 1mM EDTA). Input-1 DNA concentrations were measured by UV spectrophotometry (Nanodrop-1000 Thermo Scientific) and lysate DNA concentrations were calculated. Sizes of sonicated DNA fragments in were measured by agarose gel electrophoresis (Green et al., 2012) of the Input-1 samples.

Lysate samples were thawed, and calculated volumes of ChIP lysis buffer were added in order to normalize sample concentrations to 12.5 µg DNA in 500 µL (for Sir protein immunoprecipitations) or 1µg DNA in 500 µL (for histone immunoprecipitations). A second set of 50µL input samples (Input-2) were taken as described above. Immunoprecipitations were performed using the following antibody volumes: 2µL anti-Sir2, 0.5 µL anti-Sir3, 1µL anti Sir4 (polyclonal Rabbit antibodies, Rudner Lab), 1µL anti-H3 (Millipore), 1µL anti-pan-

H3K79me (Millipore), 1µL anti H4K16ac (Millipore). These antibody volumes were determined by test ChIP experiments to ensure that antibody saturation was avoided. Lysates were incubated with antibodies for 30 minutes on ice before 15 µL of protein A dynabeads (Life Technologies) was added to each sample. Lysates were then incubated at 4°C while rotating end-over-end for two hours. Following immunoprecipitation, lysates were washed four times with lysis buffer, and then washed once with Lithium-Cholate buffer (10mM Tris-HCl pH 8.0, 0.25 M LiCl, 0.5% NP-40, 1mM EDTA, and added just before use: 0.5% sodium deoxycholate), and once with 50/10 TE. Immunoprecipitates (IP samples) were heated to 65°C C for 15 minutes in 100µL 50/10 TE + 1% SDS and then washed with an additional 150µL 50/10 TE + 1% SDS to elute bound proteins from beads. Input-2 and IP samples were heated to 65°C overnight to reverse formaldehyde crosslinks, and samples were purified with RNAse, Proteinase, and phenol-chloroform extractions as described above with the following modifications: 10 µg RNAse A was added to Input-2 samples, and 1µg RNAse A was added to IP samples. Ethanol-precipitated Input-2 and IP samples from Sir protein immunoprecipitations were resuspended in 25µL 10/1 TE, while Input-2 and IP samples from histone immunoprecipitations were resuspended in 50µL 10/1 TE.

2.8 Quantitative PCR

For each ChIP experiment, a standard curve was generated from a single input sample, from which 5 or 6 serial 1/6 dilutions were made in 10/1 TE. All other input samples were diluted 1/6 in 10/1 TE while IP samples were not diluted. Oligo pairs were premixed and diluted to 5mM in 10mM Tris-HCl pH 8.0. Each qPCR reaction contained 9µL Master Mix (1X Qiagen HotStar PCR buffer, 0.15% Triton X-100, 0.5mM oligo mix, 0.9µm ROX reference dye (Invitrogen), 2mM dNTPs (Fisher), 1:10000 SYBR Green (Invitrogen), 0.16U

(0.4uL)/μL mix Qiagen HotStar Taq Polymerase) and 1μL DNA. qPCR reactions were performed in DiaTec 420-1378 PCR strip-tubes, and each sample was assessed in duplicates. After master mix and DNA were aliquoted into qPCR tubes, tubes were spun at 3000 rpm for 20 minutes to remove bubbles, and were loaded into the Mx3000P qPCR system (Agilent Technologies). Samples were cycled through the following thermal profile:

segment 1: (95°C for 15 minutes), 1 cycle

segment 2: (95°C for 15 seconds, 60°C for 30 seconds, 72°C for 30 seconds), 45 cycles

segment 3: (95°C for 1 minute, 60°C for 30 seconds, 95°C for 30 seconds), 1 cycle

Amplification plots were generated from fluorescence measurements taken from the SYBR and ROX dyes at the end of the 60-degree annealing period in each cycle of segment 2. Dissociation curves were generated from fluorescence measurements taken from the SYBR and ROX dyes during each incremental 1-degree increase in temperature between the 60-degree annealing period and 95 degree denaturing period in segment 3. Data were analyzed using MxPro software (Agilent Technologies). Standard curves were optimized to give efficiencies as close as possible to 100% and R^2 values greater than 0.990; experiments with curves that had efficiencies lower than 90% or higher than 110% or $R^2 < 0.990$ were repeated until standard curve efficiencies and R^2 values were within the desired range. Dissociation curves were assessed to ensure nonspecific PCR amplification was avoided. Input and IP DNA concentrations were normalized to account for variations in DNA concentrations from the 1/6 input dilution used in the standard curve. Undiluted input DNA concentrations were set to 10% (representing the 50μL input sample taken from the 500μL lysate volume), and IP DNA concentrations were calculated accordingly. Sir protein

enrichments were measured at the telomeric *URA3* locus, as well as at a euchromatic *ACT1* locus (see Table S1.4 for qPCR oligo sequences).

For the Sir3-LexA ChIP samples, qPCR was performed as described above, with several modifications. Phusion was used instead of Hot Star Taq, and the qPCR master mix was modified to include the following ingredients: 1X HF PCR buffer (Fisher), 3.5% DMSO (New England Biolabs), 0.5mM oligo mix, 0.9µm ROX reference dye (Invitrogen), 2mM dNTPs (Fisher), 1:10000 SYBR Green (Invitrogen), 0.04uL/µL mix Phusion Polymerase. Sir3 enrichment was measured at the A-element of *HMR-E,* the *Kluveromyces lactis URA3* (*KlURA3*) reporter gene inserted at *HMR,* and at a euchromatic *ACT1* locus (see Table S1.4 for oligo sequences). Samples were cycled through the following thermal profile:
segment 1: (98°C for 2 minutes), 1 cycle
segment 2: (98°C for 30 seconds, 60°C for 30 seconds, 72°C for 10 seconds), 45 cycles
segment 3: (98°C for 1 minute, 60°C for 30 seconds, 98°C for 30 seconds), 1 cycle

2.9 Statistical Analysis

ChIP-qPCR data for Sir protein and histone enrichment at active or silenced telomeric *URA3* (Figures 14-17) were log transformed in order to correct for nonnormality and heteroscedasticity. Data were statistically analyzed by one-way and two-way ANOVA followed by Bonferroni Post-Hoc tests using GraphPad Prism software. Statistical analysis is summarized in tables S2.1-S2.17. ChIP-qPCR data for Sir3-LexA enrichment (Figure 18D) were analyzed by Welch One-Way ANOVA and Games-Howell Post Hoc tests for data sets with unequal variances (as determined by the Levene's test), or by One-Way ANOVA and Bonferroni Post Hoc tests in the case of equal sample variances. Analysis was conducted using IBM SPSS software and is summarized in Tables S2.19-S2.22.

Chapter 3 – Results

3.1 Role of the Sir3 residues 657-660 in silent chromatin spreading

3.1.1 Sir3 residues 657-660 are required for interaction with Sir4 in vivo and for the direct interaction of Sir3 with Sir4 in vitro

The recently solved crystal structure of the C-terminal AAA+ domain of Sir3 reveals a basic loop comprising lysine and arginine residues 657-660 that extends from the surface of the molecule (Ehrentraut et al. 2011, Figure 3B). Mutation of these residues to alanine disrupted SIR complex formation *in vitro* (Ehrentraut et al., 2011). We therefore suspected that residues 657-660 were important for the Sir3-Sir4 interaction *in vivo*. We generated untagged and FLAG-tagged *sir3-2A, 3A,* and *4A* mutants in which the first two, three, or all four of the residues 657-660 were respectively mutated to alanine. These mutants expressed from *CEN* plasmids at similar levels as wild type Sir3 and Sir3-FLAG (Figure 7A). To overexpress Sir3 we used a high-copy 2-micron (2μ) YEp13 plasmid (Renauld et al 1993). Expression levels of 2μ Sir3 were determined by comparing Sir3 expression in five two-fold serial dilutions of a cell lysate containing 2μ Sir3 with Sir3 expression in cell lysate containing endogenous or *CEN* Sir3. Wild type Sir3 was expressed from the 2μ plasmid at levels almost 16-fold higher than Sir3 expressed from a *CEN* plasmid, and over 16-fold higher than endogenous Sir3 (Figure 7B), and both wild type and mutant Sir3 expressed from the 2μ plasmid at similar levels (Figure 7C).

To assess the role of Sir3 residues 657-660 *in vivo* we immunoprecipitated FLAG-tagged wild type and mutant Sir3 using a FLAG antibody. Both Sir4 and the Sir4 homologue Asf2 co-precipitated with wild type Sir3-FLAG, but not with the Sir3 mutants (Figure 8A). To ensure that the FLAG tag itself was not affecting the Sir3-Sir4 interaction, we used

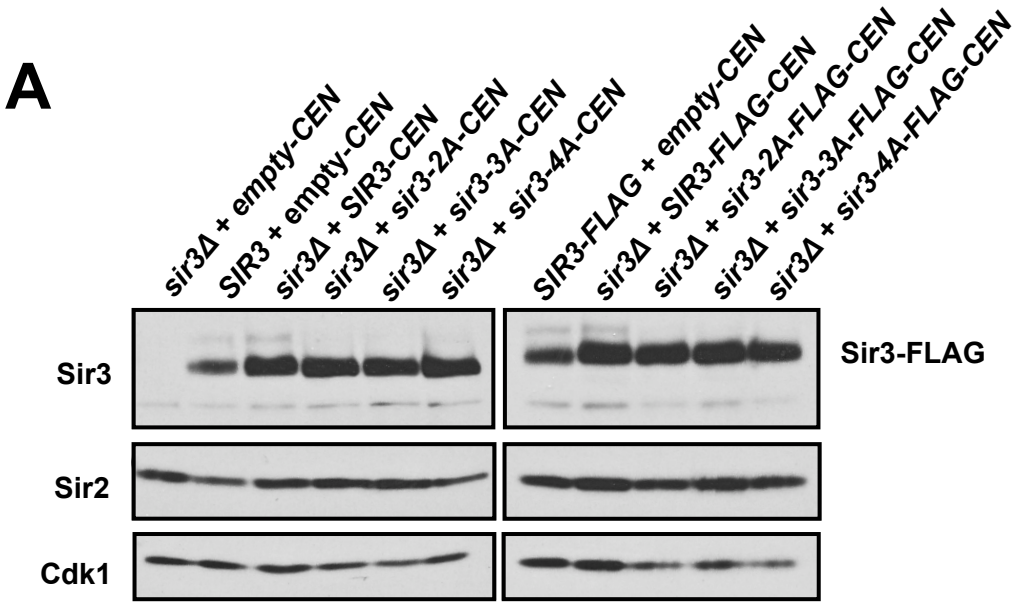
A
sir3Δ + empty-CEN
SIR3 + empty-CEN
sir3Δ + SIR3-CEN
sir3Δ + sir3-2A-CEN
sir3Δ + sir3-3A-CEN
sir3Δ + sir3-4A-CEN
SIR3-FLAG + empty-CEN
sir3Δ + SIR3-FLAG-CEN
sir3Δ + sir3-2A-FLAG-CEN
sir3Δ + sir3-3A-FLAG-CEN
sir3Δ + sir3-4A-FLAG-CEN
Sir3
Sir3-FLAG
Sir2
Cdk1

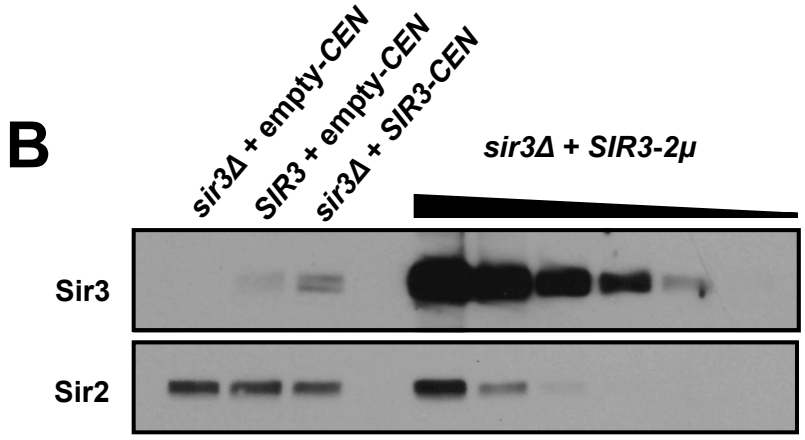
B
sir3Δ + empty-CEN
SIR3 + empty-CEN
sir3Δ + SIR3-CEN
sir3Δ + SIR3-2μ
Sir3
Sir2

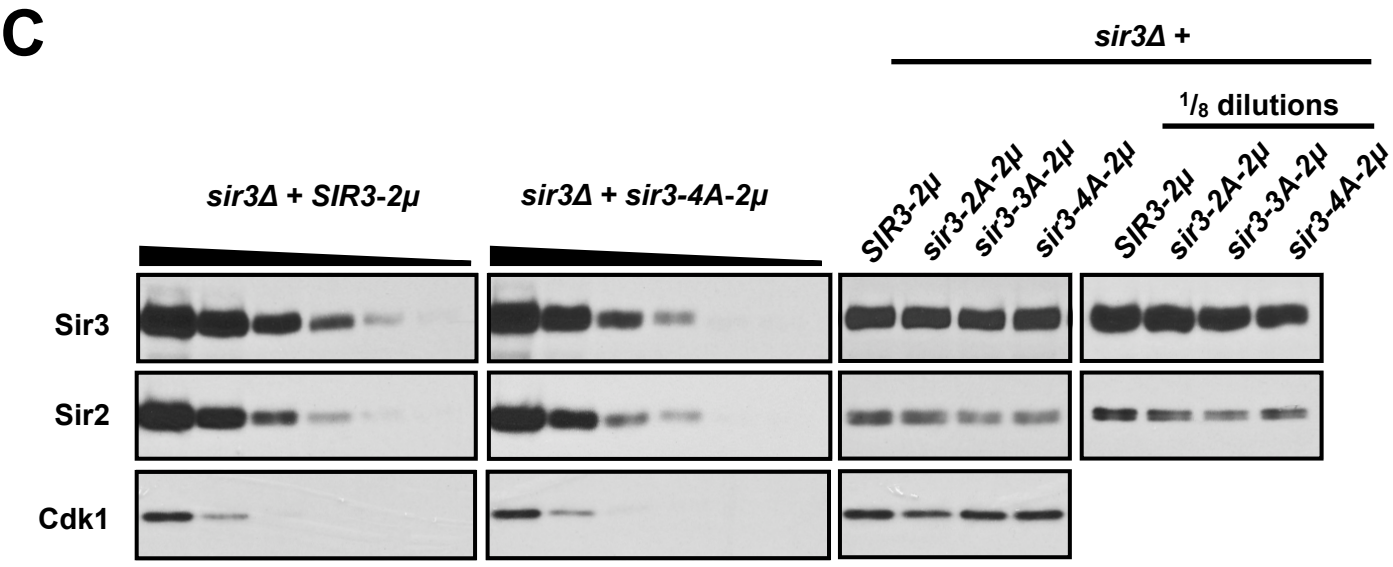
C
sir3Δ +
1/8 dilutions
sir3Δ + SIR3-2μ
sir3Δ + sir3-4A-2μ
SIR3-2μ
sir3-2A-2μ
sir3-3A-2μ
sir3-4A-2μ
SIR3-2μ
sir3-2A-2μ
sir3-3A-2μ
sir3-4A-2μ
Sir3
Sir2
Cdk1

Figure 7. Wild type Sir3 and Sir3-2A, 3A, and 4A mutants express to similar levels. **(A)** *SIR3-CEN* and *sir3-2A,3A,* and *4A-CEN* express at similar levels. A *sir3Δ* strain was transformed with an empty *CEN* plasmid, or with *CEN* plasmids expressing FLAG-tagged or untagged wild type *SIR3* or *sir3-2A, 3A,* or *4A*. Empty *CEN* plasmids were also transformed into a wild type strain and a *SIR3-FLAG* strain for use as endogenous Sir3 controls. Expression of Sir3 was assessed by Western Blotting, Sir2 and Cdk1 serve as loading controls. **(B)** *SIR3-2μ* expresses to levels over16-fold higher than endogenous Sir3. A *sir3Δ* strain was transformed with a 2μ plasmid expressing wild type *SIR3*. The undiluted *SIR3-2μ* sample and five serial two-fold dilutions were loaded alongside *sir3Δ*, endogenous *SIR3*, and *SIR3-CEN* controls, in order to determine expression levels of *SIR3-2μ* relative to that of endogenous Sir3 and Sir3-*CEN*. Sir2 serves as a loading control. *SIR3-2μ* expressed at levels over 16 fold higher than endogenous *SIR3*, and almost 16-fold higher than *SIR3-CEN*. **(C)** *SIR3-2μ* and *sir3-2A, 3A,* and *4A-2μ* express at similar levels. A *sir3Δ* strain was transformed with *SIR3-2μ* or *sir3-2A, 3A,* or *4A-2μ*. Panels 1 and 2: Serial 2-fold dilutions of *SIR3-2μ* and *sir3-4A-2μ* samples. Panel 3: undiluted *SIR3, sir3-2A, 3A,* and *4A-2μ* samples. Panel 4: 1/8 dilutions of the samples in panel 3; during visualization of the Western blot, the 1/8 dilutions were exposed for a longer period of time than the undiluted samples in Panel 3. Sir2 and Cdk1 serve as loading controls.

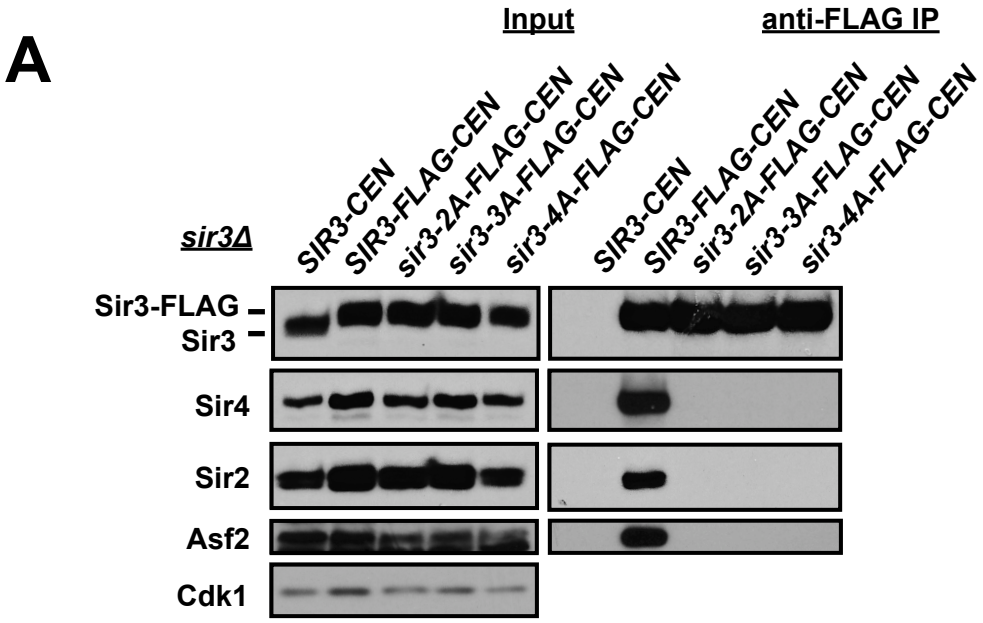
A
Input
anti-FLAG IP
sir3Δ
SIR3-CEN
SIR3-FLAG-CEN
sir3-2A-FLAG-CEN
sir3-3A-FLAG-CEN
sir3-4A-FLAG-CEN
Sir3-FLAG
Sir3
Sir4
Sir2
Asf2
Cdk1

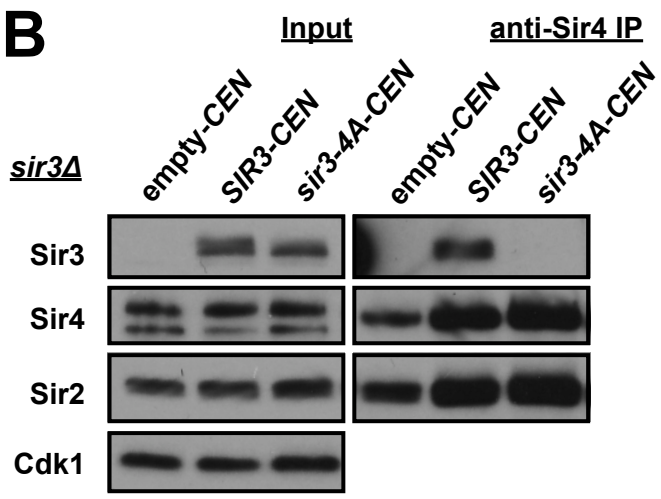
B
Input
anti-Sir4 IP
sir3Δ
empty-CEN
SIR3-CEN
sir3-4A-CEN
Sir3
Sir4
Sir2
Cdk1

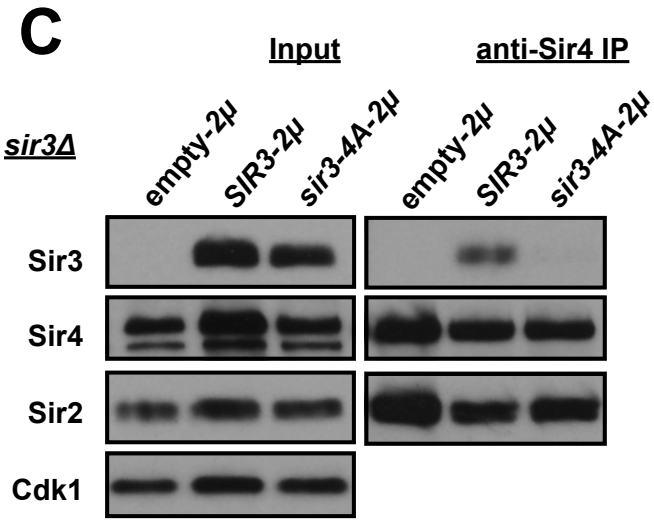
C
Input
anti-Sir4 IP
sir3Δ
empty-2μ
SIR3-2μ
sir3-4A-2μ
Sir3
Sir4
Sir2
Cdk1

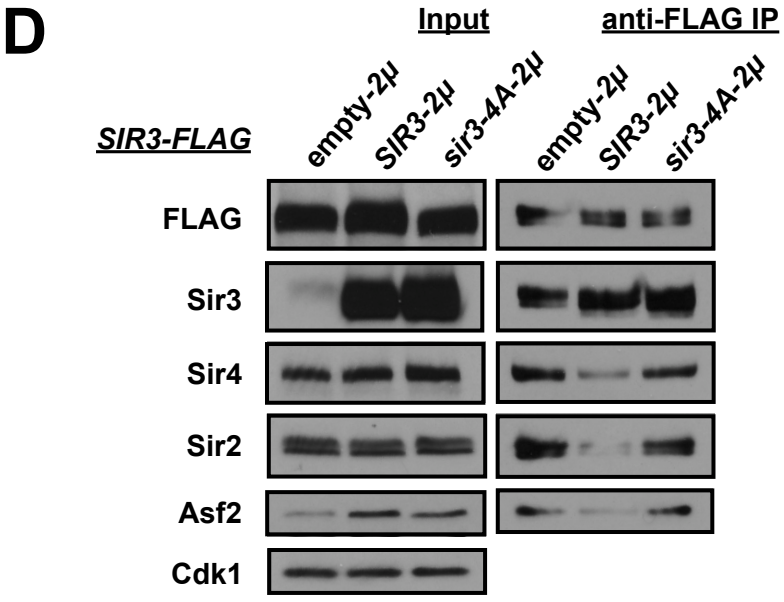
D
Input
anti-FLAG IP
SIR3-FLAG
empty-2μ
SIR3-2μ
sir3-4A-2μ
FLAG
Sir3
Sir4
Sir2
Asf2
Cdk1

Figure 8. Sir3 residues 657-660 are required for the Sir3-Sir4 and Sir3-Asf2 interactions *in vivo*. (A) FLAG-tagged Sir3-2A, 3A, and 4A do not interact with Sir4. Untagged wild type Sir3, FLAG-tagged wild type Sir3, or FLAG-tagged Sir3-2A, 3A, or 4A were expressed in a strain lacking endogenous Sir3. FLAG-tagged wild type and mutant Sir3 were immunoprecipitated with an anti-FLAG antibody (Sigma). Immunoprecipitates were assessed by Western blot. **(B, C)** Untagged Sir3-4A expressed from either a *CEN* or a *2μ* plasmid does not interact with Sir4. Wild type Sir3 and Sir3-4A were expressed from *CEN* plasmids (B), or were overexpressed from *2μ* plasmids (C) in a strain lacking endogenous Sir3. Sir4 was immunoprecipitated with a polyclonal rabbit Sir4 antibody (Rudner Lab) and immunoprecipitates were assessed by Western blot. **(D)** Overexpressed Sir3, but not Sir3-4A, can compete with Sir3-FLAG for binding to Sir4. Wild type Sir3 and Sir3-4A were overexpressed from *2μ* plasmids in a strain expressing wild type FLAG-tagged Sir3 at endogenous levels. Immunoprecipitations were performed with an anti-FLAG antibody (Sigma), and immunoprecipitates were assessed by Western blot.

polyclonal Sir3 or Sir4 antibodies to perform co-immunoprecipitations in strains expressing untagged Sir3 or Sir3-4A. The overexpression of Sir3 or Sir3-4A from a 2μ plasmid produced an excess of the Sir3 protein, causing Sir4 levels to become limiting. Thus, detectable levels of Sir4 could not be co-precipitated with overexpressed, wild type Sir3 (data not shown). However, whether expressed from a *CEN* or 2μ plasmid, wild type Sir3, but not Sir3-4A, could be co-immunoprecipitated with Sir4 (Figure 8B,C). We also tested the ability of wild type Sir3 and Sir3-4A expressed from 2μ plasmids to compete with wild type Sir3-FLAG for binding to Sir4. Overexpression of wild type Sir3, but not the Sir3 mutant, noticeably reduced the levels of Sir4 that co-precipitated with wild type Sir3-FLAG in a FLAG-immunoprecipitation (Figure 8D), showing that when overexpressed, wild type Sir3, but not Sir3-4A, could titrate Sir4 away from wild type Sir3-FLAG. Taken together, these immunoprecipitations provide strong evidence that unlike wild type Sir3, Sir3-4A cannot interact with Sir4 *in vivo*.

To determine whether Sir3 residues 657-660 are required for the direct interaction of Sir3 with Sir4, a GST-tagged Sir4 fragment containing the known Sir3 binding site was immobilized on glutathione beads. When His-tagged Sir3 or Sir4-4A fragments were applied to the beads, only the wild type Sir3 co-eluted with Sir4-GST (Figure 9, experiment performed by Carole Doré). Sir4-M1307N is a mutation in the Sir3 binding-site of Sir4 that has previously been shown to block the Sir3-Sir4 interaction (Chang et al., 2003); as expected, GST-tagged Sir4-M1307N fragments were unable to interact with either the Sir3 or Sir3-4A fragments.

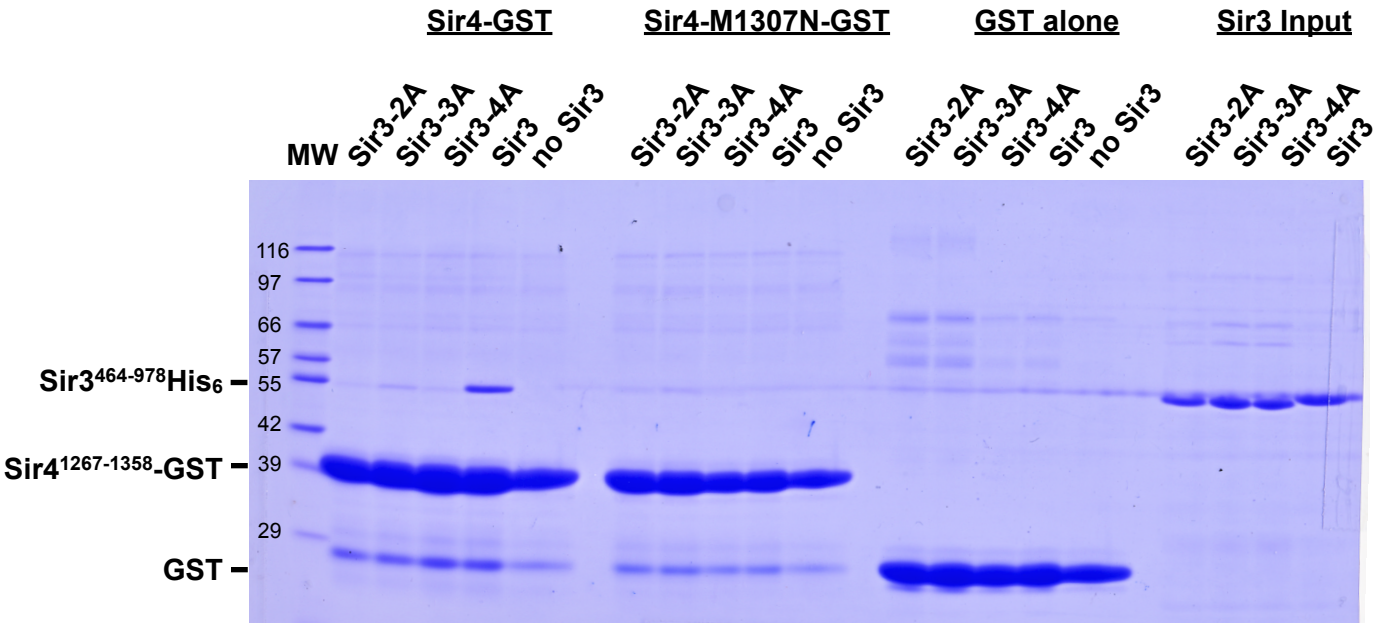
Sir4-GST
Sir4-M1307N-GST
GST alone
Sir3 Input
MW
Sir3-2A
Sir3-3A
Sir3-4A
Sir3
no Sir3
Sir3-2A
Sir3-3A
Sir3-4A
Sir3
no Sir3
Sir3-2A
Sir3-3A
Sir3-4A
Sir3
no Sir3
Sir3-2A
Sir3-3A
Sir3-4A
Sir3
116
97
66
57
55
42
39
29
Sir3464-978His6
Sir41267-1358-GST
GST

Figure 9. Sir3 residues 657-660 are required for the direct interaction of Sir3 with Sir4 *in vitro*. A GST-tagged $Sir4^{1267-1358}$ fragment containing a previously identified Sir3 binding site was incubated with glutathione resin and His_6-$Sir3^{464-978}$ or His_6-$Sir3^{464-978}$-2A, 3A, or 4A fragments. Elutates were analyzed by PAGE and Coomassie staining. Sir4-M1307N contains a mutation in the Sir4 binding site for Sir3 that prevents the Sir3-Sir4 interaction, serving as a negative control. Protein ladder gives molecular weight (MW) values in Kilodaltons. This experiment was performed by Carole Doré.

3.1.2 sir3-2A, 3A, and 4A mutants are insufficient for silent chromatin nucleation but do not block spreading in the presence of wild type Sir3

To determine whether the Sir3 mutants could nucleate telomeric and *HM* silent chromatin, we expressed these mutants in strains that lacked endogenous *SIR3*, but carried a *TRP1* reporter gene downstream of a weakened *HMR* silencer (*hmr*Δ*E::TRP1*) and a *URA3* reporter gene at *TELVII-L* (*TELVII-L::URA3*). The *TRP1* gene is required for tryptophan biosynthesis (Braus et al., 1991), thus reduced growth on media lacking tryptophan is indicative of silencing at *HMR*. In contrast, *URA3* encodes an enzyme that converts FOA into a toxic compound leading to cell death (Boeke et al., 1984), thus loss of growth on media containing FOA represents derepression of telomeric *URA3*. Whether expressed from a *CEN* or *2μ* plasmid, the Sir3 mutants were unable to compliment wild type Sir3 and initiate silencing at *HMR* or *TELVII-L* (Figure 10A). The FLAG-tagged Sir3 mutants were also unable to initiate silencing; interestingly, FLAG-tagged wild type Sir3 exhibited a slight deficiency in *HMR* but not *TELVII-L* silencing (Figure 10A), revealing that *SIR3-FLAG* cannot fully compliment untagged *SIR3*.

Sir3 is known to form dimers (Oppikofer et al., 2013b) and oligomers (Liou et al., 2005). Thus, it was possible that in the presence of wild type Sir3, the Sir3 mutants would exert a dominant negative effect by sequestering wild type Sir3 away from sites of silent chromatin nucleation and spreading. To test for a dominant negative phenotype, we expressed the Sir3 mutants in strains that also expressed wild type Sir3, and carried the *hmr*Δ*E::TRP1* and *TELVII-L::URA3* reporter genes. Silencing assays revealed that none of the untagged or FLAG-tagged Sir3 mutants expressed from *CEN* or *2μ* plasmids exerted a dominant negative effect on silencing (Figure 10B). However, in a strain with a *URA3* reporter gene located 1.0 kb from the end of *TELV-R*, Sir3-4A overexpression did cause a

A

sir3Δ HMR-E::AeB-TRP1
TELVII-L::URA3

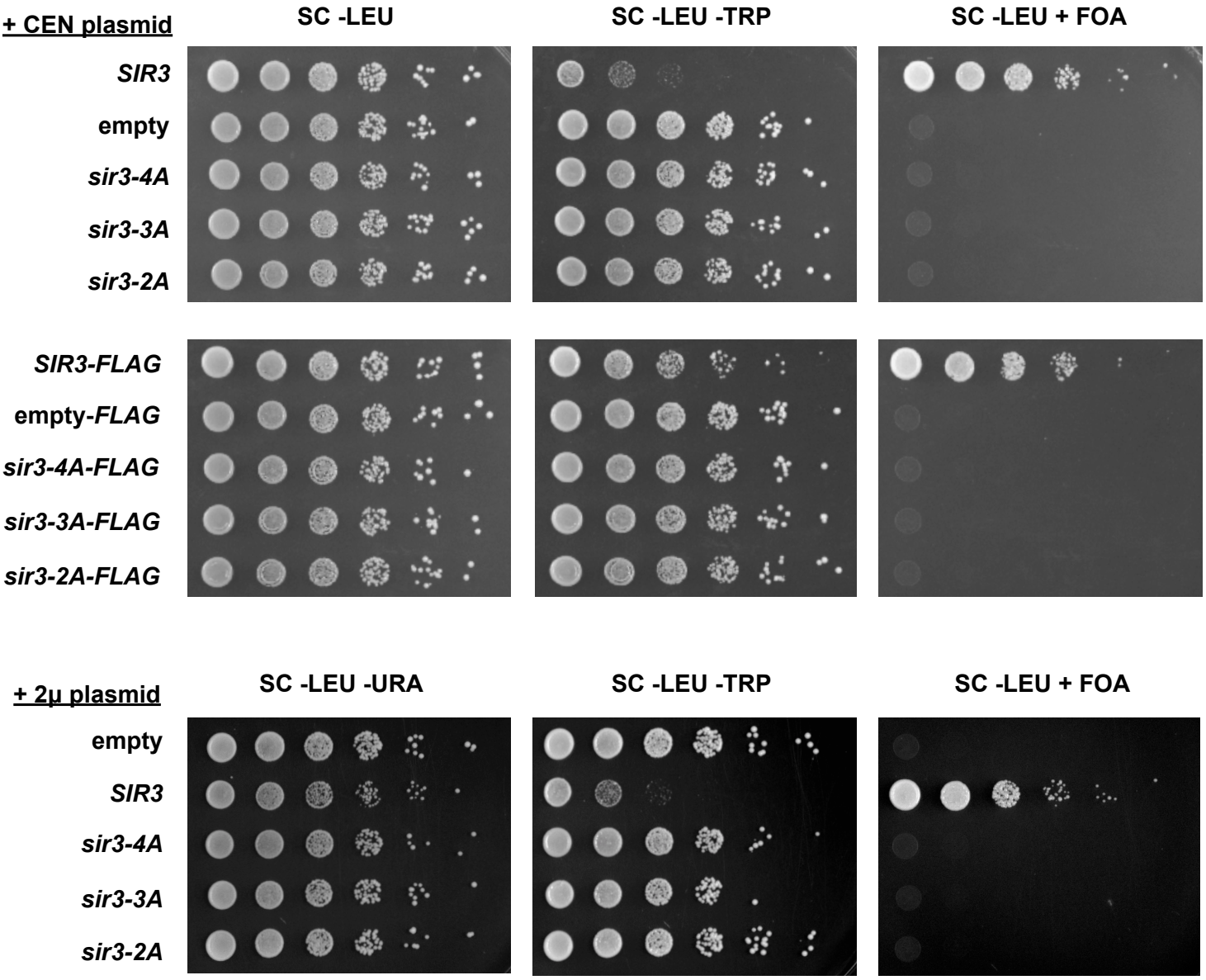

B

SIR3 HMR-E::AeB-TRP1
TELVII-L::URA3

+ CEN plasmid

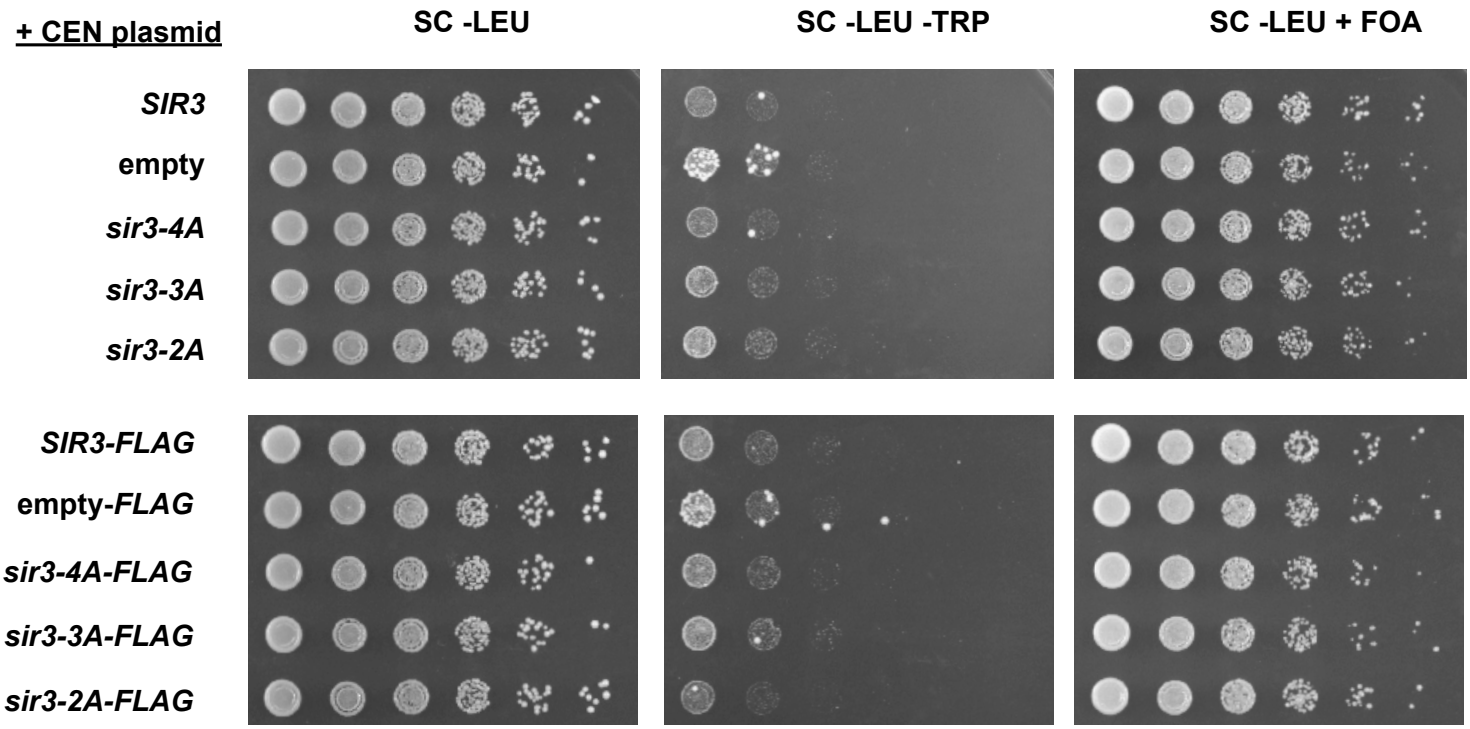

+ 2μ plasmid

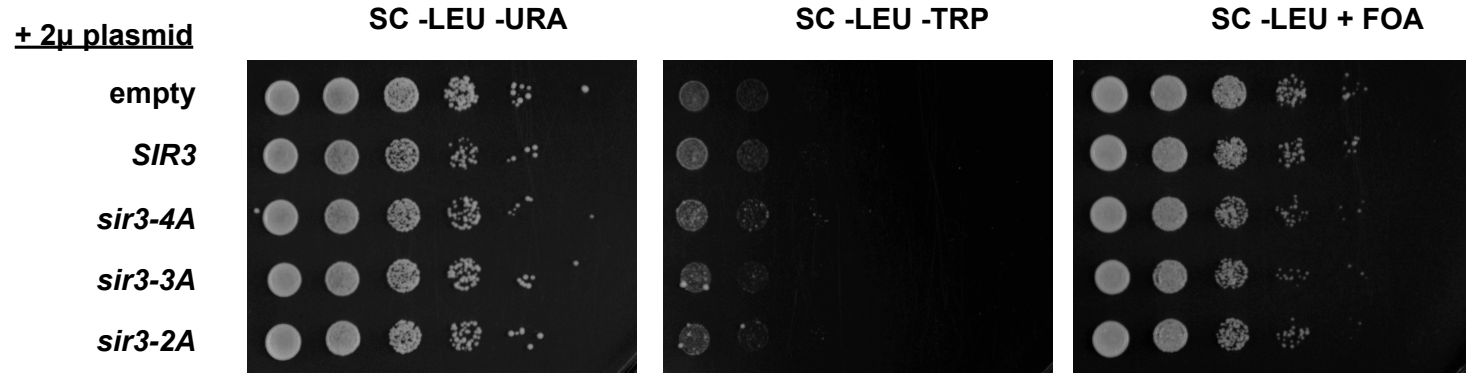

Figure 10. *sir3-2A*, *3A*, and *4A* mutants cannot nucleate silencing but do not interfere with silent chromatin spreading. **(A)** Sir3-2A, 3A, and 4A mutants cannot nucleate silencing. A *sir3Δ HMR::TRP1 TELVII-L::URA3* strain was transformed with *CEN* plasmids expressing FLAG-tagged or untagged *SIR3, sir3-2A, 3A,* or *4A,* or with *2μ* plasmids expressing untagged *SIR3, sir3-2A, 3A,* or *4A*. Ten-fold serial dilutions were spotted onto -LEU, -LEU -TRP, -LEU –URA, and –LEU FOA media to assess *HMR* and telomeric silencing. All media lacked leucine in order to maintain the transformed plasmids. **(B)** Sir3-2A, 3A, and 4A mutants do not exert a dominant negative effect on silencing. A *SIR3 HMR::TRP1 TELVII-L::URA3* strain was transformed with the plasmids described in (A) and silencing was assessed as in (A).

noticeable increase in growth on –URA media relative to a strain expressing only endogenous Sir3 (Figure 13A). Interestingly, this was not accompanied by a loss of viability of the Sir3-4A strain on FOA media. In a strain that can silence a *URA3* gene, lack of growth on –URA media represents the ability to stably maintain this silencing despite selection pressure for transcriptional activation of *URA3.* Thus, overexpression of Sir3-4A had a small negative impact on silent chromatin stability 1.0 kb from *TELV-R* but did not prevent silencing of the 1.0 kb *URA3* gene in the presence of FOA.

3.1.3 Overexpressing a Sir3 mutant that cannot bind Sir4 extends telomeric silent chromatin domains

To investigate the role of the Sir3-Sir4 interaction in silent chromatin spreading we next overexpressed either wild type Sir3 or Sir3-4A in strains carrying a *URA3* reporter gene at increasing distances from the end of *TELV-R*. These strains also expressed endogenous Sir3, to allow for the nucleation of silent chromatin. Silencing was assessed by viability on FOA both qualitatively (Figures 11 and 13) and quantitatively (Harding, 2014, unpublished data). Overexpressing any of the Sir3 mutants caused silent chromatin to spread to a similar extent as that observed when wild type Sir3 was overexpressed, albeit with a lower silencing efficiency (as measured by viability on FOA) (Figures 11 and 13). At 1.0 kb from *TELV-R*, strains overexpressing Sir3-4A were also less able to maintain silencing on –URA media than strains overexpressing Sir3 (Figure 13).

A quantitative analysis of silencing efficiency (Harding 2014, unpublished data) revealed that strains overexpressing Sir3 and strains overexpressing Sir3-4A could both silence a telomeric *URA3* gene up to 6.5 kb from the end of *TELV-R*, although silencing efficiency in the Sir3-4A strain was approximately 10-fold lower than that of the Sir3 strain

TELV-R::URA3 PPR1+

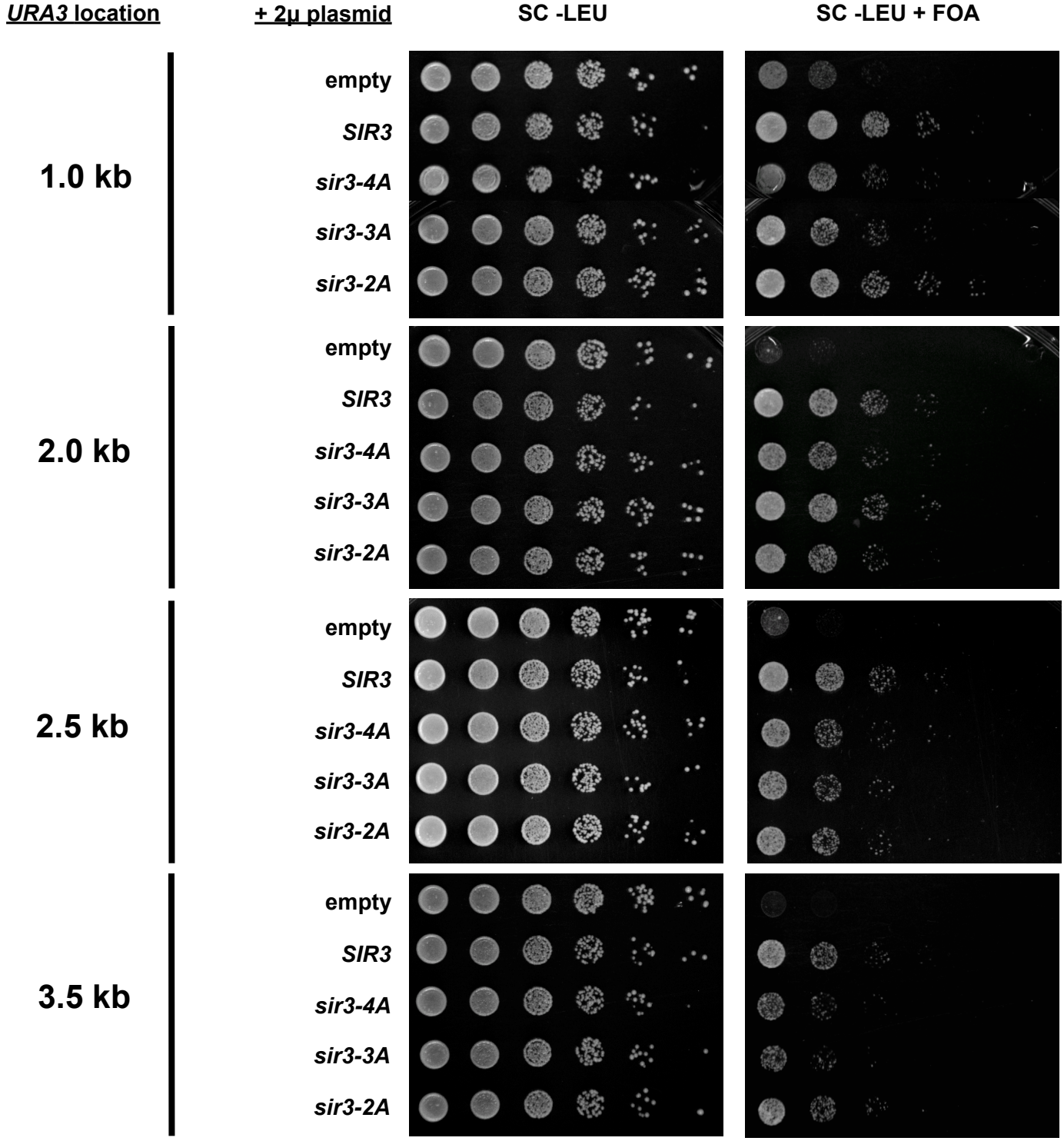

Figure 11. Sir3 and Sir3-4A mediate similar extension of silent chromatin domains. *SIR3 PPR1* strains with a *URA3* reporter gene located at 1.0, 2.0, 2.5, or 3.5 kb from the end of a modified *TELV-R* lacking a Y' element were transformed with an empty *2μ* plasmid, or *2μ* plasmids expressing *SIR3, sir3-2A, 3A,* or *4A*. Ten-fold serial dilutions were plated on –LEU and –LEU FOA media to assess silencing.

at all *URA3* loci tested. This difference in silencing efficiency was reduced by deleting Ppr1, a trans-activator of the *URA3* gene that competes with the Sir protein machinery during silent chromatin formation along a telomere containing *URA3* (Renauld et al., 1993).

3.2 Characterizing extended silent chromatin regions in epigenetically bistable OFF and ON silent chromatin states

Overexpressing either Sir3 or Sir3-4A causes a similar extension of silent chromatin domains, suggesting that a Sir3 mutant that cannot bind Sir4 may be able to mediate and participate in silent chromatin spreading. This would be possible if silent chromatin could spread either entirely in the absence of Sir4, as suggested by Strahl-Bolsinger et al (1997), or independently of the Sir3-Sir4 interaction. To characterize the architecture of the extended silent chromatin domains formed upon overexpression of Sir3 or Sir3-4A, we performed chromatin immunoprecipitation (ChIP) of the Sir proteins and histone marks in these regions.

3.2.1 Growth in selective media enriches for a cell population with transcriptional silencing or activation of a telomeric URA3 reporter gene

In a normal population of cells, sub-telomeric regions are silenced and expressed stochastically, an effect known as telomere position effect (TPE) (Figure 12) (Gottschling et al., 1990). Since our aim was to specifically analyze protein enrichment at silenced telomeres, we first isolated cells with transcriptionally silenced telomeres by adapting a method previously described (Kitada et al., 2012): Strains with a telomeric *URA3* reporter gene located either 1.0 kb or 5.5 kb from the end of *TELV-R* were grown in media containing FOA to select for silencing of the *URA3* gene prior to fixation and chromatin immunoprecipitation. We separately analyzed Sir protein enrichment along *TELV-R* in

A

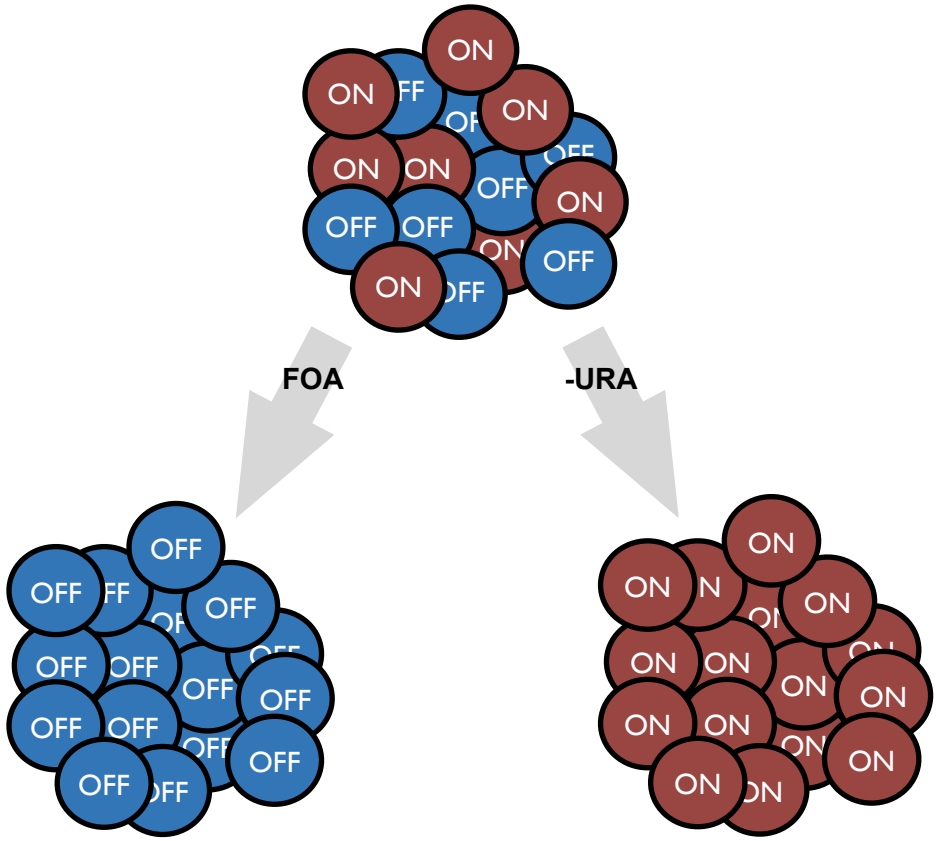

B

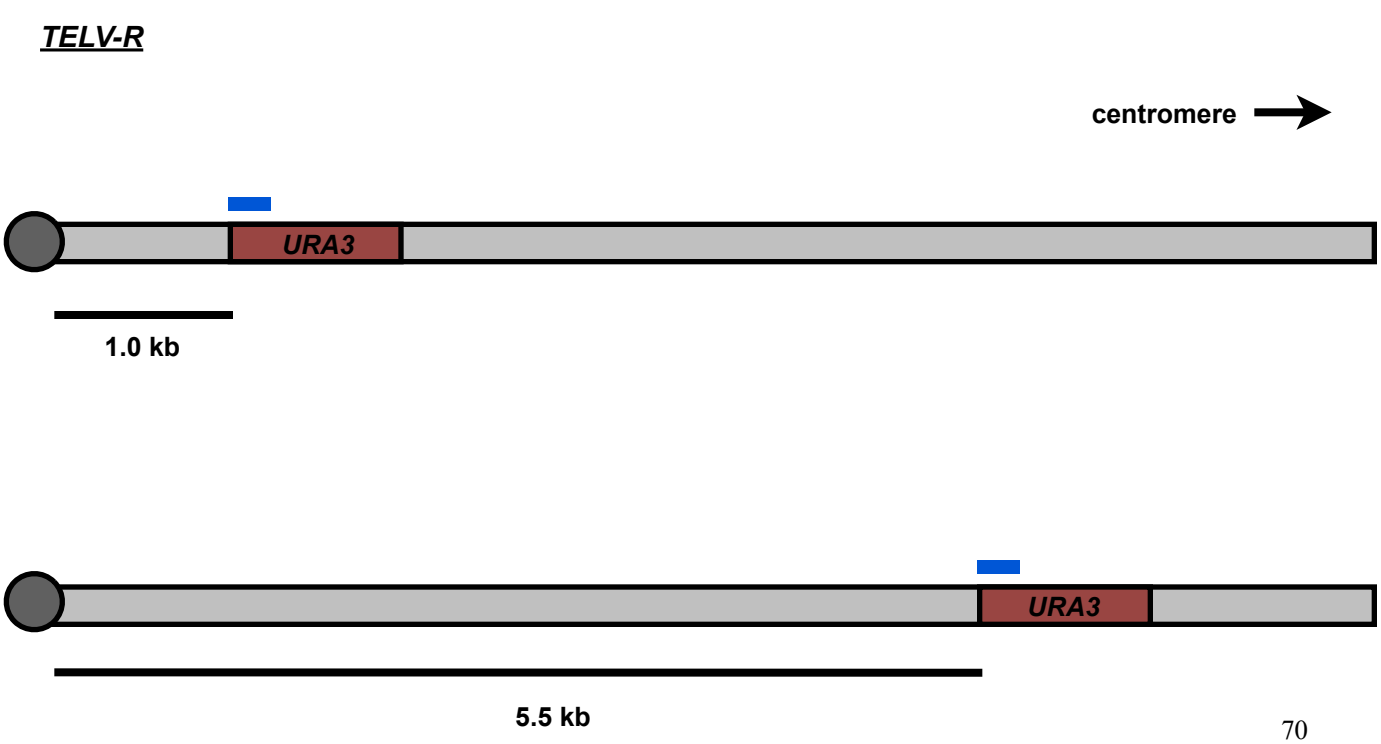

Figure 12. A method to enrich for cells with an activated or silenced telomeric *URA3* gene. (A) Strains with a telomeric *URA3* gene and that overexpressed either *SIR3* or *sir3-4A* were grown either in media containing FOA, to select for silencing of the *URA3* gene, or in –URA media, to select for *URA3* activation. Figure adapted from Kitada et al., 2012. **(B)** Strains used contain a *URA3* reporter gene under the control of its own promoter located either 1.0 or 5.5 kb from the end of *TELV-R.* The Y' element of *TELV-R* has been deleted in these strains but all other structural elements of this telomere remain intact. The *URA3* transactivator *PPR1* was also deleted in these strains (Renauld et al., 1993). Grey circle represents the G tail at the end of *TELV-R*. Blue bar denotes approximate location of qPCR probe. Diagram not to scale.

strains grown in media lacking uracil to select for transcriptional activation of the *URA3* reporter gene (Figure 12). To confirm that growth in the appropriate selective media enriched for cells with either activated or silenced *TELV-R URA3*, serial dilutions of the cultures were plated on media lacking uracil or media containing FOA to assess silencing (Figure 13). At the 1.0 kb *URA3* locus in strains overexpressing Sir3-4A, and at the 5.5 kb *URA3* locus in strains overexpressing either Sir3 or Sir3-4A, selection for silencing by FOA imparted a small but definite increase in silencing efficiency relative to the same strains grown in nonselective (SC -LEU) media. These improvements in silencing are indicated by the increased viability on FOA observed in row 7 relative to row 5 in the upper panel of Figure 13, and in rows 7 and 8 relative to rows 5 and 6 in the lower panel. The increase in silencing efficiency is especially notable at the 1.0 kb locus in strains overexpressing Sir3-4A (Figure 13, upper panel, row 7), where growth in FOA abolished the difference in silencing efficiency in strains overexpressing Sir3 and Sir3-4A.

In strains overexpressing wild-type Sir3, FOA selection also resulted in a slight increase in silencing stability at both the 1.0 kb and 5.5 kb *URA3* loci, as indicated by the reduced viability on SC –URA media in row 8 relative to row 6 in both the upper and lower panels of Figure 13. However, no discernable change in stability was observed in the strains overexpressing Sir3-4A (Figure 13). Growth in media lacking uracil led to an almost complete loss of telomeric silencing efficiency and stability at both loci, whether Sir3 or Sir3-4A was overexpressed (Figure 13).

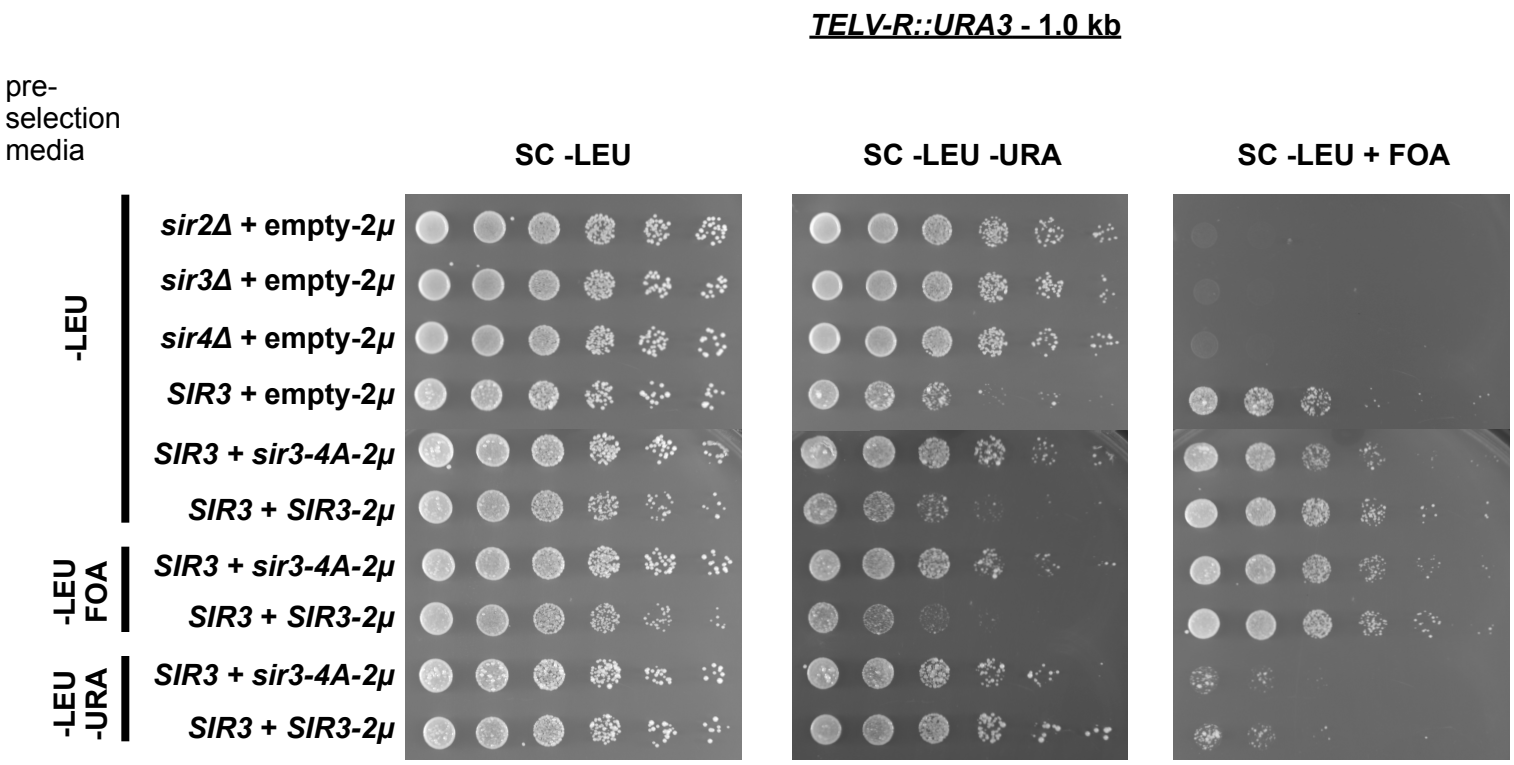
TELV-R::URA3 - 1.0 kb
pre-selection media
SC -LEU
SC -LEU -URA
SC -LEU + FOA
-LEU
-LEU FOA
-LEU -URA
sir2Δ + empty-2μ
sir3Δ + empty-2μ
sir4Δ + empty-2μ
SIR3 + empty-2μ
SIR3 + sir3-4A-2μ
SIR3 + SIR3-2μ
SIR3 + sir3-4A-2μ
SIR3 + SIR3-2μ
SIR3 + sir3-4A-2μ
SIR3 + SIR3-2μ

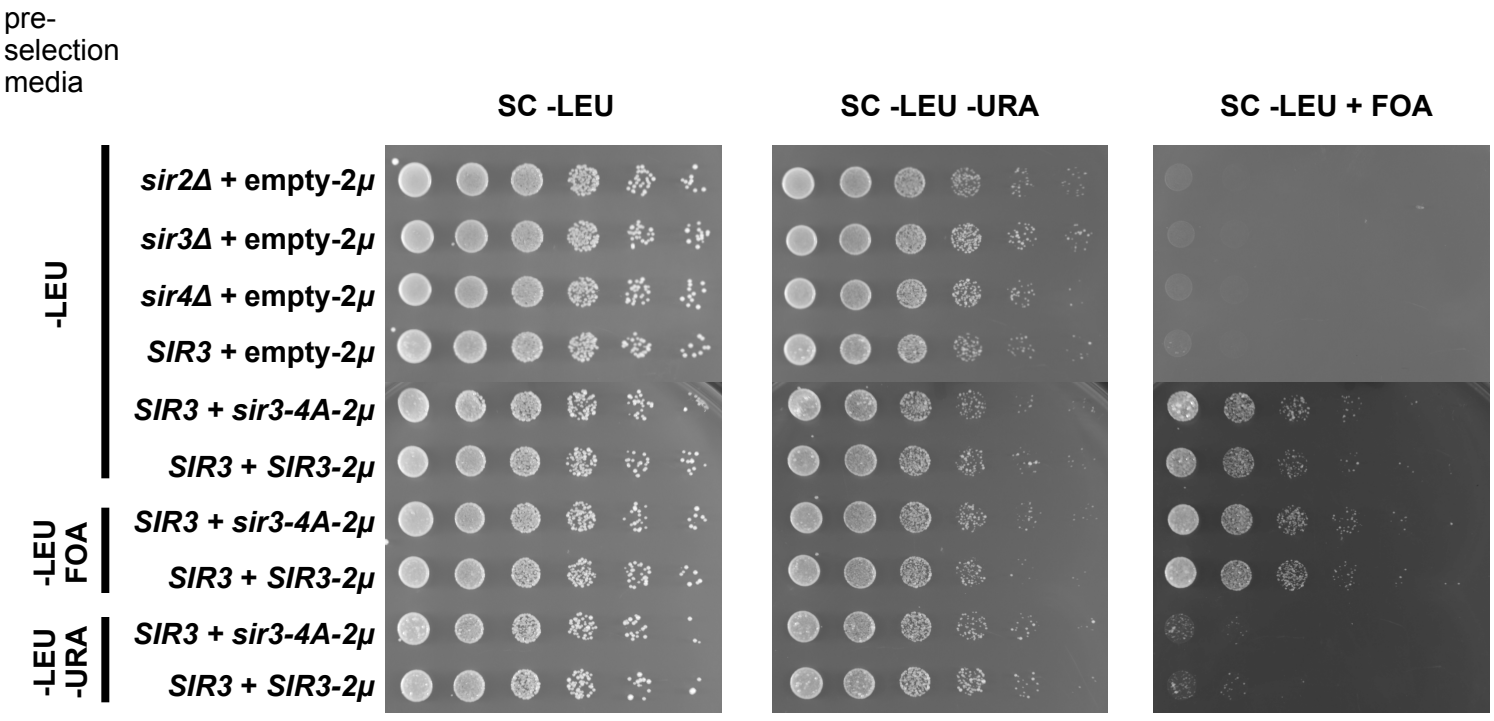
TELV-R::URA3 - 5.5 kb
pre-selection media
SC -LEU
SC -LEU -URA
SC -LEU + FOA
-LEU
-LEU FOA
-LEU -URA
sir2Δ + empty-2μ
sir3Δ + empty-2μ
sir4Δ + empty-2μ
SIR3 + empty-2μ
SIR3 + sir3-4A-2μ
SIR3 + SIR3-2μ
SIR3 + sir3-4A-2μ
SIR3 + SIR3-2μ
SIR3 + sir3-4A-2μ
SIR3 + SIR3-2μ

Figure 13. Selection for transcriptional silencing or activation of a *URA3* reporter gene near *TELV-R*. Strains described in Figure 12, with a *URA3* gene located either **(A)** 1.0 or **(B)** 5.5 kb from the end of *TELV-R* were transformed with empty, *SIR3*, or *sir3-4A 2μ* plasmids and grown in the pre-selection media indicated in the left panel. Pre-selection comprised three days growth on the indicated agar media, followed by two days of growth in the same type of liquid media at 30°C. FOA agar media contained 1g/L FOA and an additional 25mg/L uracil, while FOA liquid media contained 10mg/L FOA. Ten-fold serial dilutions of each culture were spotted on –LEU, –LEU –URA, and –LEU FOA media to assess silencing. All media lacked leucine in order to maintain plasmids.

3.2.2 Sir2, Sir3, and Sir4 spread similarly along silenced telomeres whether Sir3 or Sir3-4A is overexpressed

Using chromatin immunoprecipitation, we measured Sir protein enrichment at a *URA3* gene located either 1.0 or 5.5 kb from *TELV-R* that was silenced by growing strains overexpressing either Sir3 or Sir3-4A in media containing FOA (blue bars in Figures 14-17). Selection for silencing or activation of the telomeric *URA3* gene was not performed in control strains lacking a Sir protein or expressing endogenous levels of Sir3 (grey bars in Figures 14 – 17), due to the inability of the delete strains and the 5.5 kb *URA3* endogenous strain to silence telomeric *URA3* and grow on media containing FOA. In strains expressing only endogenous levels of Sir proteins, significant levels of Sir2 and Sir4 were detected 1.0 kb from *TELV-R* but not at the 5.5 kb locus, and Sir3 levels at the 5.5 kb locus were significant but very low relative to that at the 1.0 kb locus (Figure 14, Tables S2.1 - S2.6). Overexpressing Sir3 or Sir3-4A increased Sir2, Sir3, and Sir4 enrichment at the distal silent locus, and also caused a reduction in Sir3 enrichment at the silenced 1.0 kb locus relative to the endogenous strains (Figure 14, Tables S2.1 - S2.6). Interestingly, in no case was Sir2, Sir3, or Sir4 enrichment at any locus significantly different between Sir3 and Sir3-4A strains (Figure 14, Tables S2.1 - S2.6).

3.2.3 Low levels of Sir protein enrichment are detected at active telomeres

Several studies report significant levels of Sir3 at transcriptionally active telomeres (Kitada et al., 2012, Sperling et al., 2009) and at actively transcribed euchromatic genes (Radman-Livaja et al., 2011). We therefore also measured Sir protein enrichment in strains overexpressing either Sir3 or Sir3-4A and carrying a telomeric *URA3* gene that was transcriptionally activated by growth in –URA media (red bars in Figures 14-17). While Sir

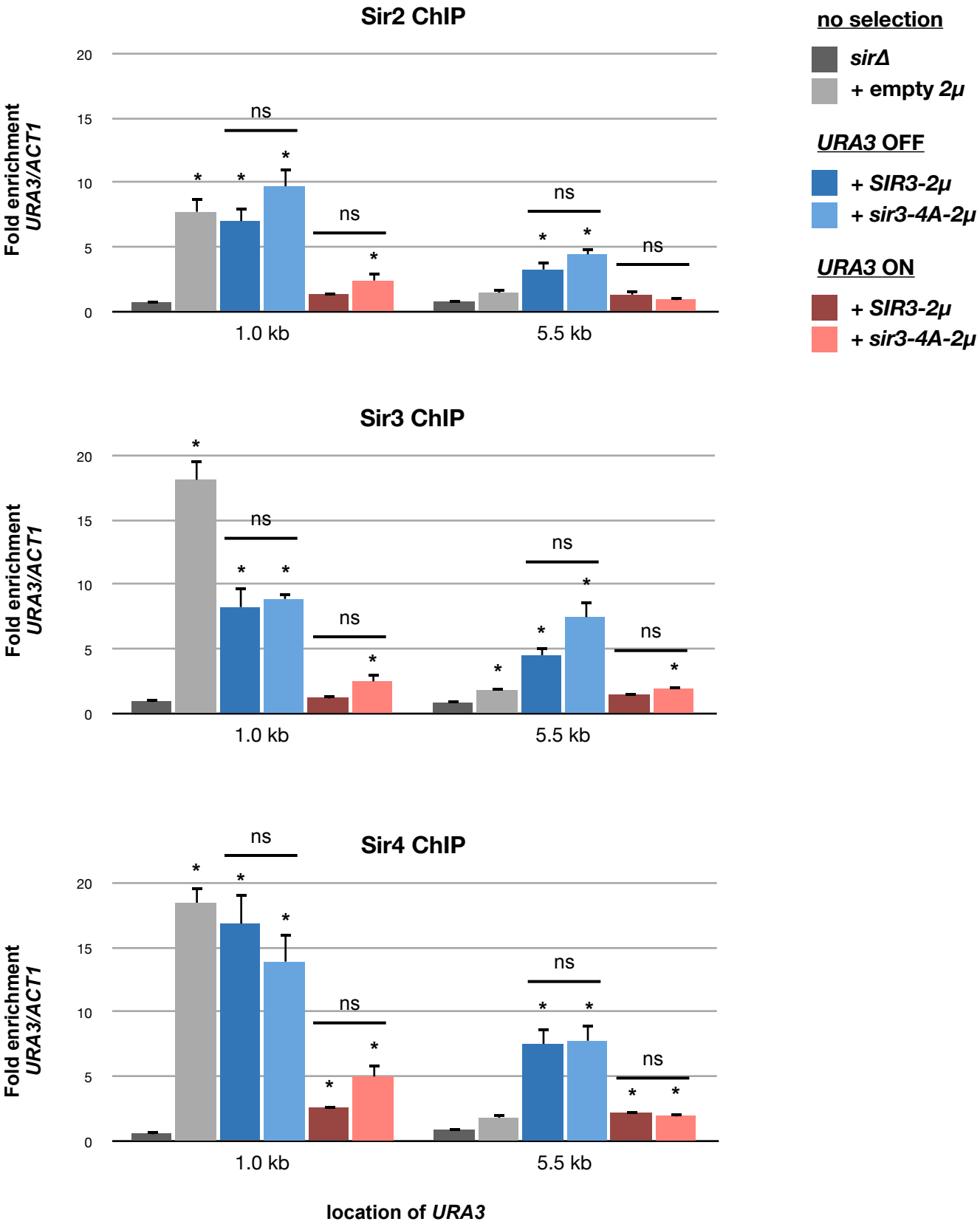
Sir2 ChIP
Sir3 ChIP
Sir4 ChIP
Fold enrichment URA3/ACT1
20
15
10
5
0
ns
*
1.0 kb
5.5 kb
location of URA3
no selection
sirΔ
+ empty 2μ
URA3 OFF
+ SIR3-2μ
+ sir3-4A-2μ
URA3 ON
+ SIR3-2μ
+ sir3-4A-2μ

Figure 14. Sir3 and Sir3-4A-mediated Sir protein spreading along active and silent telomeres. Strains described in Figures 12 and 13 with a *URA3* gene located either 1.0 kb or 5.5 kb from *TELV-R* were transformed with empty, *SIR3*, or *sir3-4A 2μ* plasmids. Strains overexpressing Sir3 or Sir3-4A were grown in –LEU FOA media (blue bars) or –LEU –URA media (red bars) as described in Figures 12 and 13 to respectively select for transcriptional silencing or activation of the telomeric *URA3* gene. Control strains that lacked a Sir protein or expressed endogenous levels of Sir2, Sir3, and Sir4 were grown in –LEU media (grey bars) and were not selected for *URA3* activation or silencing. ChIP was performed using polyclonal Sir2, Sir3, or Sir4 antibodies to measure Sir protein enrichment at the *URA3* loci. For each ChIP sample, Sir protein enrichment was normalized to the corresponding input sample, and enrichment at *URA3* was normalized to that at a euchromatic *ACT1* locus. Values represent the averages of three or more samples, with error bars representing standard errors of the means. Asterisks represent statistically significant levels of Sir protein enrichment ($p < 0.05$) relative to a *sirΔ* control (dark grey bar); ns: not statistically significant for the comparison indicated by the horizontal bar. Detailed statistical analysis can be found in tables S2.1 - S2.6.

protein enrichments at the active *URA3* locus were very low, some significant enrichments were detected (Figure 14, Tables S2.1 - S2.6). At both 1.0 kb and 5.5 kb from *TELV-R*, Sir4 was significantly enriched whether Sir3 or Sir3-4A was overexpressed. However, in strains overexpressing wild type Sir3, no significant enrichment of Sir2 or Sir3 was detected at an active *URA3* gene either 1.0 kb or 5.5 kb from the telomere. Strains overexpressing Sir3-4A showed enrichment at the 1.0 kb active *URA3* locus for low but significant levels of Sir2 and Sir3, and at the 5.5 kb locus for low but significant levels of Sir3. However, statistical comparisons between the Sir3 and Sir3-4A strains revealed no significant differences for enrichments of any of the Sir proteins (Tables S2.1 - S2.6).

3.2.4 Transcriptional activation of URA3, but not the ability of overexpressed Sir3 to interact with Sir4, affects Sir protein enrichment along telomeres

Two-way ANOVAs were performed comparing the effects of the Sir3 genotype (wild type Sir3 or Sir3-4A) and growth media (FOA media or –URA media) in strains overexpressing Sir3. At both 1.0 kb and 5.5 kb, Sir3 genotype was not found to have a significant effect on Sir2 and Sir4 enrichment (Tables S2.1, S2.2, S2.5, S2.6 b,c). Analysis by 2-way ANOVA revealed that Sir3 genotype did have a mildly significant overall effect on Sir3 enrichment at both loci (Tables S2.3b, S2.4b), however no specific significant differences in the Sir3 enrichment of Sir3 and Sir3-4A strains were detected by post-hoc comparisons (Tables S2.3c, S2.4c). Thus, Sir3-4A mutation does not appear to significantly affect Sir protein enrichment in any of the conditions tested. In contrast to genotype, the 2-way ANOVA analysis revealed that growth media had a highly significant overall effect on all Sir protein enrichments at both the 1.0 kb and 5.5 kb *URA3* loci (Tables S2.1 - 2.6b). This was confirmed by post-hoc comparisons, which showed that for each Sir protein and

telomeric locus tested, enrichment at a transcriptionally silenced *URA3* gene was significantly greater than enrichment at the corresponding active locus (Tables S2.1 - S2.6c)

3.2.5 Controlling for nucleosome occupancy does not significantly alter patterns of telomeric Sir protein enrichment

Transcriptional activation is known to reduce nucleosome occupancy (Kitada et al., 2012), which could influence the difference in Sir protein enrichment we observed at active and silenced telomeres. Indeed, chromatin immunoprecipitation revealed significantly higher H3 occupancy at a silenced or nonselected 1.0 kb *URA3* locus relative to *sir3Δ* and *sir4Δ* controls (Figure 15 and Table S2.7). Two-way ANOVA analysis revealed a significant overall effect of *URA3* activation on H3 enrichment at the 1.0 kb locus (Table S2.7b). At the 5.5 kb *URA3* locus, no significant differences in H3 enrichment were detected for strains of any genotype or selection (Figure 15 and Table S2.8). H3 enrichment also did not differ significantly between Sir3 and Sir3-4A strains at either locus (Figure 15, Tables S2.7 and S2.8). Since H3 occupancy appears to correlate with silencing, we next examined whether this relationship could account for the significant reduction of Sir protein enrichment at active *URA3* relative to that at silenced *URA3*. To measure Sir protein enrichment (or H3K79me or H4K16ac enrichment, see section 3.2.6) relative to that of H3, individual lysate samples were separated into equal aliquots, which were concomitantly subjected to immunoprecipitation of H3 and the proteins of interest. Upon normalization to H3 occupancy, trends for Sir protein enrichment remained similar to those described in Sections 3.2.2 – 3.2.4 (Figure 16, Tables S2.9 – S2.14), although Sir4 enrichment at the active 5.5 kb *URA3* locus was no longer significant. Following H3 normalization, statistical analysis did not reveal any overall effect of *SIR3* genotype on Sir4 or Sir2 enrichment, or any specific

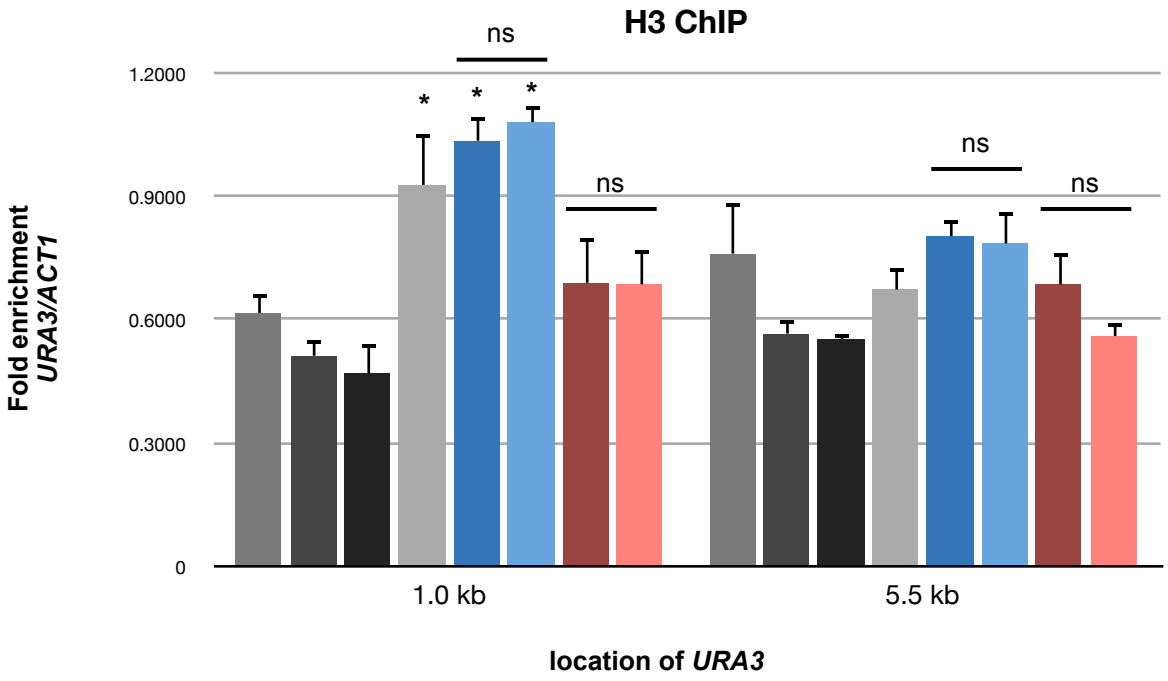
H3 ChIP
Fold enrichment
URA3/ACT1
1.2000
0.9000
0.6000
0.3000
0
ns
ns
ns
ns
*
*
*
1.0 kb
5.5 kb
location of URA3
no selection
sir2Δ
sir3Δ
sir4Δ
+ empty 2μ
URA3 OFF
+ SIR3-2μ
+ sir3-4A-2μ
URA3 ON
+ SIR3-2μ
+ sir3-4A-2μ

Figure 15. H3 occupancy correlates with telomere silencing. Strains described in Figures 12 and 13 with a *URA3* gene located either 1.0 kb or 5.5 kb from *TELV-R* were transformed with empty, *SIR3*, or *sir3-4A 2μ* plasmids. Strains were grown as described in Figures 12-14 and ChIP was performed using an H3 antibody. For each ChIP sample, H3 enrichment was normalized to the corresponding input sample, and enrichment at *URA3* was normalized to that at a euchromatic *ACT1* locus. Values represent the averages of three or more samples, with error bars representing standard errors of the means. Asterisks represent statistically significant levels of H3 enrichment ($p < 0.05$) relative to a *sir3Δ* control; ns: not statistically significant for the comparison indicated by the horizontal bar. Detailed statistical analysis can be found in tables S2.7 - S2.8.

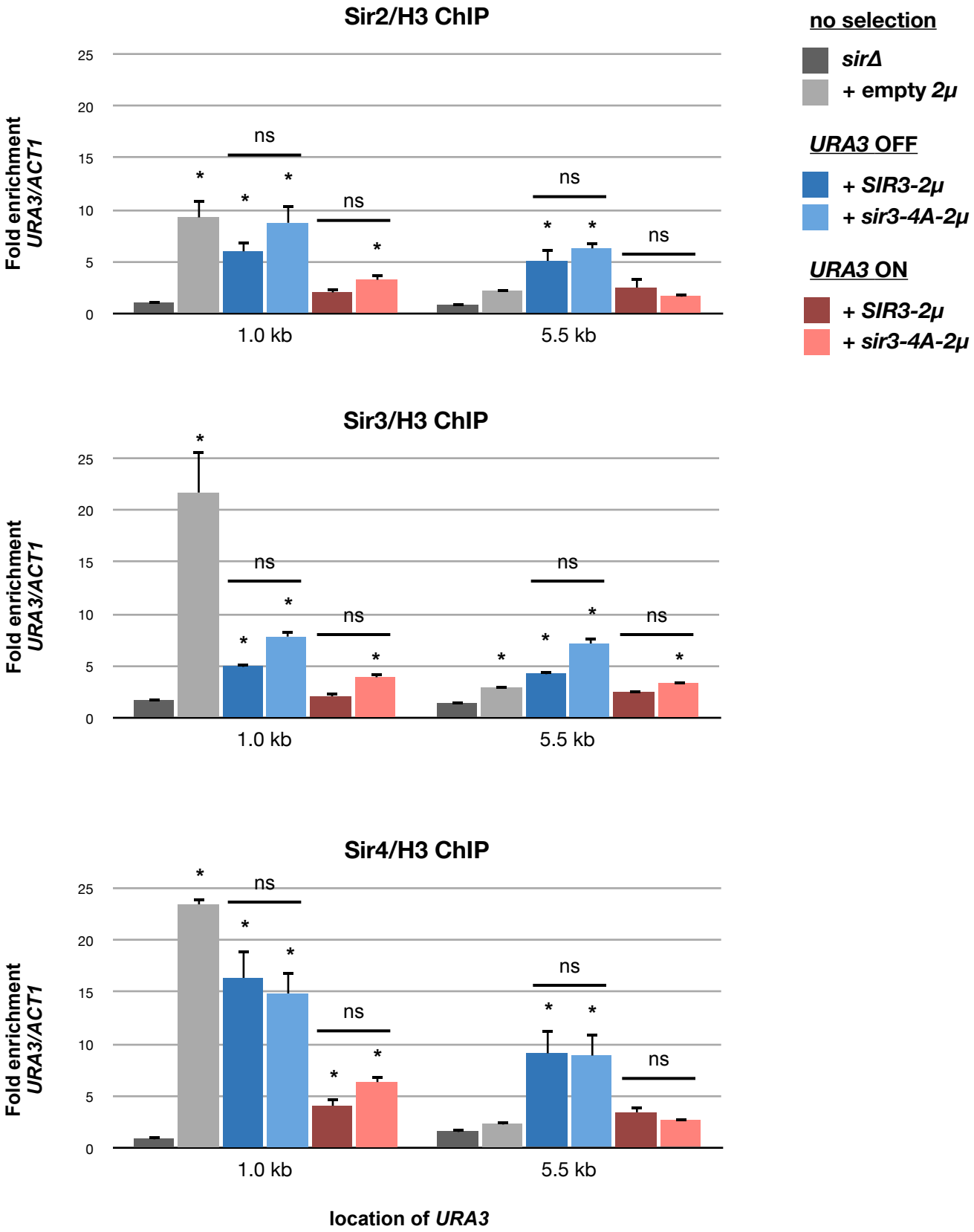
Sir2/H3 ChIP
Sir3/H3 ChIP
Sir4/H3 ChIP
Fold enrichment URA3/ACT1
25
20
15
10
5
0
ns
*
1.0 kb
5.5 kb
location of URA3
no selection
sirΔ
+ empty 2μ
URA3 OFF
+ SIR3-2μ
+ sir3-4A-2μ
URA3 ON
+ SIR3-2μ
+ sir3-4A-2μ

Figure 16. Controlling for H3 occupancy does not alter overall trends of Sir protein spreading. Strains described in Figures 12 and 13 with a *URA3* gene located either 1.0 kb or 5.5 kb from *TELV-R* were transformed with empty, *SIR3*, or *sir3-4A 2μ* plasmids. Strains were grown as described in Figures 12-14 and ChIP of was performed using Sir2, Sir3, Sir4, and H3 antibodies. For each ChIP sample, Sir protein and H3 enrichment was normalized to the corresponding input sample, and enrichment at *URA3* was normalized to that at a euchromatic *ACT1* locus. The Sir protein enrichment of each ChIP sample was further normalized to the H3 enrichment of that sample. Values represent the averages of three or more samples, with error bars representing standard errors of the means. Asterisks represent statistically significant levels of Sir protein enrichment ($p < 0.05$) relative to a *sirΔ* control; ns: not statistically significant for the comparison indicated by the horizontal bar. Detailed statistical analysis can be found in tables S2.9 - S2.14

effect of *SIR3* genotype on Sir protein enrichment (Tables S2.9 – S2.14). H3 normalization did not abolish the significant overall effect of *URA3* activation on Sir protein enrichment for all Sir proteins at both the 1.0 kb and 5.5 kb *URA3* loci, and the specific effect of *URA3* activation remained significant for all Sir proteins at the 1.0 kb *URA3* locus in strains overexpressing wild-type Sir3 (Tables S2.9 – S2.14).

3.2.6 Sir3 and Sir3-4A mediated silent chromatin extension results in similar H4K16 deacetylation and loss of H3K79 methylation

H3K79 mono, di, and trimethylation and H4K16 acetylation are important marks of active transcription that disrupt Sir-nucleosome interactions (Carmen et al., 2002; Onishi et al., 2007; Armache et al., 2011). The loss of H3K79 methylation correlates especially well with silencing (Kitada et al., 2012). In order to compare the effect of Sir3 and Sir3-4A overexpression on chromatin architecture, these histone modifications were also examined by ChIP. Pan-H3K79 methylation and H4K16 acetylation enrichment levels were normalized to H3 enrichment in order to control for differences in H3 occupancy.

As expected, endogenous levels of Sir3 were sufficient for significant loss of H3K79 methylation at the 1.0 kb but not at the 5.5 kb *URA3* locus, relative to a *sir3Δ* control. When silenced, both *URA3* loci were significantly demethylated, whether Sir3 or Sir3-4A was overexpressed. No significant loss of methylation was detected at the active *URA3* loci (Figure 17). Two-way ANOVA and post-hoc analysis revealed no significant effect of Sir3 mutation on H3K79 methylation levels (Tables S2.15 and S2.16). However, *URA3* activation was found to have an overall effect on H3K79 methylation (Tables S2.15 and S2.16). Unlike loss of H3K79 methylation, significant differences in the levels of H4K16 acetylation were not detected under any condition. However, at the 1.0 kb *URA3* locus in the endogenous Sir3

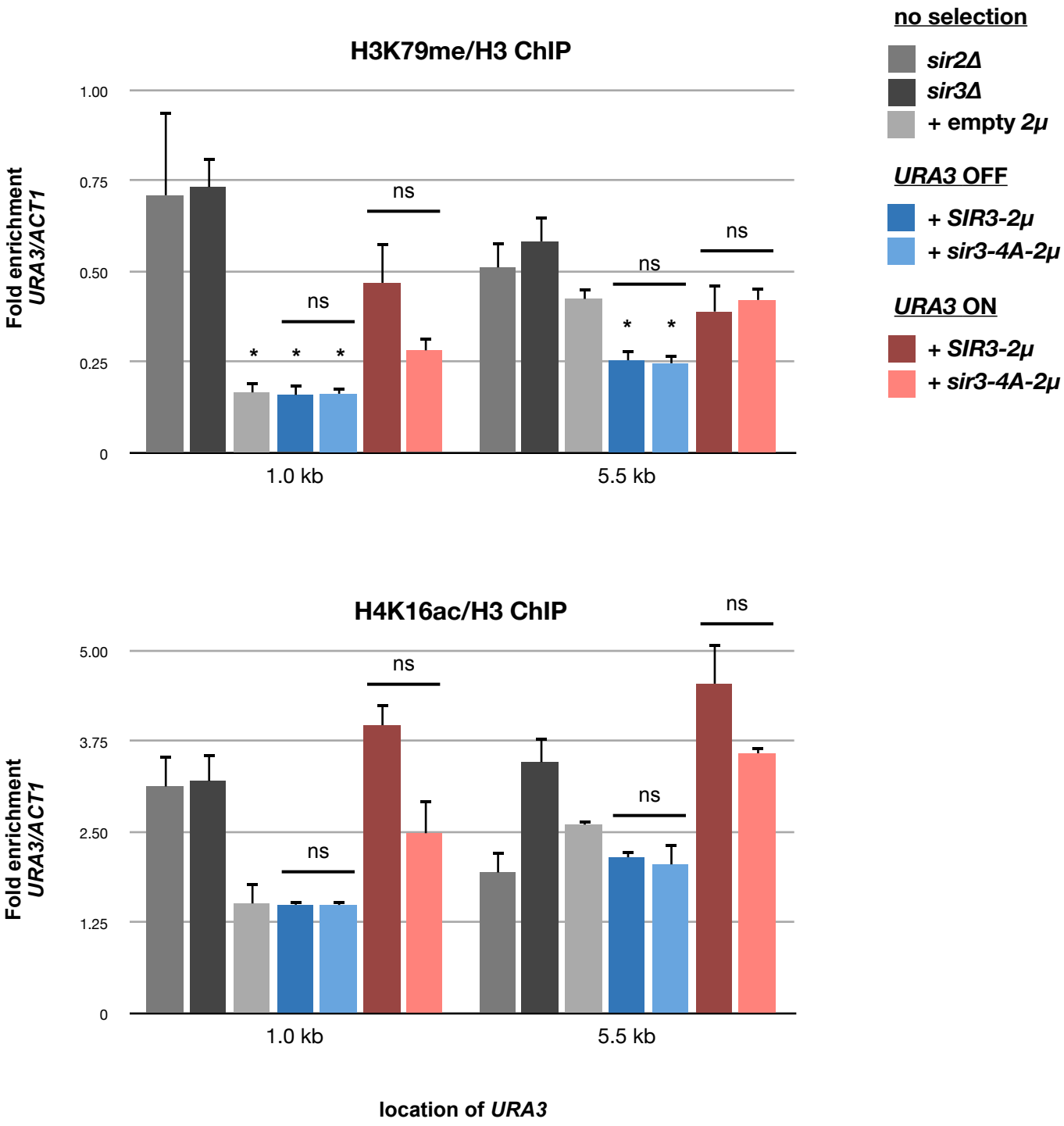
H3K79me/H3 ChIP
Fold enrichment URA3/ACT1
1.00
0.75
0.50
0.25
0
ns
ns
ns
ns
*
*
*
*
*
1.0 kb
5.5 kb
H4K16ac/H3 ChIP
Fold enrichment URA3/ACT1
5.00
3.75
2.50
1.25
0
ns
ns
ns
ns
1.0 kb
5.5 kb
location of URA3
no selection
sir2Δ
sir3Δ
+ empty 2μ
URA3 OFF
+ SIR3-2μ
+ sir3-4A-2μ
URA3 ON
+ SIR3-2μ
+ sir3-4A-2μ

Figure 17. Overexpression of Sir3 or Sir3-4A leads to H4K16 deacetylation and loss of H3K79 methylation along silenced but not active telomeres. Strains described in Figures 12 and 13 with a *URA3* gene located either 1.0 kb or 5.5 kb from *TELV-R* were transformed with empty, *SIR3*, or *sir3-4A 2μ* plasmids. Strains were grown as described in Figures 12-14 and ChIP of was performed using pan-H3K79me, H4K16ac, and H3 antibodies. For each ChIP sample, H3K79me, H4K16ac, and H3 enrichment was normalized to the corresponding input sample, and enrichment at *URA3* was normalized to that at a euchromatic *ACT1* locus. The H3K79me or H4K16ac enrichment of each ChIP sample was further normalized to the H3 enrichment of that sample. Values represent the averages of three or more samples, with error bars representing standard errors of the means. Asterisks represent statistically significant levels of Sir protein enrichment ($p < 0.05$) relative to a *sir3Δ* control; ns: not statistically significant for the comparison indicated by the horizontal bar. Detailed statistical analysis can be found in tables S2.15 - S2.18.

strain, and at both silenced *URA3* loci in the strains overexpressing Sir3 or Sir3-4A, H4K16ac levels were noticeably lower than that at activated *URA3* or at *URA3* in a *sir3Δ* control.

3.3 Tethering Sir3-4A to the *HMR* silencer is not sufficient to nucleate silent chromatin in the absence of wild type Sir3

The Sir3-Sir4 interaction is required to recruit Sir3 to the silencer (Rudner et al., 2005), however it is unclear whether this interaction has additional roles during silent chromatin nucleation. We therefore wondered whether tethering the Sir3-4A mutant to the silencer would be sufficient to bypass the requirement for the Sir3-Sir4 interaction in silent chromatin nucleation. The C-terminus of Sir3 or Sir3-4A was fused to LexA, a bacterial DNA-binding protein, and the Sir3-LexA fusions were expressed in yeast strains containing four LexA-binding sites (*lexops*) at a weakened *HMR-E::Aeb* silencer (Figure 18A). Since two of the three silencer elements of *HMR-E* were mutated, *HMR* silencing in this strain could only be nucleated by LexA-mediated tethering of Sir2 or Sir3 to the *HMR-E* silencer (Wu et al., 2011). The LexA tethering strains also carried a *Kluveromyces lactis URA3* gene 1.4 kb downstream of the *HMR* silencer (Figure 18A), allowing silencing to be assessed by viability on FOA.

The tethering strains were transformed with *lexA, SIR3-lexA,* or *sir3-4A-lexA 2μ* plasmids, the latter two of which expressed Sir3-LexA and Sir3-4A-LexA at similar levels to endogenous Sir3 (Figure 18B, experiment performed by Adam Rudner). In the presence of endogenous Sir3, both Sir3-LexA and Sir3-4A-LexA can nucleate silencing, however only Sir3-LexA can nucleate silencing in a strain lacking endogenous Sir3 (Figure 18C, experiment performed by Adam Rudner). Neither tethered Sir3 nor Sir3-4A were sufficient

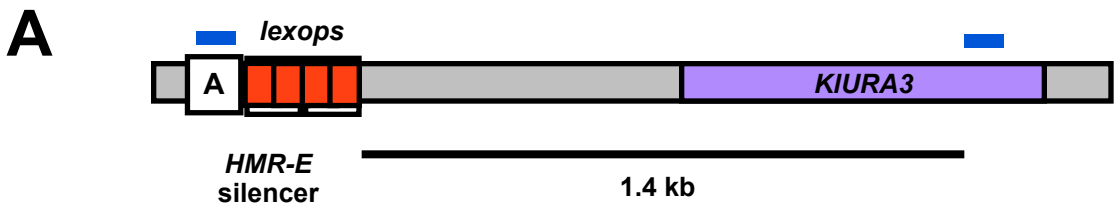
A
lexops
A
KlURA3
HMR-E
silencer
1.4 kb

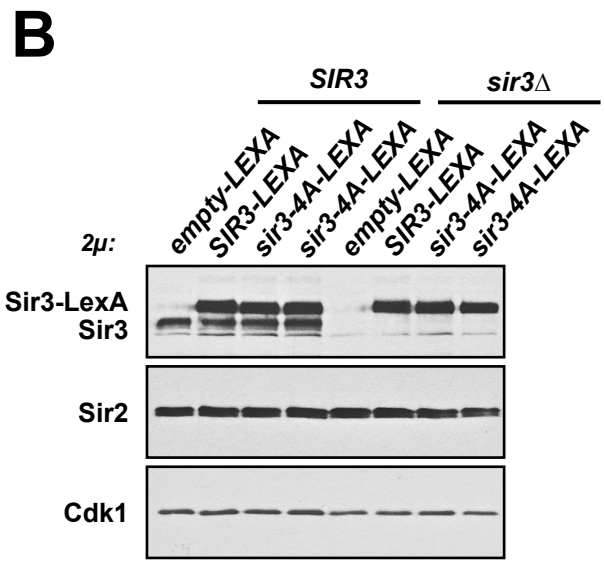
B
SIR3
sir3Δ
empty-LEXA
SIR3-LEXA
sir3-4A-LEXA
sir3-4A-LEXA
empty-LEXA
SIR3-LEXA
sir3-4A-LEXA
sir3-4A-LEXA
2μ:
Sir3-LexA
Sir3
Sir2
Cdk1

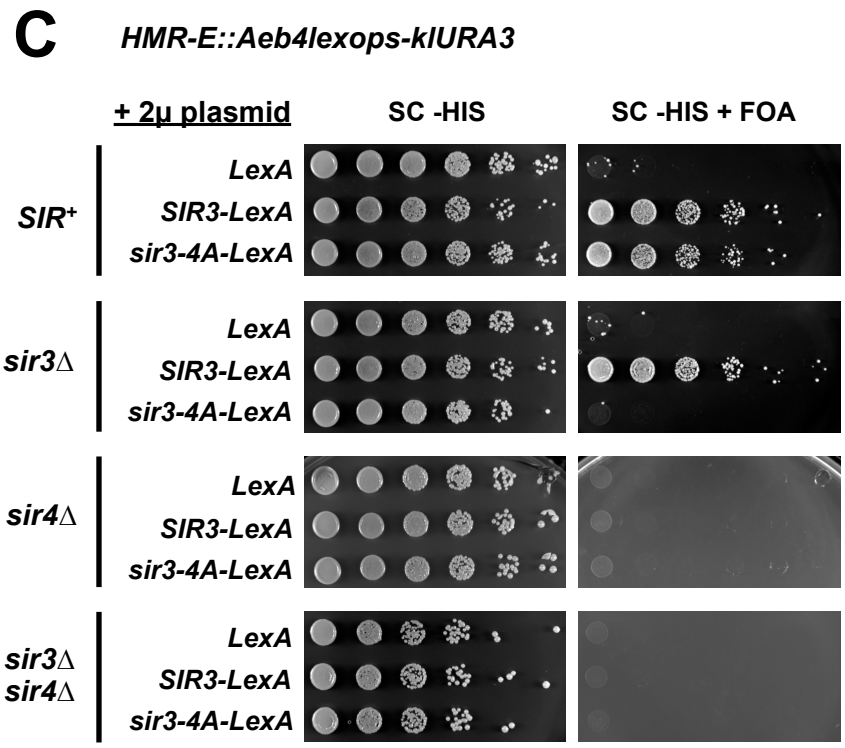
C
HMR-E::Aeb4lexops-klURA3
+ 2μ plasmid
SC -HIS
SC -HIS + FOA
SIR+
sir3Δ
sir4Δ
sir3Δ
sir4Δ
LexA
SIR3-LexA
sir3-4A-LexA

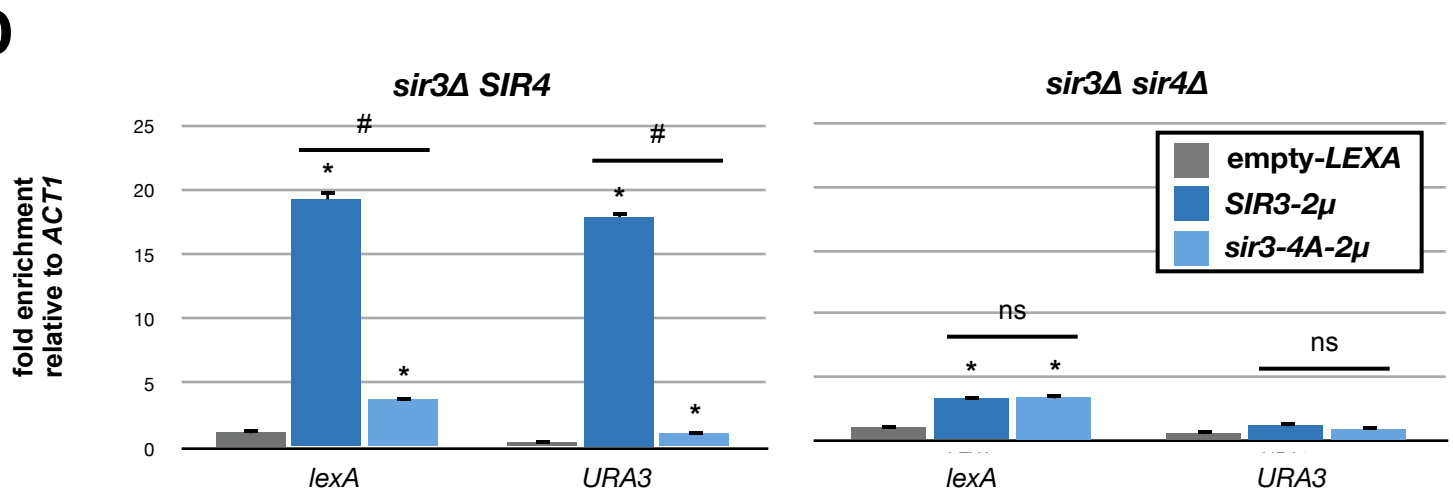
D
sir3Δ SIR4
sir3Δ sir4Δ
fold enrichment
relative to ACT1
25
20
15
10
5
0
#
*
ns
empty-LEXA
SIR3-2μ
sir3-4A-2μ
lexA
URA3

Figure 18. The Sir3-Sir4 interaction plays multiple roles in silent chromatin nucleation. **(A)** Schematic diagram showing the modified *HMR-E* silencer of LexA tethering strains. The E and B elements of the *HMR-E* silencer were replaced with four *lexops* LexA-binding sequences repeated in tandem. A *KlURA3* reporter gene replaced the *HMR a1* and *a2* genes approximately 1.4 kb downstream of the modified *HMR-E* silencer. Blue bars denote approximate locations of qPCR probes. Diagram not to scale. **(B)** Sir3-LexA and Sir3-4A-LexA express at similar levels to endogenous Sir3. LexA tethering strains described in (A) containing endogenous Sir3 or lacking Sir3 were transformed with *lexA, SIR3-lexA,* or *sir3-4A-lexA 2μ* plasmids. Sir3-LexA and Sir3-4A LexA expression was assessed by Western Blotting. Sir2 and Cdk1 serve as loading controls. Experiment performed by Adam Rudner. **(C)** Tethered Sir3-4A cannot nucleate silencing in the absence of endogenous Sir3. LexA tethering strains described in (A) expressing either all Sir proteins or lacking one or both of Sir3 and Sir4 were transformed with *lexA, SIR3-lexA,* or *sir3-4A-lexA 2μ* plasmids. Ten-fold serial dilutions were made on –HIS and –HIS FOA media to assess silencing. All media lacked histidine in order to maintain plasmids. Experiment performed by Adam Rudner. **(D)** Tethered Sir3-4A cannot nucleate Sir3 spreading in the absence of endogenous Sir3. LexA tethering strains described in (A) lacking Sir3 and either expressing or lacking Sir4 were transformed with *lexA, SIR3-lexA,* or *sir3-4A-lexA 2μ* plasmids. Sir3 enrichment at the A element of *HMR-E*, located just upstream of the LexA binding site (*LEXA*), and at the *KlURA3* reporter gene (*URA3*) (blue bars in (A)) was measured by ChIP. Enrichments are expressed as the percentage of the amount of the DNA originally present in the input sample and were normalized to enrichments at a euchromatic *ACT1* locus. Values represent the averages of three samples, with error bars representing standard errors of the means. Asterisks represent statistically significant levels of Sir protein enrichment ($p < 0.05$) relative to a *sir3Δ* control; #: statistically significant ($p<0.05$) for the comparison indicated by the horizontal bar; ns: not statistically significant for the comparison indicated by the horizontal bar. Detailed statistical analysis can be found in tables S2.19-S2.22.

to bypass the requirement of Sir4 for silencing. To assess the recruitment and spreading of Sir3-LexA and Sir3-4A-LexA, chromatin immunoprecipitation of Sir3 was performed in the tethering strains that expressed these Sir3 fusions from *2μ* plasmids but lacked endogenous Sir3. In both *SIR4* and *sir4Δ* strains, significant levels of Sir3 enrichment were detected at the A-element of *HMR-E*, located just upstream of the LexA binding site, whether Sir3-LexA or Sir3-4A-LexA was expressed (Figure 18D, Tables S2.19 and S2.21). In the *SIR4* strain but not the *sir4Δ* strain, Sir3-LexA enrichment at the A-element was significantly higher than that of Sir3-4A-LexA (Tables S2.19). Spreading of Sir3 to the *KlURA3* reporter gene required the presence of Sir4, and Sir3-LexA was significantly more enriched than Sir3-4A-LexA at this downstream locus (Figure 18D, Tables S2.20 and S2.22).

Chapter 4 – Discussion

4.1 Characterization of the Sir3-Sir4 binding interface

The Sir3 lysine and arginine residues KKRK 657-660 were previously found to play a role in the Sir3-Sir4 interaction (Ehrentraut et al., 2011), however this study did not directly examine the role of these residues in the Sir3-Sir4 interaction *in vivo*. We mutated these four residues to alanine, generating the Sir3-4A mutant, which expressed stably at levels similar to wild type Sir3 (Figure 7A,C). Multiple co-immunoprecipitations failed to detect interaction between Sir3-4A and Sir4 (Figure 8), suggesting that the Sir3 residues 657–660 are essential for *in vivo* interaction between Sir3 and Sir4. Furthermore, *in vitro* analysis (Figure 9) showed that a fragment of Sir3 containing residues 657 to 660 interacted directly with a fragment of Sir4 containing residues M1307, E1310, and I1311, which are known to be required for Sir3 binding (Chang et al., 2003). This interaction was abolished in the Sir3-4A mutant, suggesting that the Sir3 residues 657-660 are required for direct interaction of the Sir3 and Sir4 fragments. As no other Sir3-Sir4 binding interface has been identified, it is likely that the binding sites formed by Sir3 residues 657-660 and Sir4 residues 1307-1311 interact directly. The Sir3 amino acids 657-660 form a loop at the surface of the Sir3 protein, with basic residues K657 and R659 predicted to extend outward from the loop (Figure 3B; Ehrentraut et al., 2011). These residues may make contact with the negatively charged E1310 residue of Sir4, which extends from the surface of the Sir4 coiled-coil (Figure 4B; Chang et al., 2003). The second residue of the KKRK loop, K658, extends inward toward the loop's center. We found that mutation of only K657 and K658 is sufficient to block the Sir3-Sir4 interaction, suggesting that the integrity of the KKRK loop is critical in this interaction.

The Sir4 homologue Asf2 is highly similar to Sir4 in sequence, and like Sir4, its overexpression disrupts silencing (Le et al., 1997). However, the role of Asf2 in silencing remains unclear. Unpublished work shows that the Sir3 binding site in Sir4 is conserved in Asf2 (Callebaut, 2014), and that mutation of this binding site in Asf2 abolishes the Asf2-Sir3 interaction (Williams and Rudner, 2014). Mutation of the Sir3 KKRK loop also abolished interaction of Sir3 with Asf2 (Figure 8 A,D), suggesting that Sir3-Sir4 and Sir3-Asf2 share the same binding interface. Asf2 may therefore compete with Sir4 for binding to Sir3; indeed, overexpression of Asf2 disrupts the interaction between Sir3 and Sir4 (Rudner, 2003, unpublished data).

4.2 Sir3-4A cannot nucleate silent chromatin but participates in silent chromatin spreading

The inability of Sir3-4A to restore silencing in a strain lacking wild type Sir3 (Figure 10A) shows that the Sir3-Sir4 interaction plays a critical role in at least one step of the process of silent chromatin formation. Since overexpression of Sir3-4A in a wild type Sir3 background was sufficient to extend silent chromatin regions (Figures 11, 13), this mutant was able to participate in silent chromatin spreading. Thus, the functional deficiency of the Sir3-4A mutant likely lies in an earlier step of silent chromatin nucleation. The role of the Sir3-Sir4 interaction in silent chromatin nucleation has been documented in a previous study, which showed that mutations in Sir4 blocking the Sir3-Sir4 interaction also prevented recruitment of Sir3 to *HM* and telomeric silencers (Rudner et al., 2005). Thus, the nucleation defect of Sir3-4A may be due, in part, to its inability to be recruited to silencers by Sir4.

In strains expressing wild type Sir3, expression or overexpression of the Sir3 mutants did not block silent chromatin spreading at *HMR*, *TELVII-L*, or along *TELV-R* (Figures 10B,

13). The slight dominant negative effect of Sir3-4A overexpression on the ability to maintain repression of a *URA3* gene 1.0 kb from *TELV-R* on media lacing uracil (Figure 13) likely results from a reduced stability of Sir3-4A-mediated silencing. The inability to observe this dominant negative effect on FOA viability suggests that it has a very minor overall impact on silencing.

Overexpression of either Sir3 or the Sir3-4A mutant was sufficient to extend silencing up to 6.5 kb along *TELV-R* (Harding, 2014, unpublished data), although silencing efficiency of the Sir3 mutant strains was approximately 10-fold lower than that of wild type Sir3 at each locus tested (Figures 11 and 13, and Harding 2014). This is consistent with previous findings that show silencing can be mediated by N-terminal Sir3 fragments that do not interact with Sir4 (Connelly et al., 2006; Gotta et al., 1998), and supports a model for either Sir4-independent or Sir3-Sir4 interaction independent silencing (Figure 19A,B). The reduced ability for strains overexpressing Sir3-4A to maintain *URA3* silencing relative to strains overexpressing wild type Sir3 indicates that Sir3-4A-mediated silent chromatin is less stable than that formed by wild type Sir3. Indeed, deletion of the *URA3* trans-activator *PPR1* (which destabilizes *URA3* silencing (Renauld et al., 1993)) improved the efficiency of Sir3-4A silencing relative to that of Sir3 (Harding, 2014), suggesting that the Sir3-Sir4 interaction, while not required for silent chromatin spreading, may function in the stable inheritance of the silenced state.

4.3 Selection for transcriptional activation or silencing of a telomeric *URA3* gene

Growth in liquid media containing FOA caused a noticeable increase in Sir3-4A mediated silencing efficiency of a *URA3* gene located 1.0 kb from the telomere, and slightly increased silencing at the 5.5 kb locus in both Sir3 and Sir3-4A strains (Figure 13).

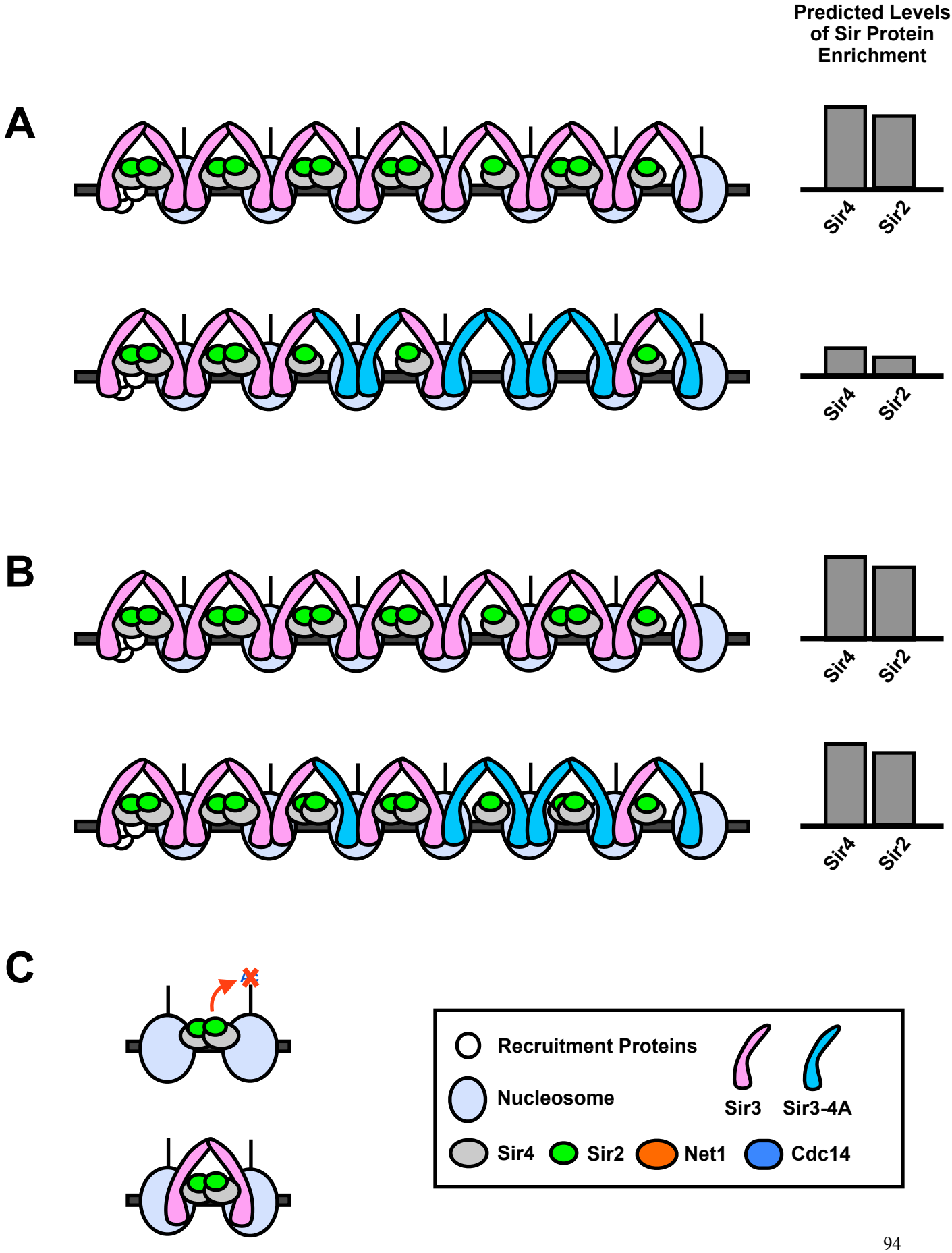
Predicted Levels of Sir Protein Enrichment
A
Sir4
Sir2
Sir4
Sir2
B
Sir4
Sir2
Sir4
Sir2
C
Recruitment Proteins
Nucleosome
Sir4
Sir2
Net1
Cdc14
Sir3
Sir3-4A

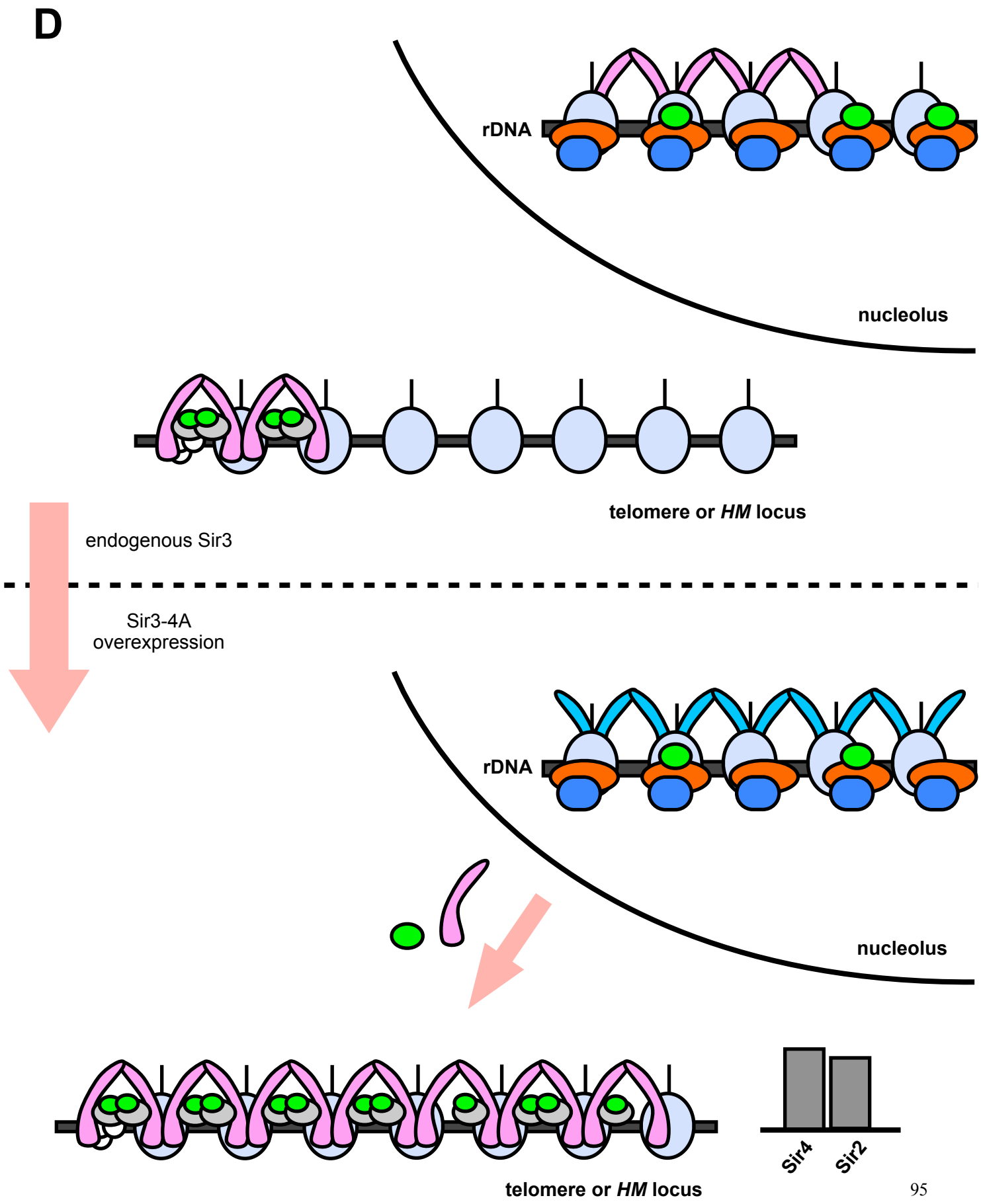
D
rDNA
nucleolus
telomere or *HM* locus
endogenous Sir3
Sir3-4A
overexpression
rDNA
nucleolus
Sir4
Sir2
telomere or *HM* locus

Figure 19. Three models for Sir3-4A mediated silent chromatin extension. (A) Model 1: silent chromatin spreading does not require Sir4. In this model, overexpression of the Sir3-4A mutant would generate silent chromatin extensions with diminished Sir4 and Sir2 enrichment relative to that of silent chromatin extensions formed by overexpressing wild type Sir3. Grey bars represent predicted Sir2 and Sir4 enrichment within extended telomeric silent chromatin based on Model 1. **(B)** Model 2: silent chromatin spreading requires Sir4 but not the Sir3-Sir4 interaction. In this model, Sir3 and Sir3-4A form heterochromatin extensions with similar levels of Sir4 and Sir2. Grey bars represent predicted Sir2 and Sir4 enrichment within extended telomeric silent chromatin based on Model 2. **(C)** According to Model 2, the Sir4/Sir2 subcomplex is normally recruited both through its interaction with H4K16-acetylated nucleosomes (upper panel) and through interaction with Sir3 (lower panel). In extended silent chromatin formed by overexpressing Sir3-4A, Sir4/Sir2 can only be recruited by interacting with nucleosomes. **(D)** Model 3: overexpressed Sir3-4A localizes to the nucleolus, releasing a sequestered pool of Sir2 and Sir3 that mediates silent chromatin extension. In this model, Sir3-4A does not participate directly in telomeric silent chromatin extension. Grey bars represent predicted Sir2 and Sir4 enrichment within extended telomeric silent chromatin based on Model 3.

These observed silencing improvements reflected an increased proportion of the cell population with the ability to silence telomeric *URA3*, confirming that growth in FOA can be used as a selection pressure for increased telomeric *URA3* silencing. Of the FOA-selected strains, the least drastic increase in silencing efficiency occurred at the 1.0 kb *URA3* locus when wild type Sir3 was overexpressed, as this strain had already neared a maximal level of silencing efficiency prior to FOA selection. The ability for FOA selection to slightly increase silencing stability (as measured by lack of growth on –URA media) in the Sir3 strains but not the Sir3-4A strains provides further support for a defect in the stability of silent chromatin extensions that form in the absence of a Sir3-Sir4 interaction. Just as FOA media can be used to select for *URA3* silencing, growth in –URA media can be used to effectively select against silencing of the *URA3* gene, abolishing both silencing efficiency and stability of the Sir3 and Sir3-4A strains. Our findings are in agreement with the results of Kitada et al. (2012), who showed by qRT-PCR that growth in FOA media significantly reduced the transcription of *TELVII-L URA3* relative to that of strains grown in –URA media or strains lacking Sir3.

4.4 Overexpression of Sir3 increased Sir protein enrichment along a silenced *TELV-R*

In strains expressing endogenous Sir3, significant levels of the Sir proteins and loss of H3K79 methylation at the 1.0 kb but not the 5.5 kb *URA3* locus correlated well with the ability of the endogenous strains to silence *URA3* only at the 1.0 kb locus. The ability of overexpressed Sir3 or Sir3-4A to significantly increase the enrichment of all three Sir proteins and decrease H3K79 methylation at the silenced 5.5 kb locus was consistent with the observed rescue of silencing in this region (Figures 13 -17). Our findings are supported by previous work, which also showed that Sir3 overexpression led to increased Sir3 enrichment along several telomeres (Strahl-Bolsinger et al., 1997). Methylation of H3K79 is

a mark of active transcription (Altaf et al., 2007; Armache et al., 2011) and the loss of this mark correlates with transcriptional silencing (Kitada et al., 2012). Indeed, we showed that relative to enrichment in a *sir3Δ* strain, H3K79 methylation in strains overexpressing Sir3 or Sir3-4A is significantly lower at silenced 1.0 kb and 5.5 kb *URA3* loci but not at the corresponding active loci. Although a higher amount of variability prevented detection of significant differences in H4K16 acetylation, our results suggest that the loss of this chromatin mark also correlates with silencing (Figure 17). While H4K16 deacetylation is required for silencing (Johnson et al., 2009; Oppikofer et al., 2011), Kitada et al recently showed that in strains expressing endogenous Sir3, H4K16 appears to be deacetylated at both an active and silenced *TELVII-L*. In contrast, our findings indicate that H4K16ac levels are higher at an active *TELV-R URA3* gene than at the silenced gene. This discrepancy may be a result of differences in the telomeres examined; alternatively, the overexpression of Sir3 may cause more pronounced H4K16 deacetylation at silenced telomeres than at active telomeres.

Overexpression of Sir3 or Sir3-4A was found to reduce the enrichment of Sir3 at the 1.0 kb *URA3* locus, relative to the endogenous Sir3 strain. This decrease was likely an artifact of normalizing Sir3 enrichment at *URA3* to background levels at a euchromatic *ACT1* locus, since background Sir3 enrichment at *ACT1* increased substantially upon Sir3 or Sir3-4A overexpression (Figures S1, S2).

4.5 Silent chromatin spreading requires Sir4 but not the Sir3-Sir4 interaction

The ability for Sir3-4A overexpression to mediate heterochromatin extensions suggests two possible models for silent chromatin spreading (Figure 19 A,B):

Model 1: silent chromatin can spread independently of Sir4 **Model 2:** silent chromatin spreading requires Sir4 but not the Sir3-Sir4 interaction

In a 1997 study by Strahl-Bolsinger et al., the authors performed ChIP to measure Sir protein enrichment in extended regions of heterochromatin along native *TELV-R* and *TELVI-R*. The high levels of Sir3 and relatively low levels of Sir4 and Sir2 within extended silent chromatin regions provided support for Model 1. However, these findings do not preclude the possibility that other factors blocked the detection of significant levels of Sir4 and Sir2 in these regions. To further examine the role of Sir4 and Sir2 in silent chromatin spreading, we compared Sir4 and Sir2 enrichment in extended chromatin regions mediated by overexpression of Sir3 and Sir3-4A. Model 1 would be supported by the detection of negligible levels of Sir4 and Sir2 within extended chromatin regions, or by significantly lower levels of Sir4 and Sir2 enrichment in silent chromatin extensions formed by Sir3-4A than in those formed by Sir3 (Figure 19A). However, our results show that Sir4 and Sir2 enrichment at the 5.5 kb silenced *URA3* locus becomes significant upon overexpression of either Sir3 or Sir3-4A. Furthermore, when comparing strains overexpressing Sir3 with those overexpressing Sir3-4A, we detected no significant differences in Sir4 or Sir2 enrichment, or in the loss of H3K79me or H4K16ac (Figures 14-17, Tables S2.1-S2.18) in silent chromatin extensions. Our results therefore argue against Model 1, suggesting that Sir4 and Sir2 are critical components of both silent chromatin nucleation and spreading.

The ability to detect significant levels of Sir4 and Sir2 in silent chromatin extensions mediated by Sir3-4A overexpression supports Model 2, and indicates that the Sir4/Sir2 subcomplex can be recruited to extended chromatin regions independently of interaction with Sir3 (Figure 19 B); this recruitment likely occurs through interactions of Sir4/Sir2 with the nucleosome. In strains overexpressing wild-type Sir3, Sir4/Sir2 may be recruited both through Sir3-Sir4 and Sir4/Sir2-nucleosome interactions (Figure 19C). A previous study provides evidence that Sir4/Sir2 preferentially associates with H4K16-acetylated

nucleosomes and that active deacetylation of H4K16 by Sir2 improves binding of the Sir complex to nucleosomes (Oppikofer et al., 2011). This is supported by work from our lab showing that while deletion of the H4K16 acetyltransferase Sas2 greatly reduces silencing in a *ppr1Δ TELV-R* 2.0 kb *URA3* strain overexpressing Sir3, loss of Sas2 completely abolishes silencing in this strain when Sir3-4A is overexpressed (Konci and Rudner, unpublished data, 2014). These findings are consistent with a model in which an interaction with H4K16-acetylated nucleosomes is the sole mechanism of Sir4/Sir2 recruitment to Sir3-4A mediated silent chromatin extensions. Since Sir2 actively deacetylates H4K16, recruitment of Sir4/Sir2 to the nucleosome may depend on a direct interaction between Sir2 and H4K16ac, although such an interaction has not been characterized. A Sir2-H4K16ac interaction may require the binding of Sir4 to Sir2, as Sir4 has been shown to induce conformational changes in Sir2 that allosterically stimulate Sir2 deacetylase activity (Hsu et al., 2013). Interaction of Sir4/Sir2 with the H4K16-acetylated nucleosome may also depend on Sir4-nucleosome interactions. Future work identifying and characterizing the nucleosome interaction interfaces of Sir4 and Sir2 will be essential in understanding the nature of Sir3-interaction independent recruitment of Sir4/Sir2 to extended silent chromatin regions.

Unlike the findings of Strahl-Bolsinger et al., our results show significant levels of Sir4 and Sir2 in extended silent chromatin regions. This discrepancy may have been influenced by several factors, including telomere-specific silencing mechanisms, a mixed population of cells with active and silenced telomeres in the Strahl-Bolsinger study, or ChIP artifacts that may prevent detection of chromatin binding proteins under certain conditions. The Stahl-Bolsinger study examined native *TELV-R* and *TELVI-R*, which may require different amounts of Sir2 and Sir4 than the synthetic, Y' element-lacking *TELV-R* used in our analysis. However, overexpression of Sir3 resulted in similar patterns of silent chromatin

spreading along a native and a Y'-lacking *TELV-R* (Renauld et al., 1993), making it unlikely that the presence or absence of the Y' element influenced the requirement for Sir2 and Sir4 in silent chromatin spreading. A more probable explanation for the inability of the Strahl-Bolsinger study to detect significant Sir4 and Sir2 in extended silent chromatin regions was their use of a mixed population of cells with active and silenced telomeres. The far lower levels of Sir protein enrichment at active telomeres present in the cell population may have negatively influenced the overall Sir protein enrichments measured by Strahl-Bolsinger et al. This possibility is supported by *TELVI-R* ChIP experiments performed in our lab using the same oligos as those employed in the Strahl-Bolsinger study (Harding, 2014, unpublished data). The strains used in these ChIP experiments overexpressed Sir3 or Sir3-4A and were not selected for transcriptional activation or silencing of *TELVI-R.* While Sir3 enrichment was maintained along the telomere, Sir2 and Sir4 enrichment decreased rapidly with increasing distance from the end of *TELVI-R*, (Harding, 2014), a finding similar to that of Strahl-Bolsinger et al (1997).

A recent study showed that formaldehyde crosslinking used in ChIP experiments causes silent chromatin to adopt structures that block the recovery of bound proteins (Thurtle et al., 2014). These structures may reduce the detectable levels of Sir protein enrichment within silent chromatin regions. It is possible that differences in antibody efficiencies caused this effect to be more pronounced for Sir2 and Sir4 detection in the Strahl-Bolsinger et al study. Importantly, Strahl-Bolsinger et al failed to detect Sir2 enrichment 0.77 kb from *TELVI-R* in the strain overexpressing Sir3, and Sir3 and Sir4 enrichment was not detected near the *TELV-R* X-element silencer in a strain with endogenous Sir3 levels. Thus, the results of the Strahl-Bolsinger study may have also been influenced by factors preventing the detection of Sir4 and Sir2 in extended silent chromatin regions.

Our results support Model 2, suggesting that silent chromatin spreading requires Sir4, but can occur independently of the Sir3-Sir4 interaction. However, our findings could also be indicative of a third model (Figure 19D), adapted from a proposal made by Gotta et al (1998). The authors overexpressed an N-terminal Sir3 fragment (Sir3N) that could not dimerize or bind Sir4 but was nevertheless capable of mediating silent chromatin extensions. Fluorescence microscopy revealed that GFP-tagged Sir3N was concentrated in the nucleolus and co-localized with rDNA, rather than forming distinct foci characteristic of wild type Sir3 (Gotta et al., 1998). The authors also found that overexpression of Sir3N abolished rDNA silencing, and caused a redistribution of Sir2 from rDNA to telomeric foci. Relocalization of Sir2 alone could not fully explain the silent chromatin extensions mediated by Sir3N overexpression, thus the authors proposed a model in which Sir3N localized to the nucleolus, releasing both Sir2 and a pool of Sir3 normally sequestered by the rDNA, to mediate silent chromatin extension at telomeres. Although Sir3 does not play a role in rDNA silencing, more recent work has confirmed significant levels of Sir3 enrichment at the rDNA repeats (Radman-Livaja et al., 2011). Interestingly, deletion of Sir4 increases localization of Sir3 to the nucleolus (Gotta et al., 1997) as does removal of Sir4 residues 1237-1358, which are necessary for both Sir4-Rap1 and Sir4-Sir3 interactions (Kennedy et al., 1997). The deletion of Sir4 may also cause a slight increase in Sir3 enrichment at the rDNA repeats (Hoppe et al., 2002). The ability of Sir4 to interact with Rap1 and Sir3 may therefore be essential in maintaining Sir3 enrichment at the telomeres, preventing Sir3 from being redistributed to the nucleolus. If so, the inability of Sir3N and Sir3-4A to interact with Sir4 may cause these proteins to be preferentially recruited to the nucleolus, where they could play an indirect role in extending telomeric silencing by releasing Sir2 and wild-type Sir3. These results are summarized in Model 3 (Figure 19D).

Model 3: A pool of Sir2 and Sir3 is normally sequestered in the nucleolus, and is unable to participate in silent chromatin spreading. The Sir3-4A mutant does not participate directly in silent chromatin spreading, but instead is preferentially recruited to rDNA repeats. Wild type Sir2 and Sir3 are released from the nucleolus, and participate directly in silent chromatin extension.

In the case of Model 3, the reduced silencing ability of overexpressed Sir3-4A (Figures 11 and 13) may result from a limited pool of wild type Sir3 that can be displaced from the nucleolus, and/or from defects in the ability of the Sir3-4A mutant to release this wild type Sir3. In contrast, overexpressed wild type Sir3 would be able to participate directly in silent chromatin spreading. Future work in our laboratory will test Model 3 by performing ChIP in strains overexpressing FLAG-tagged Sir3 and Sir3-4A in order to determine whether Sir3-4A is enriched in telomeric silent chromatin.

Fluorescence microscopy imaging of GFP-tagged silencing proteins normally reveals several bright foci, which represent clusters of telomeres. Overexpression of Sir3 decreases the average number of these foci, while increasing their overall intensity, an effect that is thought to represent telomere hyperclustering and which correlates with the level of Sir3 expression (Ruault et al., 2011). Telomere hyperclustering may increase local concentrations of the Sir proteins and trans-interactions between telomeres, which could in turn influence the formation of chromatin superstructures and facilitate silent chromatin extensions. The effect of telomere hyperclustering may work in conjunction with Sir3-Sir4 interaction independent Sir protein spreading (Model 2) or with Sir3 released from the nucleolus (Model 3) to promote silent chromatin spreading. Since overexpression of a silencing-deficient Sir3 mutant can promote telomere hyperclustering (Ruault et al., 2011), this process is more likely to occur upstream, rather than downstream of silencing. To further understand mechanism of Sir3-mediated telomere hyperclustering, the domains, interactions, and

residues of Sir3 involved in this process must be elucidated. Mutants of Sir3 and other silencing proteins can then be used to investigate the role of telomere hyperclustering in silent chromatin extension.

4.6 Sir proteins do not spread similarly along active and silenced telomeres

Although we detected significant levels of some Sir proteins at active telomeric *URA3*, Sir protein enrichment at the activated genes was quite low, and was significantly reduced compared to enrichment at the corresponding silenced loci (Figures 14, 16). In fact, the ability of silent chromatin structure to mask Sir protein enrichment (Thurtle et al., 2014) may have lowered detectable levels of Sir protein enrichment at the silenced *URA3* loci, causing us to underestimate the loss of Sir protein enrichment caused by *URA3* activation. Thus, while low levels of Sir2, Sir3, and Sir4 may localize to transcriptionally active regions, this enrichment is unlikely to result from a mechanism of Sir protein spreading similar to that which occurs in silenced regions. Our findings contrast with those of Kitada et al., who found no significant differences in Sir3 enrichment at an active or silenced *URA3* gene up to 1.0 kb from the end of *TELVII-L.* This discrepancy may have been caused by differences in the mechanisms of Sir protein spreading between *TELV-R* and *TELVII-L*, but may also result from the high levels of Sir3 present in our strains. It is possible that Sir3 overexpression could cause the Sir proteins to re-localize away from a transcriptionally active *TELV-R* to other telomeres.

A recent study identified a common artifact in ChIP experiments, in which protein enrichment is nonspecifically overrepresented at actively transcribed regions (Teytelman et al., 2013). Thus, the significant levels of Sir proteins detected at active *URA3* both in our work and in that of Kitada et al. might be a result of this artifact. Interestingly, the strains

used in our ChIP experiments lacked the *URA3* trans-activator Ppr1, which was present in the Kitada et al. strains and may have led to increased transcription of *URA3* at active telomeres. If active *URA3* is subject to the ChIP artifact described above, increased activation of *URA3* in the Kitada et al. strains may have led to the apparent similarity in Sir3 enrichment between active and silenced telomeres.

4.7 During nucleation, the Sir3-Sir4 interaction is important for more than recruitment of Sir3 to the chromatin

We wondered whether the primary role of the Sir3-Sir4 interaction was the recruitment of Sir3 to the silencer during nucleation. If so, the requirement for this interaction could be bypassed by tethering Sir3-LexA fusion proteins to *lex*-operator sites inserted at a silencer (Figure 20). Chromatin immunoprecipitation confirmed that Sir3-LexA and Sir3-4A-LexA fusions could be efficiently tethered to an *HMR* silencer using this method (Figure 18D). This tethering did not require Sir4, indicating that the targeting of the Sir3 fusions occurred through interaction of LexA with the *lex*-operator sites within the *HMR* silencer. However, Sir4 was required for the spreading of Sir3 to the *KlURA3* gene located 1.4 kb downstream of the LexA binding site and for the silencing of this gene (Figure 18 C, D), providing further support for its essential role in silent chromatin spreading.

At the LexA binding site, Sir3-LexA enrichment in the *SIR4+* strain was far higher than Sir3 enrichment in any of the other conditions tested. This was likely a result of the ability of Sir3-LexA to spread over 1.4 kb to the adjacent *klURA3* gene. Average sonication shear sizes for ChIP experiments were approximately 500 bp, resulting in significant overlap between detection of Sir3 enrichment at the LexA site and detection of Sir3 at downstream regions. In addition, recruitment of Sir3-LexA to the silencer was likely enhanced by

neighboring Sir3-Sir4 interactions. Overlap between Sir3 detection at the LexA binding site and *KlURA3* gene was likely also the cause of the very low but significant levels of Sir3-4A-LexA enrichment detected at *KlURA3* in the *sir3Δ SIR4* strain.

In the absence of wild type Sir3, tethered Sir3-4A could not mediate silencing of *KlURA3*, nor spreading of Sir3 to the *KlURA3* gene at levels biologically relevant for silencing. Thus, tethering of Sir3-4A to the *HMR* silencer was not sufficient to bypass the requirement for the Sir3-Sir4 interaction in silent chromatin nucleation. Since Sir3-4A-LexA could be efficiently recruited to the silencer, our findings indicate that the Sir3-Sir4 interaction plays multiple roles in silent chromatin nucleation, and is essential for more than the recruitment of Sir4 to the silencer. Chang et al (2003) propose that the Sir3-Sir4 interaction mediates a conformational change that is essential for the function of the Sir complex in silencing. During nucleation, such a conformational change in the SIR complex may perform a specific templating function, promoting recruitment of additional Sir complexes and causing changes in chromatin structure that favor silent chromatin spreading (Figure 20 D).

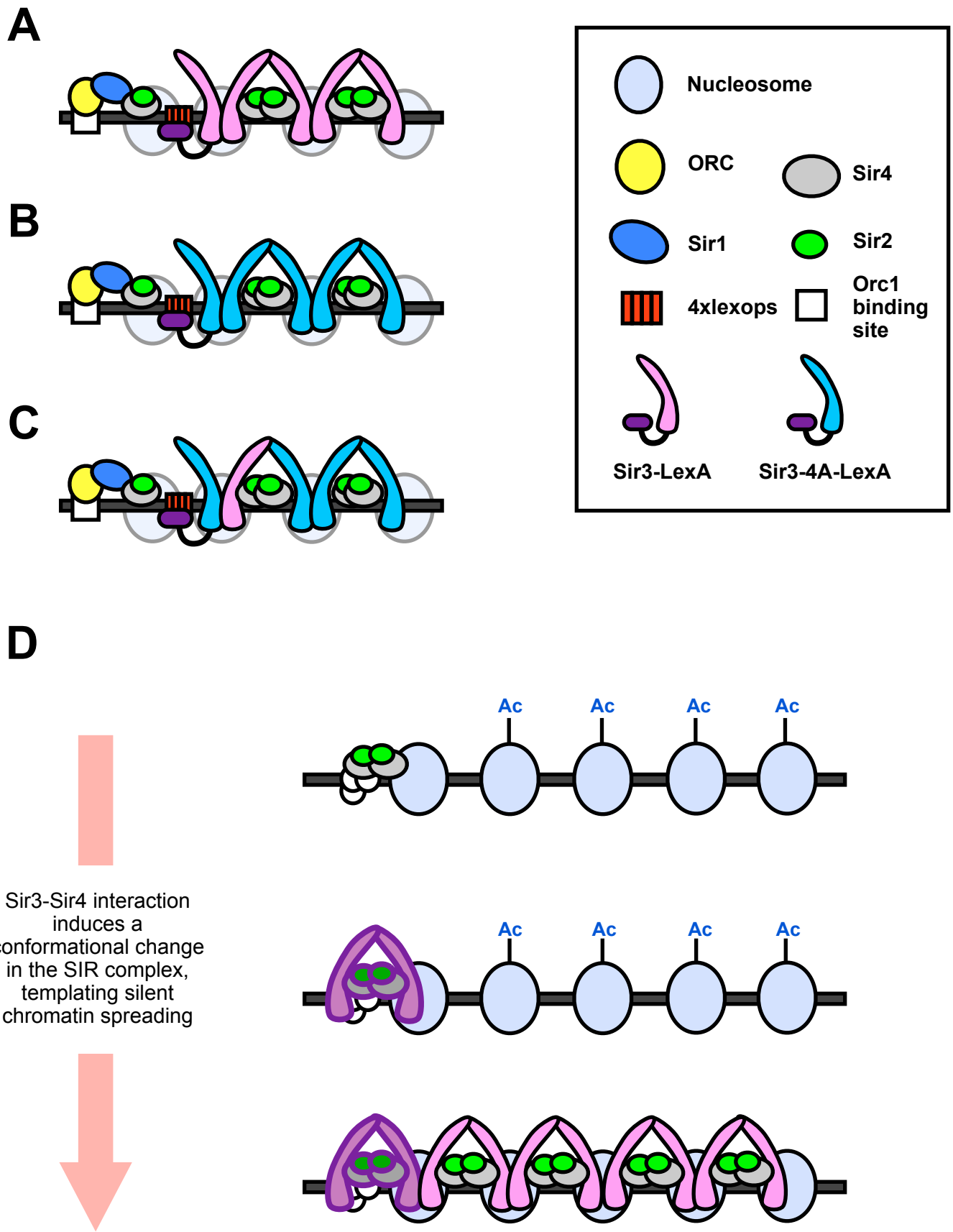
A
B
C
Nucleosome
ORC
Sir4
Sir1
Sir2
4xlexops
Orc1 binding site
Sir3-LexA
Sir3-4A-LexA
D
Ac
Ac
Ac
Ac
Sir3-Sir4 interaction induces a conformational change in the SIR complex, templating silent chromatin spreading
Ac
Ac
Ac
Ac

Figure 20. Testing for multiple roles of the Sir3-Sir4 interaction in silent chromatin nucleation. (A) Tethering wild type Sir3-LexA to a LexA binding site located within a weakened *HMR-E::Aeb* silencer was previously shown to be sufficient for silent chromatin nucleation (Wu et al., 2011). **(B)** If the only role of the Sir3-Sir4 interaction is the recruitment of Sir3 during silent chromatin nucleation, this requirement would be bypassed by the tethering of Sir3-4A-LexA to the *HMR* silencer. **(C)** Tethered Sir3-4A-LexA can only nucleate silent chromatin in the presence of endogenous Sir3, suggesting that the Sir3-Sir4 interaction plays multiple roles in silent chromatin nucleation. **(D)** During nucleation, the Sir3-Sir4 interaction may be required for a conformational change in the SIR complex (indicated by the highlighted nucleating SIR complex) that favors recruitment of additional SIR complexes and silent chromatin spreading.

References

Ai, W., Bertram, P.G., Tsang, C.K., Chan, T.F., and Zheng, X.F.S. (2002). Regulation of subtelomeric silencing during stress response. Mol. Cell *10*, 1295–1305.

Alper, B.J., Job, G., Yadav, R.K., Shanker, S., Lowe, B.R., and Partridge, J.F. (2013). Sir2 is required for Clr4 to initiate centromeric heterochromatin assembly in fission yeast. Embo J. *32*, 2321–2335.

Altaf, M., Utley, R.T., Lacoste, N., Tan, S., Briggs, S.D., and Côté, J. (2007). Interplay of chromatin modifiers on a short basic patch of histone H4 tail defines the boundary of telomeric heterochromatin. Mol. Cell *28*, 1002–1014.

Amberg, D.C., Burke, D.J., and Strathern, J.N. (2005). Methods in Yeast Genetics: A Cold Spring Harbor Laboratory Course Manual, 2005 Edition.

Amberg, D.C., Burke, D.J., and Strathern, J.N. (2006). High-efficiency transformation of yeast. CSH Protocols.

Anderson, C.W., Baum, P.R., and Gesteland, R.F. (1973). Processing of Adenovirus 2-Induced Proteins. J Virol *12*, 241-252.

Armache, K.J., Garlick, J.D., Canzio, D., Narlikar, G.J., and Kingston, R.E. (2011). Structural Basis of Silencing: Sir3 BAH Domain in Complex with a Nucleosome at 3.0 A Resolution. Science *334,* 977-982.

Arnaudo, N., Fernández, I.S., McLaughlin, S.H., Peak-Chew, S.Y., Rhodes, D., and Martino, F. (2013). The N-terminal acetylation of Sir3 stabilizes its binding to the nucleosome core particle. Nat. Struct. Mol. Biol. *20*, 1119–1121.

Arnerić, M., and Lingner, J. (2007). Tel1 kinase and subtelomere-bound Tbf1 mediate preferential elongation of short telomeres by telomerase in yeast. EMBO Rep *8*, 1080–1085.

Bannister, A. J., Kouzarides, T. (2011). Regulation of chromatin by histone modifications. Nature Cell Research *21,* 381-395.

Bedford, M.T. (2007). Arginine Methylation at a Glance. Journal of Cell Science. *120,* 4243-4246.

Bell, S.P., Mitchell, J., Leber, J., Kobayashi, R., and Stillman, B. (1995). The multidomain structure of Orc1p reveals similarity to regulators of DNA replication and transcriptional silencing. Cell *83*, 563–568.

Bernard, P., Maure, J.F., Partridge, J.F., Genier, S., Javerzat, J.P., and Allshire, R.C. (2001). Requirement of heterochromatin for cohesion at centromeres. Science *294*, 2539–2542.

Bi, X., Braunstein, M., Shei, G.J., and Broach, J.R. (1999). The yeast HML I silencer defines a heterochromatin domain boundary by directional establishment of silencing. Proc. Natl. Acad. Sci. U.S.a. *96*, 11934–11939.

Blander, G., and Guarente, L. (2004). The Sir2 family of protein deacetylases. Annu. Rev. Biochem. *73*, 417–435.

Boeke, J.D., Croute, F., and Fink, G.R. (1984). A positive selection for mutants lacking orotidine-5?-phosphate decarboxylase activity in yeast: 5-fluoro-orotic acid resistance. Mol Gen Genet *197*, 345–346.

Bose, M.E., McConnell, K.H., Gardner-Aukema, K.A., Müller, U., Weinreich, M., Keck, J.L., and Fox, C.A. (2004). The origin recognition complex and Sir4 protein recruit Sir1p to yeast silent chromatin through independent interactions requiring a common Sir1p domain. Molecular and Cellular Biology *24*, 774–786.

Bottomley, M.J. (2004). Structures of protein domains that create or recognize histone modifications. EMBO Reports, *5,* 464-469.

Boulton, S.J., and Jackson, S.P. (1998). Components of the Ku-dependent non-homologous end-joining pathway are involved in telomeric length maintenance and telomeric silencing. Embo J. *17*, 1819–1828.

Braus, G.H. (1991). Aromatic Amino Acid Biosynthesis in the Yeast *Saccharomyces cerevisiae:* a Model System for the Regulation of a Eukaryotic Biosynthetic Pathway. Microbiological Reviews, *55*, 349-370

Buchberger, J.R., Onishi, M., Li, G., Seebacher, J., Rudner, A.D., Gygi, S.P., and Moazed, D. (2008). Sir3-nucleosome interactions in spreading of silent chromatin in Saccharomyces cerevisiae. Molecular and Cellular Biology *28*, 6903–6918.

Buck, S.W., and Shore, D. (1995). Action of a RAP1 carboxy-terminal silencing domain reveals an underlying competition between HMR and telomeres in yeast. Genes Dev. *9*, 370–384.

Bupp, J.M., Martin, A.E., Stensrud, E.S., and Jaspersen, S.L. (2007). Telomere anchoring at the nuclear periphery requires the budding yeast Sad1-UNC-84 domain protein Mps3. J. Cell Biol. *179*, 845–854.

Buscaino, A., Lejeune, E., Audergon, P., Hamilton, G., Pidoux, A., and Allshire, R.C. (2013). Distinct roles for Sir2 and RNAi in centromeric heterochromatin nucleation, spreading and maintenance. Embo J. *32*, 1250–1264.

Callebaut, I. (2014). Conservation of the Sir4 Coiled-Coil domain in Asf2. Unpublished laboratory work, Université Pierre et Marie Curie, France.

Canzio, D., Chang, E.Y., Shankar, S., Kuchenbecker, K.M., Simon, M.D., Madhani, H.D., Narlikar, G.J., and Al-Sady, B. (2011). Chromodomain-mediated oligomerization of HP1

suggests a nucleosome-bridging mechanism for heterochromatin assembly. Mol. Cell *41*, 67–81.

Canzio, D., Liao, M., Naber, N., Pate, E., Larson, A., Wu, S., Marina, D.B., Garcia, J.F., Madhani, H.D., Cooke, R., et al. (2013). A conformational switch in HP1 releases auto-inhibition to drive heterochromatin assembly. Nature *496*, 377–381.

Carmen, A.A., Milne, L., and Grunstein, M. (2002). Acetylation of the yeast histone H4 N terminus regulates its binding to heterochromatin protein SIR3. J. Biol. Chem. *277*, 4778–4781.

Carrozza, M.J., Utley, R.T., Workman, J.L., and Cote, J. (2003). The diverse functions of histone acetyltransferases complexes. Trends in Genetics *19,* 321-329.

Chang, J.-F., Hall, B.E., Tanny, J.C., Moazed, D., Filman, D., and Ellenberger, T. (2003). Structure of the coiled-coil dimerization motif of Sir4 and its interaction with Sir3. Structure *11*, 637–649.

Chen, L., and Widom, J. (2005). Mechanism of transcriptional silencing in yeast. Cell *120*, 37–48.

Chen, Y., Rai, R., Zhou, Z.-R., Kanoh, J., Ribeyre, C., Yang, Y., Zheng, H., Damay, P., Wang, F., Tsujii, H., et al. (2011). A conserved motif within RAP1 has diversified roles in telomere protection and regulation in different organisms. Nat. Struct. Mol. Biol. *18*, 213–221.

Chou, C.-C., Li, Y.-C., and Gartenberg, M.R. (2008). Bypassing Sir2 and O-acetyl-ADP-ribose in transcriptional silencing. Mol. Cell *31*, 650–659.

Cohen, J. (1962). Position-Effect Variegation at Several Closely Linked Loci in *Drosophila melanogaster*. Genetics. *47,* 647-659.

Coïc, E., Richard, G.-F., and Haber, J.E. (2006). Saccharomyces cerevisiae donor preference during mating-type switching is dependent on chromosome architecture and organization. Genetics *173*, 1197–1206.

Connelly, J.J., Yuan, P., Hsu, H.-C., Li, Z., Xu, R.-M., and Sternglanz, R. (2006). Structure and function of the Saccharomyces cerevisiae Sir3 BAH domain. Molecular and Cellular Biology *26*, 3256–3265.

Cubizolles, F., Martino, F., Perrod, S., and Gasser, S.M. (2006). A homotrimer-heterotrimer switch in Sir2 structure differentiates rDNA and telomeric silencing. Mol. Cell *21*, 825–836.

Delcuve, G.P., Khan, D.H., and Davie, J.R. (2012). Roles of histone deacetylases in epigenetic regulation: emerging paradigms from studies with inhibitors. Clin Epigenetics *4*, 5.

Demerec, M. (1940). Genetic behavior of euchromatic segments inserted into heterochromatin. Genetics *25,* 618-627.
Duggan, N.M. and Tang, Z.I. (2010). The Formation of Heterochromatin. Nature Education *3,* 5.

Edwards, C.R., Dang, W., and Berger, S.L. (2011). Histone H4 lysine 20 of Saccharomyces cerevisiae is monomethylated and functions in subtelomeric silencing. Biochemistry *50*, 10473–10483.

Ehrentraut, S., Hassler, M., Oppikofer, M., Kueng, S., Weber, J.M., Mueller, J.W., Gasser, S.M., Ladurner, A.G., and Ehrenhofer-Murray, A.E. (2011). Structural basis for the role of the Sir3 AAA+ domain in silencing: interaction with Sir4 and unmethylated histone H3K79. Genes Dev. *25*, 1835–1846.

Fadloun, A., Eid, A., and Torres-Padilla, M.-E. (2013). Mechanisms and dynamics of heterochromatin formation during mammalian development: closed paths and open questions. Curr. Top. Dev. Biol. *104*, 1–45.

Förstemann, K., Höss, M., and Lingner, J. (2000). Telomerase-dependent repeat divergence at the 3' ends of yeast telomeres. Nucleic Acids Research *28*, 2690–2694.

Freitas-Junior, L.H., Hernandez-Rivas, R., Ralph, S.A., Montiel-Condado, D., Ruvalcaba-Salazar, O.K., Rojas-Meza, A.P., Mancio-Silva, L., Leal-Silvestre, R.J., Gontijo, A.M., Shorte, S., et al. (2005). Telomeric heterochromatin propagation and histone acetylation control mutually exclusive expression of antigenic variation genes in malaria parasites. Cell *121*, 25–36.

Gallegos-García, V., Pan, S.-J., Juárez-Cepeda, J., Ramírez-Zavaleta, C.Y., Martin-del-Campo, M.B., Martínez-Jiménez, V., Castaño, I., Cormack, B., and Las Peñas, De, A. (2012). A novel downstream regulatory element cooperates with the silencing machinery to repress EPA1 expression in Candida glabrata. Genetics *190*, 1285–1297.

Gao, L., and Gross, D.S. (2008). Sir2 silences gene transcription by targeting the transition between RNA polymerase II initiation and elongation. Molecular and Cellular Biology *28*, 3979–3994.

Gartenberg, M. (2009). Heterochromatin and the cohesion of sister chromatids. Chromosome Res *17*, 229–238.

Gartenberg, M.R., Neumann, F.R., Laroche, T., Blaszczyk, M., and Gasser, S.M. (2004). Sir-mediated repression can occur independently of chromosomal and subnuclear contexts. Cell *119*, 955–967.

Georgel, P.T., Palacios DeBeer, M.A., Pietz, G., Fox, C.A., and Hansen, J.C. (2001). Sir3-dependent assembly of supramolecular chromatin structures in vitro. Proc. Natl. Acad. Sci. U.S.a. *98*, 8584–8589.

Ghidelli, S., Donze, D., Dhillon, N., and Kamakaka, R.T. (2001). Sir2p exists in two

nucleosome-binding complexes with distinct deacetylase activities. Embo J. *20*, 4522–4535.

Gietz, R.D., and Schiestl, R.H. (2007). High-efficiency yeast transformation using the LiAc/SS carrier DNA/PEG method. Nat Protoc *2*, 31–34.

Goetze, H., Wittner, M., Hamperl, S., Hondele, M., Merz, K., Stoeckl, U., and Griesenbeck, J. (2010). Alternative chromatin structures of the 35S rRNA genes in Saccharomyces cerevisiae provide a molecular basis for the selective recruitment of RNA polymerases I and II. Molecular and Cellular Biology *30*, 2028–2045.

Gotta, M., Laroche, T., Formenton, A., Maillet, L., Scherthan, H., and Gasser, S.M. (1996). The clustering of telomeres and colocalization with Rap1, Sir3, and Sir4 proteins in wild-type Saccharomyces cerevisiae. J. Cell Biol. *134*, 1349–1363.

Gotta, M., Palladino, F., and Gasser, S.M. (1998). Functional characterization of the N terminus of Sir3p. Molecular and Cellular Biology *18*, 6110–6120.

Gotta, M., Strahl-Bolsinger, S., Renauld, H., Laroche, T., Kennedy, B.K., Grunstein, M., and Gasser, S.M. (1997). Localization of Sir2p: the nucleolus as a compartment for silent information regulators. Embo J. *16*, 3243–3255.

Gottschling, D.E., Aparicio, O.M., Billington, B.L., and Zakian, V.A. (1990). Position effect at S. cerevisiae telomeres: reversible repression of Pol II transcription. Cell *63*, 751–762.

Grandin, N., Reed, S.I., and Charbonneau, M. (1997). Stn1, a new Saccharomyces cerevisiae protein, is implicated in telomere size regulation in association with Cdc13. Genes Dev. *11*, 512–527.

Green, M.R., and Sambrook J. (2012). Molecular Cloning, A Laboratory Manual. Cold Spring Harbor Laboratory Press.

Greider, C.W., and Blackburn, E.H. (1989). A telomeric sequence in the RNA of Tetrahymena telomerase required for telomere repeat synthesis. Nature *337*, 331–337.

Grewal, S.I.S., and Elgin, S.C.R. (2002). Heterochromatin: new possibilities for the inheritance of structure. Curr. Opin. Genet. Dev. *12*, 178–187.

Grewal, S.I.S., and Moazed, D. (2003). Heterochromatin and Epigenetic Control of Gene Expression. Science *301*, 798–802.

Grunstein, M., and Gasser, S.M. (2013). Epigenetics in Saccharomyces cerevisiae. Cold Spring Harb Perspect Biol *5*.

Hall, B.E., Buchberger, J.R., Gerber, S.A., Ambrosio, A.L.B., Gygi, S.P., Filman, D., Moazed, D., and Ellenberger, T. (2008). Autoregulation of the yeast Sir2 deacetylase by reaction and trapping of a pseudosubstrate motif in the active site. RSCB Protein Data Bank, PDB ID 2HJH.

Halme, A., Bumgarner, S., Styles, C., and Fink, G.R. (2004). Genetic and epigenetic regulation of the FLO gene family generates cell-surface variation in yeast. Cell *116*, 405–415.

Hanson, P.I., and Whiteheart, S.W. (2005). AAA+ proteins: have engine, will work. Nat Rev Mol Cell Biol *6*, 519–529.

Harding, K. (2014). Silencing Proteins Sir3 and Sir4 have Distinct Roles in the Assembly of Silent Chromatin in Budding Yeast. M.Sc. Thesis, uOttawa.

Harding, K., Gerson, R.J., Doré, C., Pilon, S., and Rudner, A.D. (in preparation). The Interaction between Sir3 and Sir4 is dispensible for spreading of silent chromatin in budding yeast.

Hecht, A., Laroche, T., Strahl-Bolsinger, S., Gasser, S.M., and Grunstein, M. (1995). Histone H3 and H4 N-termini interact with SIR3 and SIR4 proteins: a molecular model for the formation of heterochromatin in yeast. Cell *80*, 583–592.

Herskowitz, I. (1988). Life cycle of the budding yeast *Saccharomyces cerevisiae*. Microbiology and Molecular Biology Reviews. *52,* 536-553.

Hickman, M.A., Froyd, C.A., and Rusche, L.N. (2011). Reinventing heterochromatin in budding yeasts: Sir2 and the origin recognition complex take center stage. Eukaryotic Cell *10*, 1183–1192.

Hild, M., and Paro, R. (2003). Anti-silencing from the core: a histone H2A variant protects euchromatin. Nat. Cell Biol. *5*, 278–280.

Hoppe, G.J., Tanny, J.C., Rudner, A.D., Gerber, S.A., Danaie, S., Gygi, S.P., and Moazed, D. (2002). Steps in assembly of silent chromatin in yeast: Sir3-independent binding of a Sir2/Sir4 complex to silencers and role for Sir2-dependent deacetylation. Molecular and Cellular Biology *22*, 4167–4180.

Hsu, H.-C., Wang, C.-L., Wang, M., Yang, N., Chen, Z., Sternglanz, R., and Xu, R.-M. (2013). Structural basis for allosteric stimulation of Sir2 activity by Sir4 binding. Genes Dev. *27*, 64–73.

Hughes, T.R., Weilbaecher, R.G., Walterscheid, M., and Lundblad, V. (2000). Identification of the single-strand telomeric DNA binding domain of the Saccharomyces cerevisiae Cdc13 protein. Proc. Natl. Acad. Sci. U.S.a. *97*, 6457–6462.

Jackson, M. D., and J. M. Denu. (2002). Structural identification of 2'- and 3'-O-acetyl-ADP-ribose as novel metabolites derived from the Sir2 family of beta-NAD+-dependent histone/protein deacetylases. J. Biol. Chem. *277,* 18535–18544.

Jiang, C., and Pugh, B.F. (2009). Nucleosome positioning and gene regulation: advances through genomics. Nat Rev Genet *10*, 161–172.

Johnson, A., Li, G., Sikorski, T.W., Buratowski, S., Woodcock, C.L., and Moazed, D. (2009). Reconstitution of heterochromatin-dependent transcriptional gene silencing. Mol. Cell *35*, 769–781.

Kamakaka, R.T., and Biggins, S. (2005). Histone Variants: deviants? Genes & Dev. *19,* 295-316.

Katan-Khaykovich, Y., and Struhl, K. (2005). Heterochromatin formation involves changes in histone modifications over multiple cell generations. Embo J. *24*, 2138–2149.

Kato, S., Inoue, K., and Youn, M.-Y. (2010). Emergence of the osteo-epigenome in bone biology. IBMS BoneKEy *7*, 314–324.

Kunkel, T.A. (1985). Rapid and efficient site-specific mutagenesis without phenotypic selection. Proc. Natl. Acad. Sci. U.S.a. *82*, 488–492.

Kurdistani, S, and Grunstein, M. (2003). Histone Acetylation and Deacetylation in Yeast. Nature *4*, 276-284.

Kennedy, B.K., Gotta, M., Sinclair, D.A., Mills, K., McNabb, D.S., Murthy, M., Pak, S.M., Laroche, T., Gasser, S.M., and Guarente, L. (1997). Redistribution of silencing proteins from telomeres to the nucleolus is associated with extension of life span in S. cerevisiae. Cell *89*, 381–391.

King, D.A., Hall, B.E., Iwamoto, M.A., Win, K.Z., Chang, J.-F., and Ellenberger, T. (2006). Domain structure and protein interactions of the silent information regulator Sir3 revealed by screening a nested deletion library of protein fragments. J. Biol. Chem. *281*, 20107–20119.

Kitada, T., Kuryan, B.G., Tran, N.N.H., Song, C., Xue, Y., Carey, M., and Grunstein, M. (2012). Mechanism for epigenetic variegation of gene expression at yeast telomeric heterochromatin. Genes Dev. *26*, 2443–2455.

Klose, R.J., Gardner, K.E., Liang, G., Erdjument-Bromage, H., Tempst, P., and Zhang, Y. (2007). Demethylation of histone H3K36 and H3K9 by Rph1: a vestige of an H3K9 methylation system in Saccharomyces cerevisiae? Molecular and Cellular Biology *27*, 3951–3961.

Konci, R., and Rudner, A.D. (2014). The effects of *SAS2* deletion on silencing in strains overexpressing *SIR3* or *sir3-4A*. Unpublished laboratory work, University of Ottawa.

Kostriken, R., Strathern, J.N., Klar, A.J., Hicks, J.B., and Heffron, F. (1983). A site-specific endonuclease essential for mating-type switching in Saccharomyces cerevisiae. Cell *35*, 167–174.

Kueng, S., Tsai-Pflugfelder, M., Oppikofer, M., Ferreira, H.C., Roberts, E., Tsai, C., Roloff, T.-C., Sack, R., and Gasser, S.M. (2012). Regulating repression: roles for the sir4 N-terminus in linker DNA protection and stabilization of epigenetic states. PLOS Genetics *8*, e1002727.

Laroche, T., Martin, S.G., Gotta, M., Gorham, H.C., Pryde, F.E., Louis, E.J., and Gasser, S.M. (1998). Mutation of yeast Ku genes disrupts the subnuclear organization of telomeres. Curr. Biol. *8*, 653–656.

Le, S., Davis, C., Konopka, J.B., and Sternglanz, R. (1997). Two new S-phase-specific genes from Saccharomyces cerevisiae. Yeast *13*, 1029–1042.

Lee, J., Lee, T., Lee, Y.-W., Yun, S.-H., and Turgeon, B.G. (2003). Shifting fungal reproductive mode by manipulation of mating type genes: obligatory heterothallism of Gibberella zeae. Mol. Microbiol. *50*, 145–152.

Li, E. (2002). Chromatin modification and epigenetic reprogramming in mammalian development. Nat Rev Genet *3*, 662–673.

Liaw, H., and Lustig, A.J. (2006). Sir3 C-terminal domain involvement in the initiation and spreading of heterochromatin. Molecular and Cellular Biology *26*, 7616–7631.

Liou, G.-G., Tanny, J.C., Kruger, R.G., Walz, T., and Moazed, D. Assembly of the SIR Complex and Its Regulation by *O*-Acetyl-ADP-Ribose, a Product of NAD-Dependent Histone Deacetylation.

Longtine, M.S., McKenzie, A., Demarini, D.J., Shah, N.G., Wach, A., Brachat, A., Philippsen, P., and Pringle, J.R. (1998). Additional modules for versatile and economical PCR-based gene deletion and modification in Saccharomyces cerevisiae. Yeast *14*, 953–961.

Loo, S., and Rine, J. (1994). Silencers and domains of generalized repression. Science *264*, 1768-1771.

Lundblad, V., and Zhou, H. (2001). Manipulation of plasmids from yeast cells. Curr Protoc Mol Biol *Chapter 13*, Unit13.9.

Luo, K., Vega-Palas, M.A., and Grunstein, M. (2002). Rap1-Sir4 binding independent of other Sir, yKu, or histone interactions initiates the assembly of telomeric heterochromatin in yeast. Genes Dev. *16*, 1528–1539.

Luo, Z., and van Vuuren, H.J.J. (2008). Stress-induced production, processing and stability of a seripauperin protein, Pau5p, in Saccharomyces cerevisiae. FEMS Yeast Res. *8*, 374–385.

Lustig, A.J., Liu, C., Zhang, C., and Hanish, J.P. (1996). Tethered Sir3p nucleates silencing at telomeres and internal loci in Saccharomyces cerevisiae. Molecular and Cellular Biology *16*, 2483–2495.

Mahoney, D.J., and Broach, J.R. (1989). The HML mating-type cassette of Saccharomyces cerevisiae is regulated by two separate but functionally equivalent silencers. Molecular and Cellular Biology *9*, 4621–4630.

Mancio-Silva, L., Rojas-Meza, A.P., Vargas, M., Scherf, A., and Hernandez-Rivas, R.

(2008). Differential association of Orc1 and Sir2 proteins to telomeric domains in Plasmodium falciparum. J. Cell. Sci. *121*, 2046–2053.

Marks, P.A., Rifkind, R.A., Richon, V.M., Breslow, R., Miller, T., and Kelly, W.K. (2001). Histone deacetylases and Cancer: Causes and Therapies. Nature *1,* 194-202.

Martino, F., Kueng, S., Robinson, P., Tsai-Pflugfelder, M., van Leeuwen, F., Ziegler, M., Cubizolles, F., Cockell, M.M., Rhodes, D., and Gasser, S.M. (2009). Reconstitution of yeast silent chromatin: multiple contact sites and O-AADPR binding load SIR complexes onto nucleosomes in vitro. Mol. Cell *33*, 323–334.

Martínez-Jiménez, V., Ramírez-Zavaleta, C.Y., Orta-Zavalza, E., Díaz de León, G., Gutiérrez-Escobedo, G., Ponce de León, A., Sifuentes-Osornio, J., Bobadilla Del Valle, M., Las Peñas, De, A., and Castaño, I. (2013). Sir3 Polymorphisms in Candida glabrata Clinical Isolates. Mycopathologia *175*, 207–219.

Marvin, M.E., Becker, M.M., Noel, P., Hardy, S., Bertuch, A.A., and Louis, E.J. (2009). The association of yKu with subtelomeric core X sequences prevents recombination involving telomeric sequences. Genetics *183*, 453–67–1SI–13SI.

Meneghini, M.D., Wu, M., and Madhani, H.D. (2003). Conserved histone variant H2A.Z protects euchromatin from the ectopic spread of silent heterochromatin. Cell *112*, 725–736.

Mersfelder, E.L., and Parthun, M.R. (2006). The tale beyond the tail: histone core domain modifications and the regulation of chromatin structure. Nucleic Acids Research, *34*, 2653-2662.

Meshorer, E., and Misteli, T. (2006). Chromatin in pluripotent embryonic stem cells and differentiation. Nat Rev Mol Cell Biol *7*, 540–546.

Mishra, K., and Shore, D. (1999). Yeast Ku protein plays a direct role in telomeric silencing and counteracts inhibition by rif proteins. Curr. Biol. *9*, 1123–1126.

Moazed, D., Kistler, A., Axelrod, A., Rine, J., and Johnson, A.D. (1997). Silent information regulator protein complexes in Saccharomyces cerevisiae: a SIR2/SIR4 complex and evidence for a regulatory domain in SIR4 that inhibits its interaction with SIR3. Proc. Natl. Acad. Sci. U.S.a. *94*, 2186–2191.

Moazed, D. (2001). Common themes in mechanisms of gene silencing. Mol. Cell *8*, 489–498.

Mondoux, M.A., Scaife, J.G., and Zakian, V.A. (2007). Differential nuclear localization does not determine the silencing status of Saccharomyces cerevisiae telomeres. Genetics *177*, 2019–2029.

Moretti, P., Freeman, K., Coodly, L., and Shore, D. (1994) Evidence that a complex of SIR proteins interacts with the silencer and telomere-binding protein RAP1. Genes Dev. *8,* 2257-2269.

Moretti, P., and Shore, D. (2001). Multiple interactions in Sir protein recruitment by Rap1p at silencers and telomeres in yeast. Molecular and Cellular Biology *21*, 8082–8094.

Muller, H.J. (1930) Types of visible variations induced by X-rays in Drosophila. J. Genet. *22,* 299–335.

Murphy, G.A., Spedale, E.J., Powell, S.T., Pillus, L., Schultz, S.C., and Chen, L. (2003). The Sir4 C-terminal coiled coil is required for telomeric and mating type silencing in Saccharomyces cerevisiae. J. Mol. Biol. *334*, 769–780.

Musselman, C.A., and Kutateldze, T.G. (2011). Handpicking epigenetic marks with PHD fingers. Nucleic Acids Research. *39,* 9061-9071.

Newell-Price, J., Clark, A.J., and King, P. (2000). DNA methylation and silencing of gene expression. Trends Endocrinol. Metab. *11*, 142–148.

Ng, H.H., Feng, Q., Wang, H., Erdjument-Bromage, H., Tempst, P., Zhang, Y., and Struhl, K. (2002). Lysine methylation within the globular domain of histone H3 by Dot1 is important for telomeric silencing and Sir protein association. Genes Dev. *16*, 1518–1527.

Nguyen, A.T., and Zhang, Y. (2011). The diverse funcitons of Dot1 and H3K79 methylation. Genes&Dev. *25,* 1345-1358.

Nonaka, N., Kitajima, T., Yokobayashi, S., Xiao, G., Yamamoto, M., Grewal, S.I.S., and Watanabe, Y. (2002). Recruitment of cohesin to heterochromatic regions by Swi6/HP1 in fission yeast. Nat. Cell Biol. *4*, 89–93.

Oberdoerffer, P., and Sinclair, D.A. (2007). The role of nuclear architecture in genomic instability and ageing. Nat Rev Mol Cell Biol *8*, 692–702.

Olins, D.E., and Olins, A.L. (2003). Chromatin history: our view from the bridge. Nature Reviews Molecular Cell Biology, *4,* 809 – 814.

Onishi, M., Liou, G.-G., Buchberger, J.R., Walz, T., and Moazed, D. (2007). Role of the conserved Sir3-BAH domain in nucleosome binding and silent chromatin assembly. Mol. Cell *28*, 1015–1028.

Oppikofer, M., Kueng, S., Martino, F., Soeroes, S., Hancock, S.M., Chin, J.W., Fischle, W., and Gasser, S.M. (2011). A dual role of H4K16 acetylation in the establishment of yeast silent chromatin. Embo J. *30*, 2610–2621.

Oppikofer, M., Kueng, S., and Gasser, S.M. (2013a). SIR-nucleosome interactions: structure-function relationships in yeast silent chromatin. Gene *527*, 10–25.

Oppikofer, M., Kueng, S., Keusch, J.J., Hassler, M., Ladurner, A.G., Gut, H., and Gasser, S.M. (2013b). Dimerization of Sir3 via its C-terminal winged helix domain is essential for yeast heterochromatin formation. Embo J. *32*, 437-449

Osborne, E.A., Dudoit, S., and Rine, J. (2009). The establishment of gene silencing at single-cell resolution. Nature Genetics, *41*, 800-807

Park, Y., Hanish, J., and Lustig, A.J. (1998). Sir3p domains involved in the initiation of telomeric silencing in Saccharomyces cerevisiae. Genetics *150*, 977–986.

Pryde, F.E., and Louis, E.J. (1999). Limitations of silencing at native yeast telomeres. Embo J. *18*, 2538–2550.

Radman-Livaja, M., Ruben, G., Weiner, A., Friedman, N., Kamakaka, R., and Rando, O.J. (2011). Dynamics of Sir3 spreading in budding yeast: secondary recruitment sites and euchromatic localization. Embo J. *30*, 1012–1026.

Ramakrishnan, V. (1997). Histone Structure and the Organization of the Nucleosome. Annu. Rev. Biophys. Biomol. Struct. *26,* 83-112.

Ray, A., Hector, R.E., Roy, N., Song, J.-H., Berkner, K.L., and Runge, K.W. (2003). Sir3p phosphorylation by the Slt2p pathway effects redistribution of silencing function and shortened lifespan. Nat. Genet. *33*, 522–526.

Raynaud, C., Mallory, A.C., Latrasse, D., Jégu, T., Bruggeman, Q., Delarue, M., Bergounioux, C., and Benhamed, M. (2014). Chromatin meets the cell cycle. J. Exp. Bot. *65*, 2677–2689.

Renauld, H., Aparicio, O.M., Zierath, P.D., Billington, B.L., Chhablani, S.K., and Gottschling, D.E. (1993). Silent domains are assembled continuously from the telomere and are defined by promoter distance and strength, and by SIR3 dosage. Genes Dev. *7*, 1133–1145.

Rivier, D.H., Ekena, J.L., and Rine, J. (1999). HMR-I is an origin of replication and a silencer in Saccharomyces cerevisiae. Genetics *151*, 521–529.

Ropero, S., Esteller, M. (2007). The role of histone deacetlases (HDACs) in human cancer. Molecular Oncology *1,* 19-25.

Roth, S.Y., Denu, J.M., and Allis, C.D. (2001). Histone Acetyltransferases. Annu. Rev. Biocehem. *70,* 81-120.

Roy, R., Meier, B., McAinsh, A.D., Feldmann, H.M., and Jackson, S.P. (2004). Separation-of-function mutants of yeast Ku80 reveal a Yku80p-Sir4p interaction involved in telomeric silencing. J. Biol. Chem. *279*, 86–94.

Ruault, M., De Meyer, A., Loiodice, I., and Taddei, A. (2011). Clustering heterochromatin: Sir3 promotes telomere clustering independently of silencing in yeast. J. Cell Biol. *192*, 417-431

Rudner, A.D., Hall, B.E., Ellenberger, T., and Moazed, D. A. (2005). Nonhistone Protein-Protein Interaction Required for Assembly of the SIR Complex and Silent Chromatin.

Molecular and Cellular Biology *25*, 4514–4528.

Rudner, A.D. Overexpression of Asf2 disrupts the Sir3-Sir4 interaction (2003). Unpublished laboratory work, University of Ottawa.

Rusche, L.N., Kirchmaier, A.L., and Rine, J. (2002). Ordered Nucleation and Spreading of Silenced Chromatin in *Saccharomyces cerevisiae*. Molecular Biology of the Cell.

Rusche, L.N. Kirchmaier, A.L., and Rine, J. (2003). The Establishment, Inheritance, and Function of Silenced Chromatin in *Saccharomyces Cerevisiae*. Annu. Rev. Biochem. *72,* 481-516.

Salvi, J.S., Chan, J.N.Y, Pettigrew, C., Liu, T.T., Wu, J.D., and Mekhail, K. (2013). Enforcement of a lifespan-sustaining distribution of Sir2 between telomeres, mating-type loci, and rDNA repeats by Rif1. Aging Cell *12,* 67-75.

Sampath, V., Yuan, P., Wang, I.X., Prugar, E., van Leeuwen, F., and Sternglanz, R. (2009). Mutational analysis of the Sir3 BAH domain reveals multiple points of interaction with nucleosomes. Molecular and Cellular Biology *29*, 2532–2545.

Schober, H., Ferreira, H., Kalck, V., Gehlen, L.R., and Gasser, S.M. (2009). Yeast telomerase and the SUN domain protein Mps3 anchor telomeres and repress subtelomeric recombination. Genes Dev. *23*, 928–938.

Sekinger, E.A., and Gross, D.S. (2001). Silenced chromatin is permissive to activator binding and PIC recruitment. Cell *105*, 403–414.

Shankaranarayana, G.D., Motamedi, M.R., Moazed, D., and Grewal, S.I.S. (2003). Sir2 regulates histone H3 lysine 9 methylation and heterochromatin assembly in fission yeast. Curr. Biol. *13*, 1240–1246.

Shi, T., Bunker, R.D., Mattarocci, S., Ribeyre, C., Faty, M., Gut, H., Scrima, A., Rass, U., Rubin, S.M., Shore, D., et al. (2013). Rif1 and Rif2 shape telomere function and architecture through multivalent Rap1 interactions. Cell *153*, 1340–1353.

Shou, W., Seol, J.H., Shevchenko, A., Baskerville, C., Moazed, D., Chen, Z.W., Jang, J., Shevchenko, A., Charbonneau, H., and Deshaies, R.J. (1999). Exit from mitosis is triggered by Tem1-dependent release of the protein phosphatase Cdc14 from nucleolar RENT complex. Cell *97*, 233–244.

Singer, M.S., Kahana, A., Wolf, A.J., Meisinger, L.L., and al, E. (1998). Identification of high-copy disruptors of telomeric silencing in Saccharomyces cerevisiae. ….

Sperling, A.S., and Grunstein, M. (2009). Histone H3 N-terminus regulates higher order structure of yeast heterochromatin. Proceedings of the National Academy of Sciences *106*, 13153–13159.

Stancheva, I. (2011). Revisiting heterochromatin in embryonic stem cells. PLOS Genetics *7*,

e1002093.

Stone, E.M., and Pillus, L. (1996). Activation of an MAP kinase cascade leads to Sir3p hyperphosphorylation and strengthens transcriptional silencing. J. Cell Biol. *135*, 571–583.

Strahl-Bolsinger, S., Hecht, A., Luo, K., and Grunstein, M. (1997). SIR2 and SIR4 interactions differ in core and extended telomeric heterochromatin in yeast. Genes & Dev. *11,* 83-93

Straight, A.F., Shou, W., Dowd, G.J., Turck, C.W., Deshaies, R.J., Johnson, A.D., and Moazed, D. (1999). Net1, a Sir2-associated nucleolar protein required for rDNA silencing and nucleolar integrity. Cell *97*, 245–256.

Suka, N., Luo, K., and Grunstein, M. (2002). Sir2p and Sas2p opposingly regulate acetylation of yeast histone H4 lysine16 and spreading of heterochromatin. Nat. Genet. *32*, 378–383.

Sun, Z., and Allis, C.D. (2002). Ubiquitination of Histone H2B regulates H3 methylation and Gene Silencing in Yeast. Letters to Nature *418,* 104-108.

Sussel, L., and Shore, D. (1991). Separation of transcriptional activation and silencing functions of the RAP1-encoded repressor/activator protein 1: isolation of viable mutants affecting both silencing and telomere length. Proc. Natl. Acad. Sci. U.S.a. *88*, 7749–7753.

Swygert, S.G., Manning, B.J., Senapati, S., Kaur, P., Lindsay, S., Demeler, B., and Peterson, C.L. (2014). Solution-state conformation and stoichiometry of yeast Sir3 heterochromatin fibres. Nat Commun *5*, 4751.

Taddei, A., Hediger, F., Neumann, F.R., Bauer, C., and Gasser, S.M. (2004). Separation of silencing from perinuclear anchoring functions in yeast Ku80, Sir4 and Esc1 proteins. Embo J. *23*, 1301–1312.

Taddei, A., Van Houwe, G., Nagai, S., Erb, I., van Nimwegen, E., and Gasser, S.M. (2009). The functional importance of telomere clustering: global changes in gene expression result from SIR factor dispersion. Genome Res. *19*, 611–625.

Takahashi, Y.-H., Schulze, J.M., Jackson, J., Hentrich, T., Seidel, C., Jaspersen, S.L., Kobor, M.S., and Shilatifard, A. (2011). Dot1 and histone H3K79 methylation in natural telomeric and HM silencing. Mol. Cell *42*, 118–126.

Tanny, J.C., Kirkpatrick, D.S., Gerber, S.A., Gygi, S.P., and Moazed, D. (2004). Budding yeast silencing complexes and regulation of Sir2 activity by protein-protein interactions. Molecular and Cellular Biology *24*, 6931–6946.

Teytelman, L., Thurtle, D.M., Rine, J., and van Oudenaarden, A. (2013). Highly expressed loci are vulnerable to misleading ChIP localization of multiple unrelated proteins. Proceedings of the National Academy of Sciences *110*, 18602–18607.

Thomas, J.O., and Kornberg, R. D. (1975). An octamer of histones in chromatin and free in solution. Proc. Nat. Acad. Sci. USA *72*, 2626-2630.

Thompson, J.S., Ling, X., and Grunstein, M. (1994). Histone H3 amino terminus is required for telomeric and silent mating locus repression in yeast. Nature *369*, 245–247.

Thurtle, D.M., and Rine, J. (2014). The molecular topography of silenced chromatin in Saccharomyces cerevisiae. Genes Dev. *28*, 245–258.

Torres-Machorro, A.L., and Pillus, L. (2014). Bypassing the Requirement for an Essential MYST Acetyltransferase. Genetics *197*, 851–863.

Trojer, P., and Reinberg, D. (2007). Facultative Heterochromatin: Is there a Distinctive Molecular Signature? Molecular Cell, *28,* 1-13.

Van de Vosse, D.W., Wan, Y., Lapetina, D.L., Chen, W.-M., Chiang, J.-H., Aitchison, J.D., and Wozniak, R.W. (2013). A role for the nucleoporin Nup170p in chromatin structure and gene silencing. Cell *152*, 969–983.

Van Leeuwen, F., Gafken, P.R., and Gottschling, D.E. (2002). Dot1p modulates silencing in yeast by methylation of the nucleosome core. Cell *109*, 745–756.

Varunan, S.M., Tripathi, J., Bhattacharyya, S., Suhane, T., and Bhattacharyya, M.K. (2013). Plasmodium falciparum origin recognition complex subunit 1 (PfOrc1) functionally complements Δsir3 mutant of Saccharomyces cerevisiae. Mol. Biochem. Parasitol. *191*, 28–35.

Vassilopoulos, A., Fritz, K.S., Petersen, D.R., and Gius, D. (2011). The human sirtuin family: Evolutionary divergences and Functions. Human Genomics. *5,* 485-496.
Verdel, A., and Moazed, D. (2005). RNAi-directed assembly of heterochromatin in fission yeast. FEBS Letters *579,* 5872-5878.

Wahlin, J., and Cohn, M. (2000). Saccharomyces cerevisiae RAP1 binds to telomeric sequences with spatial flexibility. Nucleic Acids Research *28*, 2292–2301.

Wang, F., Li, G., Altaf, M., Lu, C., Currie, M.A., Johnson, A., and Moazed, D. (2013). Heterochromatin protein Sir3 induces contacts between the amino terminus of histone H4 and nucleosomal DNA. Proceedings of the National Academy of Sciences *110*, 8495–8500.

Wang, X., Connelly, J.J., Wang, C.-L., and Sternglanz, R. (2004). Importance of the Sir3 N terminus and its acetylation for yeast transcriptional silencing. Genetics *168*, 547–551.

Wellinger, R.J., and Zakian, V.A. (2012). Everything you ever wanted to know about Saccharomyces cerevisiae telomeres: beginning to end. Genetics *191*, 1073–1105.

Williams, E., and Rudner, A.D. (2014). Mutation of conserved residues in Asf2 blocks interaction of Asf2 with Sir3. Unpublished laboratory work, University of Ottawa.

Wu, C.-S., Chen, Y.-F., and Gartenberg, M.R. (2011). Targeted sister chromatid cohesion by Sir2. PLOS Genetics *7*, e1002000.

Wutz, A. (2011). Gene silencing in X-chromosome inactivation: advances in understanding facultative heterochromatin formation. Nat Rev Genet *12*, 542–553.

Xu, F., Zhang, Q., Zhang, K., Xie, W., and Grunstein, M. (2007). Sir2 deacetylates histone H3 lysine 56 to regulate telomeric heterochromatin structure in yeast. Mol. Cell *27*, 890–900.

Yang, B., and Kirchmaier, A.L. (2006). Bypassing the catalytic activity of SIR2 for SIR protein spreading in Saccharomyces cerevisiae. Molecular Biology of the Cell *17*, 5287–5297.

Yang, B., Britton, J., and Kirchmaier, A.L. (2008). Insights into the impact of histone acetylation and methylation on Sir protein recruitment, spreading, and silencing in Saccharomyces cerevisiae. J. Mol. Biol. *381*, 826–844.

Yang, D., Fang, Q., Wang, M., Ren, R., Wang, H., He, M., Sun, Y., Yang, N., and Xu, R.-M. (2013). Nα-acetylated Sir3 stabilizes the conformation of a nucleosome-binding loop in the BAH domain. Nat. Struct. Mol. Biol. *20*, 1116–1118.

Yasuhara, J.C., and Wakimoto, B.T. (2006). Oxymoron no more: the expanding world of heterochromatic genes. Trends in Genetics. *22*, 330-338.

Zhang, X., Yu, Q., Olsen, L., and Bi, X. (2012). Functions of protosilencers in the formation and maintenance of heterochromatin in Saccharomyces cerevisiae. PLOS One *7*, e37092.

Zhu, Q., Pao, G.M., Huynh, A.M., Suh, H., Tonnu, N., Nederlof, P.M., Gage, F.H., and Verma, I.M. (2011). BRCA1 tumour suppression occurs via heterochromatin-mediated silencing. Nature *477*, 179–184.

Zhu, X., and Gustafsson, C.M. (2009). Distinct differences in chromatin structure at subtelomeric X and Y' elements in budding yeast. PLOS One *4*, e6363.

Contributions of Collaborators

Carole Doré – Figure 9 and construction of some of the strains and plasmids used in this study
Adam Rudner – Figure 18 B, C and construction of some of the strains and plasmids used in this study
Katherine Harding – quantitative silencing assays discussed in Results section 3.1.3 and construction of strains ADR 7325, 7327

Appendix

Appendix 1 – Strains, Plasmids, and Primers used in this Study

Table S1.1 Yeast strains used in this study

Strain	Genotype	Origin (previous name)
ADR 2764	W303 *MAT**α** SIR3-3xFLAG-kanMX*	Rudner Lab
ADR 3101	W303 *MAT**a** sir4Δ::natMX*	Rudner Lab
ADR 3353	W303 *MAT**a** sir3Δ::kanMX*	Rudner Lab
ADR 3632	W303 *MAT**a** sir2Δ::HIS3*	Rudner Lab
ADR 3684	*MAT**a** ade2-101 his3-Δ200 leu2-Δ1 lys2-801 trp1-Δ1 ura3-52 TelV-R::URA3 (2kb) DIU5(2-13)*	Renauld et al 1993 (UCC506)
ADR 3685	*MAT**a** ade2-101 his3-Δ200 leu2-Δ1 lys2-801 trp1-Δ1 ura3-52 TelV-R::URA3 (1kb) DIU5(2-13)*	Renauld et al 1993 (UCC507)
ADR 3686	*MAT**a** ade2-101 his3-Δ200 leu2-Δ1 lys2-801 trp1-Δ1 ura3-52 TelV-R::URA3 (3.5kb) DIU5(2-13)*	Renauld et al 1993 (UCC508)
ADR 3687	*MAT**a** ade2-101 his3-Δ200 leu2-Δ1 lys2-801 trp1-Δ1 ura3-52 TelV-R::URA3 (2.5kb) DIU5(2-13)*	Renauld et al 1993 (UCC509)
ADR 3689	*MAT**a** ade2-101 his3-Δ200 leu2-Δ1 lys2-801 trp1-Δ1 ura3-52 TelV-R::URA3 (1kb) DIU5(2-13) ppr1Δ::HIS3*	Renauld et al 1993 (UCC519)
ADR 4006	W303 *MAT**a** bar1Δ*	Rudner Lab
ADR 4062	W303 *MAT**a** hmrΔE::TRP1, TelVII-L::URA3*	Rudner Lab
ADR 5010	W303 *MAT**α** hmrE::Aeb4xlexops-KlURA3-HMRI*	Chou et al 2008 (JN19)
ADR 5012	W303 *MAT**α** hmrE::Aeb4xlexops-KlURA3-HMRI sir4Δ::kanMX*	Chou et al 2008 (CCC47)
ADR 5469	W303 *MAT**a** hmrΔE::TRP1, TelVII-L::URA3 sir3Δ::kanMX*	Rudner Lab
ADR 6213	*MAT**a** ade2-101 his3-Δ200 leu2-Δ1 lys2-801 trp1-Δ1 ura3-52 TelV-R::URA3 (5.5kb) DIU5(2-13) ppr1Δ::HIS3*	Renauld et al 1993 (UCC523)
ADR 6460	W303 *MAT**α** hmrE::Aeb4xlexops-KlURA3-HMRI sir3Δ::hphMX*	This Study
ADR 6461	W303 *MAT**α** hmrE::Aeb4xlexops-KlURA3-HMRI sir3Δ::hphMX sir4Δ::kanMX*	This Study
ADR 7092	*MAT**a** ade2-101 his3-Δ200 leu2-Δ1 lys2-801 trp1-Δ1 ura3-52 TelV-R::URA3 (1kb) DIU5(2-13) ppr1Δ::HIS3 sir3Δ::hphMX*	This Study
ADR 7097	*MAT**a** ade2-101 his3-Δ200 leu2-Δ1 lys2-801 trp1-Δ1 ura3-52 TelV-R::URA3 (5.5kb) DIU5(2-13) ppr1Δ::HIS3 sir3Δ::hphMX*	This Study
ADR 7098	*MAT**a** ade2-101 his3-Δ200 leu2-Δ1 lys2-801 trp1-Δ1 ura3-52 TelV-R::URA3 (1kb) DIU5(2-13) ppr1Δ::HIS3 sir4Δ::kanMX*	This Study
ADR 7101	*MAT**a** ade2-101 his3-Δ200 leu2-Δ1 lys2-801 trp1-Δ1 ura3-52 TelV-R::URA3 (5.5kb) DIU5(2-13) ppr1Δ::HIS3 sir4Δ::kanMX*	This Study
ADR 7325	*MAT**a** ade2-101 his3-Δ200 leu2-Δ1 lys2-801 trp1-Δ1 ura3-52 TelV-R::URA3 (1kb) DIU5(2-13) ppr1Δ::HIS3 sir2Δ::natMX*	This Study
ADR 7327	*MAT**a** ade2-101 his3-Δ200 leu2-Δ1 lys2-801 trp1-Δ1 ura3-52 TelV-R::URA3 (5.5kb) DIU5(2-13) ppr1Δ::HIS3 sir2Δ::natMX*	This Study

Table S1.2 Plasmids used in this study

Plasmid	Genotype	Origin (previous name)
P1	*KanMx*	Rudner Lab
pAR357	*CEN-LEU2*	Rudner Lab
pAR359	*GST*	Rudner Lab
pAR411	pGEX24 *GST-SIR4*$^{1267-1358}$	Rudner Lab
pAR412	pGEX24 *GST-sir4-M1307N*$^{1267-1358}$	Rudner Lab
pAR469	*2μ-SIR3-LEU2*	Rudner Lab
pAR512	*CEN-SIR3-LEU2*	Rudner Lab
pAR534	*2μ-LEU2*	Rudner Lab
pAR787	*2μ-LEXA-HIS3*	Wu et al 2011 (pBTM116His3)
pAR788	*2μ-SIR3-LEXA-HIS3*	Wu et al 2011 (pCSW14)
pAR790	*2μ-LexA-SIR2*$^{78-562}$*-HIS3*	Wu et al 2011 (pCSW22)
pAR979	*CEN-SIR3-3xFLAG-LEU2*	Rudner Lab
pAR982	*CEN-sir3-4A-LEU2*	This Study
pAR984	*CEN-sir-3A-LEU2*	This Study
pAR985	*CEN-sir3-2A-LEU2*	This Study
pAR986	*CEN-sir3-3A-3xFLAG-LEU2*	This Study
pAR988	*CEN-sir3-2A-3xFLAG-LEU2*	This Study
pAR1009	*sir3-2A*$^{464-978}$*-His*$_6$	Rudner Lab
pAR1011	*sir3-4A*$^{464-978}$*His*$_6$	Rudner Lab
pAR1012	*SIR3*$^{464-978}$*-His*$_6$	Rudner Lab
pAR1017	*2μ-sir3-4A-LEU2*	This Study
pAR1020	*2μ-SIR3-LEU2*	This Study
pAR1023	*2μ-sir3-3A-LEU2*	This Study
pAR1042	*sir3-3A*$^{464-978}$*-His*$_6$	Rudner Lab
pAR1056	*2μ-sir3-2A-LEU2*	This Study
pAR1061	*GST-SIR4*$^{1198-1358}$	Rudner Lab
pAR1062	*GST-sir4-I1311N*$^{1198-1358}$	Rudner Lab
pAR1064	*CEN-sir3-4A-3xFLAG-LEU2*	This Study
pAR1189	*2μ-sir3-4A-LEXA-HIS3*	This Study
pJB116	pBluescript-KS-*SIR3*	Rudner Lab

Table S1.3 primers used for site-directed mutagenesis of Sir3

Primer	Sequence	Sir3 mutation
977	TGTCCCGAAAGCTGCAGCCGCCGCGACACTAATATT	*4A*
978	TGTCCCGAAAGCTGCAGCCGCCAAGACACTAATA	*3A*
979	TGTCCCGAAAGCTGCAGCAAGAAAGACACTA	*2A*

Table S1.4 qPCR primers used in this study

Primer	Sequence	Target gene
499	GCCTTCTACGTTTCCATCCA	*ACT1*
501	CGTAAATTGGAACGACGTGA	*ACT1*
1236	CCCAGTATTCTTAACCCAACTGC	*URA3*
1237	GCAGCACGTTCCTTATATGTAGC	*URA3*
1493	CATCATTGTTGGCAGAGGAC	*KlURA3*
1494	CTGATTCTCTTTTGGTACGCTTC	*KlURA3*
1501	ACGTATCTTGTACCCTTTTTATTGC	*HMR-E* (A element)
1503	AAAGTTTTGTTTGCAAATGTGG	*HMR-E* (A element)

Sequences of all other primers used in this study are available upon request

Appendix 2 – Statistical Analysis

In the Two-Way ANOVA Tables S2.1b to S2.18b, "Row Factor" refers to the genotype of the overexpressed Sir3 (wild-type or *sir3-4A*). "Column Factor" refers to the growth media (FOA or –URA) used to select for transcriptional silencing or activation of the *URA3* gene.

Tables S2.1 - Sir2 – 1.0 kb

Table S2.1a One-Way ANOVA summary (analysis of all 6 conditions) for Sir2 (1.0 kb)

ANOVA table	SS	DF	MS	F (DFn	DFd)	P value
Treatment (between columns)	5.90128	5	1.18026	F (5	25) = 34.7063	P < 0.0001
Residual (within columns)	0.850174	25	0.034007			
Total	6.75146	30				

Table S2.1b Two-Way ANOVA summary (SIR3-2u and sir3-4A-2u in FOA and –URA only) for Sir2 (1.0 kb)

ANOVA table	SS	DF	MS	F (DFn	DFd)	% of total variation	P value
Interaction	0.00852488	1	0.00852488	F (1	16) = 0.190950	0.274455	P = 0.6680
Row Factor	0.155201	1	0.155201	F (1	16) = 3.47636	4.99662	P = 0.0807
Column Factor	2.22807	1	2.22807	F (1	16) = 49.9070	71.7319	P < 0.0001
Residual	0.714313	16	0.0446445				

Table S2.1c Post-hoc comparisons for Sir2 (1.0 kb)

Post-Hoc Comparison	Bonferroni's multiple comparisons test	Adjusted P value
Sir2 delete vs.	empty	< 0.0001
	SIR3 OFF	< 0.0001
	sir3-4A OFF	< 0.0001
	SIR3 ON	0.1769
	sir3-4A ON	0.0012
SIR3 vs sir3-4A	OFF	> 0.9999
	ON	0.6661
OFF vs ON	SIR3	< 0.0001
	sir3-4A	0.0001

Tables S2.2 - Sir2 – 5.5 kb

Table S2.2a One-Way ANOVA summary (analysis of all 6 conditions) for Sir2 (5.5 kb)

ANOVA table	SS	DF	MS	F (DFn	DFd)	P value
Treatment (between columns)	2.47688	5	0.495376	F (5	22) = 14.2235	P < 0.0001
Residual (within columns)	0.766217	22	0.0348281			
Total	3.2431	27				

Table S2.2b Two-Way ANOVA summary (SIR3-2u and sir3-4A-2u in FOA and –URA only) for Sir2 (5.5 kb)

ANOVA table	SS	DF	MS	F (DFn	DFd)	% of total variation	P value
Interaction	0.0657283	1	0.0657283	F (1	14) = 2.08657	3.63121	0.1706
Row Factor	0.00474951	1	0.00474951	F (1	14) = 0.150775	0.262391	0.7036
Column Factor	1.29375	1	1.29375	F (1	14) = 41.0704	71.4741	< 0.0001
Residual	0.44101	14	0.0315007				

Table S2.2c Post-hoc comparisons for Sir2 (5.5 kb)

Post-Hoc Comparison	Bonferroni's multiple comparisons test	Adjusted P value
Sir2 delete vs.	empty	0.4017
	SIR3 OFF	< 0.0001
	sir3-4A OFF	< 0.0001
	SIR3 ON	0.7599
	sir3-4A ON	> 0.9999
SIR3 vs sir3-4A	OFF	> 0.9999
	ON	> 0.9999
OFF vs ON	SIR3	0.0268
	sir3-4A	0.0002

Tables S2.3 - Sir3 – 1.0 kb

Table S2.3a One-Way ANOVA summary (analysis of all 6 conditions) for Sir3 (1.0 kb)

ANOVA table	SS	DF	MS	F (DFn	DFd)	P value
Treatment (between columns)	8.79959	5	1.75992	F (5	34) = 70.3716	P < 0.0001
Residual (within columns)	0.850304	34	0.0250089			
Total	9.64989	39				

Table S2.3b Two-Way ANOVA summary (SIR3-2u and sir3-4A-2u in FOA and –URA only) for Sir3 (1.0 kb)

ANOVA table	SS	DF	MS	F (DFn	DFd)	% of total variation	P value
Interaction	0.0609911	1	0.0609911	F (1	22) = 2.56136	1.72503	0.1238
Row Factor	0.195699	1	0.195699	F (1	22) = 8.21849	5.53502	0.009
Column Factor	2.79392	1	2.79392	F (1	22) = 117.332	79.0213	< 0.0001
Residual	0.523864	22	0.023812				

Table S2.3c Post-hoc comparisons for Sir3 (1.0 kb)

Post-Hoc Comparison	Bonferroni's multiple comparisons test	Adjusted P value
Sir3 delete vs.	empty	< 0.0001
	SIR3 OFF	< 0.0001
	sir3-4A OFF	< 0.0001
	SIR3 ON	> 0.9999
	sir3-4A ON	0.0003
Empty vs	Sir3 OFF	0.0035
	sir3-4A OFF	0.0336
SIR3 vs sir3-4A	OFF	> 0.9999
	ON	0.0971
OFF vs ON	SIR3	< 0.0001
	sir3-4A	< 0.0001

Tables S2.4 - Sir3 – 5.5 kb

Table S2.4a One-Way ANOVA summary (analysis of all 6 conditions) for Sir3 (5.5 kb)

ANOVA table	SS	DF	MS	F (DFn	DFd)	P value
Treatment (between columns)	4.53843	5	0.907686	F (5	34) = 38.0241	P < 0.0001
Residual (within columns)	0.811626	34	0.0238713			
Total	5.35006	39				

Table S2.4b Two-Way ANOVA summary (SIR3-2u and sir3-4A-2u in FOA and –URA only) for Sir3 (5.5 kb)

ANOVA table	SS	DF	MS	F (DFn	DFd)	% of total variation	P value
Interaction	0.0110639	1	0.0110639	F (1	22) = 0.437400	0.471379	0.5152
Row Factor	0.189442	1	0.189442	F (1	22) = 7.48940	8.0712	0.012
Column Factor	1.55655	1	1.55655	F (1	22) = 61.5366	66.317	< 0.0001
Residual	0.556482	22	0.0252946				

Table S2.4c Post-hoc comparisons for Sir3 (5.5 kb)

Post-Hoc Comparison	Bonferroni's multiple comparisons test	Adjusted P value
Sir3 delete vs.	empty	0.008
	SIR3 OFF	< 0.0001
	sir3-4A OFF	< 0.0001
	SIR3 ON	0.0775
	sir3-4A ON	0.001
SIR3 vs sir3-4A	OFF	0.0716
	ON	> 0.9999
OFF vs ON	SIR3	< 0.0001
	sir3-4A	< 0.0001

Tables S2.5 - Sir4 – 1.0 kb

Table S2.5a One-Way ANOVA summary (analysis of all 6 conditions) for Sir4 (1.0 kb)

ANOVA table	SS	DF	MS	F (DFn	DFd)	P value
Treatment (between columns)	10.6115	5	2.12231	F (5	25) = 67.3783	P < 0.0001
Residual (within columns)	0.78746	25	0.0314984			
Total	11.399	30				

Table S2.5b Two-Way ANOVA summary (SIR3-2u and sir3-4A-2u in FOA and –URA only) for Sir4 (1.0 kb)

ANOVA table	SS	DF	MS	F (DFn	DFd)	% of total variation	P value
Interaction	0.169095	1	0.169095	F (1	16) = 4.33568	6.74379	0.0537
Row Factor	0.0396017	1	0.0396017	F (1	16) = 1.01541	1.57938	0.3286
Column Factor	1.70011	1	1.70011	F (1	16) = 43.5916	67.8032	< 0.0001
Residual	0.624014	16	0.0390009				

Table S2.5c Post-hoc comparisons for Sir4 (1.0 kb)

Post-Hoc Comparison	Bonferroni's multiple comparisons test	Adjusted P value
Sir4 delete vs.	empty	< 0.0001
	SIR3 OFF	< 0.0001
	sir3-4A OFF	< 0.0001
	SIR3 ON	< 0.0001
	sir3-4A ON	< 0.0001
SIR3 vs sir3-4A	OFF	> 0.9999
	ON	0.3219
OFF vs ON	SIR3	< 0.0001
	sir3-4A	0.0138

Tables S2.6 - Sir4 – 5.5 kb

Table S2.6a One-Way ANOVA summary (analysis of all 6 conditions) for Sir4 (5.5 kb)

ANOVA table	SS	DF	MS	F (DFn	DFd)	P value
Treatment (between columns)	5.84166	5	1.16833	F (5	35) = 35.1076	P < 0.0001
Residual (within columns)	1.16475	35	0.0332786			
Total	7.00641	40				

Table S2.6b Two-Way ANOVA summary (SIR3-2u and sir3-4A-2u in FOA and –URA only) for Sir4 (5.5 kb)

ANOVA table	SS	DF	MS	F (DFn	DFd)	% of total variation	P value
Interaction	0.0136811	1	0.0136811	F (1	22) = 0.362130	0.526744	0.5535
Row Factor	0.00195809	1	0.00195809	F (1	22) = 0.0518294	0.0753897	0.822
Column Factor	1.75214	1	1.75214	F (1	22) = 46.3782	67.4605	< 0.0001
Residual	0.831148	22	0.0377795				

Table S2.6c Post-hoc comparisons for Sir4 (5.5 kb)

Post-Hoc Comparison	Bonferroni's multiple comparisons test	Adjusted P value
Sir4 delete vs.	empty	0.0525
	SIR3 OFF	< 0.0001
	sir3-4A OFF	< 0.0001
	SIR3 ON	0.0013
	sir3-4A ON	0.0089
SIR3 vs sir3-4A	OFF	> 0.9999
	ON	> 0.9999
OFF vs ON	SIR3	0.0004
	sir3-4A	< 0.0001

Tables S2.7 - H3 – 1.0 kb

Table S2.7a One-Way ANOVA summary (analysis of all 8 conditions) for H3 (1.0 kb)

ANOVA table	SS	DF	MS	F (DFn	DFd)	P value
Treatment (between columns)	0.601695	7	0.0859565	F (7	30) = 6.11800	P = 0.0002
Residual (within columns)	0.421493	30	0.0140498			
Total	1.02319	37				

Table S2.7b Two-Way ANOVA summary (SIR3-2u and sir3-4A-2u in FOA and –URA only) for H3 (1.0 kb)

ANOVA table	SS	DF	MS	F (DFn	DFd)	% of total variation	P value
Interaction	0.000431657	1	0.000431657	F (1	14) = 0.0302430	0.110656	0.8644
Row Factor	0.000491692	1	0.000491692	F (1	14) = 0.0344492	0.126046	0.8554
Column Factor	0.189435	1	0.189435	F (1	14) = 13.2723	48.5622	0.0027
Residual	0.199822	14	0.014273				

Table S2.7c Post-hoc comparisons for H3 (1.0 kb)

Post-Hoc Comparison	Bonferroni's multiple comparisons test	Adjusted P value
Sir2 delete vs.	empty	0.6543
	SIR3 OFF	0.1007
	sir3-4A OFF	0.0509
	SIR3 ON	> 0.9999
	sir3-4A ON	> 0.9999
Sir3 delete vs.	empty	0.0498
	SIR3 OFF	0.0059
	sir3-4A OFF	0.0028
	SIR3 ON	> 0.9999
	sir3-4A ON	> 0.9999
Sir4 delete vs.	empty	0.0215
	SIR3 OFF	0.003
	sir3-4A OFF	0.0015
	SIR3 ON	0.8713
	sir3-4A ON	0.856
SIR3 vs sir3-4A	OFF	> 0.9999
	ON	> 0.9999
OFF vs ON	SIR3	0.3668
	sir3-4A	0.2041

Tables S2.8 - H3 – 5.5 kb

Table S2.8a One-Way ANOVA summary (analysis of all 8 conditions) for H3 (5.5 kb)

ANOVA table	SS	DF	MS	F (DFn	DFd)	P value
Treatment (between columns)	0.106308	7	0.0151868	F (7	21) = 1.68721	P = 0.1665
Residual (within columns)	0.189025	21	0.00900117			
Total	0.295332	28				

Table S2.8b Two-Way ANOVA summary (SIR3-2u and sir3-4A-2u in FOA and –URA only) for H3 (5.5 kb)

ANOVA table	SS	DF	MS	F (DFn	DFd)	% of total variation	P value
Interaction	0.00339174	1	0.00339174	F (1	10) = 0.452909	2.70141	0.5162
Row Factor	0.00787214	1	0.00787214	F (1	10) = 1.05119	6.26989	0.3294
Column Factor	0.0406754	1	0.0406754	F (1	10) = 5.43150	32.3965	0.042
Residual	0.0748879	10	0.00748879				

Table S2.8c Post-hoc comparisons for H3 (5.5 kb)

Post-Hoc Comparison	Bonferroni's multiple comparisons test	Adjusted P value
Sir2 delete vs.	empty	> 0.9999
	SIR3 OFF	> 0.9999
	sir3-4A OFF	> 0.9999
	SIR3 ON	> 0.9999
	sir3-4A ON	> 0.9999
Sir3 delete vs.	empty	> 0.9999
	SIR3 OFF	0.5556
	sir3-4A OFF	0.9173
	SIR3 ON	> 0.9999
	sir3-4A ON	> 0.9999
Sir4 delete vs.	empty	> 0.9999
	SIR3 OFF	0.622
	sir3-4A OFF	0.9855
	SIR3 ON	> 0.9999
	sir3-4A ON	> 0.9999
SIR3 vs sir3-4A	OFF	> 0.9999
	ON	> 0.9999
OFF vs ON	SIR3	> 0.9999
	sir3-4A	> 0.9999

Tables S2.9 - Sir2/H3 – 1.0 kb

Table S2.9a One-Way ANOVA summary(analysis of all 6 conditions) for Sir2/H3 (1.0 kb)

ANOVA table	SS	DF	MS	F (DFn	DFd)	P value
Treatment (between columns)	2.95114	5	0.590229	F (5	19) = 14.7052	P < 0.0001
Residual (within columns)	0.762613	19	0.0401375			
Total	3.71376	24				

Table S2.9b Two-Way ANOVA summary (SIR3-2u and sir3-4A-2u in FOA and –URA only) for Sir2/H3 (1.0 kb)

ANOVA table	SS	DF	MS	F (DFn	DFd)	% of total variation	P value
Interaction	0.00589882	1	0.00589882	F (1	12) = 0.137065	0.401067	0.7177
Row Factor	0.125841	1	0.125841	F (1	12) = 2.92404	8.55605	0.113
Column Factor	0.822603	1	0.822603	F (1	12) = 19.1140	55.9296	0.0009
Residual	0.51644	12	0.0430367				

Table S2.9c Post-hoc comparisons for Sir2/H3 (1.0 kb)

Post-Hoc Comparison	Bonferroni's multiple comparisons test	Adjusted P value
Sir2 delete/H3 vs.	empty	< 0.0001
	SIR3 OFF	0.0002
	sir3-4A OFF	< 0.0001
	SIR3 ON	0.7359
	sir3-4A ON	0.0245
SIR3 vs sir3-4A	OFF	> 0.9999
	ON	> 0.9999
OFF vs ON	SIR3	0.023
	sir3-4A	0.0773

Tables S2.10 - Sir2/H3 – 5.5 kb

Table S2.10a One-Way ANOVA summary (analysis of all 6 conditions) for Sir2/H3 (5.5 kb)

ANOVA table	SS	DF	MS	F (DFn	DFd)	P value
Treatment (between columns)	1.83626	5	0.367252	F (5	13) = 6.81509	P = 0.0025
Residual (within columns)	0.700544	13	0.053888			
Total	2.5368	18				

Table S2.10b Two-Way ANOVA summary (SIR3-2u and sir3-4A-2u in FOA and –URA only) for Sir2/H3 (5.5 kb)

ANOVA table	SS	DF	MS	F (DFn	DFd)	% of total variation	P value
Interaction	0.0220773	1	0.0220773	F (1	8) = 0.361228	1.82893	0.5645
Row Factor	0.00327454	1	0.00327454	F (1	8) = 0.0535778	0.27127	0.8228
Column Factor	0.692825	1	0.692825	F (1	8) = 11.3360	57.395	0.0098
Residual	0.48894	8	0.0611175				

Table S2.10c Post-hoc comparisons for Sir2/H3 (5.5 kb)

Post-Hoc Comparison	Bonferroni's multiple comparisons test	Adjusted P value
Sir2 delete/H3 vs.	empty	0.2272
	SIR3 OFF	0.0058
	sir3-4A OFF	0.0017
	SIR3 ON	0.3914
	sir3-4A ON	0.6708
SIR3 vs sir3-4A	OFF	> 0.9999
	ON	> 0.9999
OFF vs ON	SIR3	0.5182
	sir3-4A	0.0943

Tables S2.11 - Sir3/H3 –1.0 kb

Table S2.11a One-Way ANOVA summary (analysis of all 6 conditions) for Sir3/H3 (1.0 kb)

ANOVA table	SS	DF	MS	F (DFn	DFd)	P value
Treatment (between columns)	3.4856	5	0.69712	F (5	19) = 26.5670	P < 0.0001
Residual (within columns)	0.498561	19	0.0262401			
Total	3.98416	24				

Table S2.11b Two-Way ANOVA summary (SIR3-2u and sir3-4A-2u in FOA and –URA only) for Sir3/H3 (1.0 kb)

ANOVA table	SS	DF	MS	F (DFn	DFd)	% of total variation	P value
Interaction	0.00844577	1	0.00844577	F (1	12) = 0.348423	0.780415	0.566
Row Factor	0.22967	1	0.22967	F (1	12) = 9.47482	21.2222	0.0096
Column Factor	0.55322	1	0.55322	F (1	12) = 22.8226	51.1192	0.0005
Residual	0.29088	12	0.02424				

Table S2.11c Post-hoc comparisons for Sir3/H3 (1.0 kb)

Post-Hoc Comparison	Bonferroni's multiple comparisons test	Adjusted P value
Sir3 delete/H3 vs.	empty	< 0.0001
	SIR3 OFF	0.0029
	sir3-4A OFF	< 0.0001
	SIR3 ON	> 0.9999
	sir3-4A ON	0.0463
Empty vs.	SIR3 OFF	0.0005
	sir3-4A ON	0.0209
SIR3 vs sir3-4A	OFF	> 0.9999
	ON	0.2426
OFF vs ON	SIR3	0.0188
	sir3-4A	0.1138

Tables S2.12 - Sir3/H3 – 5.5 kb

Table S2.12a One-Way ANOVA summary (analysis of all 6 conditions) for Sir3/H3 (5.5 kb)

ANOVA table	SS	DF	MS	F (DFn	DFd)	P value
Treatment (between columns)	1.07537	5	0.215073	F (5	13) = 11.7266	P = 0.0002
Residual (within columns)	0.238428	13	0.0183406			
Total	1.31379	18				

Table S2.12b Two-Way ANOVA summary (SIR3-2u and sir3-4A-2u in FOA and –URA only) for Sir3/H3 (5.5 kb)

ANOVA table	SS	DF	MS	F (DFn	DFd)	% of total variation	P value
Interaction	0.00405428	1	0.00405428	F (1	8) = 0.408941	0.91988	0.5404
Row Factor	0.10121	1	0.10121	F (1	8) = 10.2088	22.9637	0.0127
Column Factor	0.256163	1	0.256163	F (1	8) = 25.8383	58.121	0.0009
Residual	0.0793127	8	0.00991409				

Table S2.12c Post-hoc comparisons for Sir3/H3 (5.5 kb)

Post-Hoc Comparison	Bonferroni's multiple comparisons test	Adjusted P value
Sir3 delete/H3 vs.	empty	0.0409
	SIR3 OFF	0.002
	sir3-4A OFF	< 0.0001
	SIR3 ON	0.2009
	sir3-4A ON	0.0133
SIR3 vs sir3-4A	OFF	0.6086
	ON	> 0.9999
OFF vs ON	SIR3	0.3414
	sir3-4A	0.0967

Tables S2.13 - Sir4/H3 –1.0 kb

Table S2.13a One-Way ANOVA summary (analysis of all 6 conditions) for Sir4/H3 (1.0 kb)

ANOVA table	SS	DF	MS	F (DFn	DFd)	P value
Treatment (between columns)	4.0614	5	0.812281	F (5	12) = 46.0989	P < 0.0001
Residual (within columns)	0.211445	12	0.0176204			
Total	4.27285	17				

Table S2.13b Two-Way ANOVA summary (SIR3-2u and sir3-4A-2u in FOA and –URA only) for Sir4/H3 (1.0 kb)

ANOVA table	SS	DF	MS	F (DFn	DFd)	% of total variation	P value
Interaction	0.0436056	1	0.0436056	F (1	8) = 1.72675	4.42899	0.2253
Row Factor	0.022513	1	0.022513	F (1	8) = 0.891498	2.28662	0.3727
Column Factor	0.716409	1	0.716409	F (1	8) = 28.3693	72.765	0.0007
Residual	0.202024	8	0.025253				

Table S2.13c Post-hoc comparisons for Sir4/H3 (1.0 kb)

Post-Hoc Comparison	Bonferroni's multiple comparisons test	Adjusted P value
Sir4 delete/H3 vs.	empty	< 0.0001
	SIR3 OFF	< 0.0001
	sir3-4A OFF	< 0.0001
	SIR3 ON	0.0008
	sir3-4A ON	< 0.0001
SIR3 vs sir3-4A	OFF	> 0.9999
	ON	0.7208
OFF vs ON	SIR3	0.001
	sir3-4A	0.0477

Tables S2.14 - Sir4/H3 – 5.5 kb

Table S2.14a One-Way ANOVA summary (analysis of all 6 conditions) for Sir4/H3 (5.5 kb)

ANOVA table	SS	DF	MS	F (DFn	DFd)	P value
Treatment (between columns)	1.32164	5	0.264328	F (5	12) = 8.50733	P = 0.0012
Residual (within columns)	0.372848	12	0.0310707			
Total	1.69449	17				

Table S2.14b Two-Way ANOVA summary (SIR3-2u and sir3-4A-2u in FOA and –URA only) for Sir4/H3 (5.5 kb)

ANOVA table	SS	DF	MS	F (DFn	DFd)	% of total variation	P value
Interaction	0.00442709	1	0.00442709	F (1	8) = 0.108871	0.47012	0.7499
Row Factor	0.00508099	1	0.00508099	F (1	8) = 0.124952	0.539559	0.7329
Column Factor	0.606877	1	0.606877	F (1	8) = 14.9244	64.4453	0.0048
Residual	0.325308	8	0.0406635				

Table S2.14c Post-hoc comparisons for Sir4/H3 (5.5 kb)

Post-Hoc Comparison	Bonferroni's multiple comparisons test	Adjusted P value
Sir3 delete/H3 vs.	empty	> 0.9999
	SIR3 OFF	0.0028
	sir3-4A OFF	0.0029
	SIR3 ON	0.4893
	sir3-4A ON	> 0.9999
SIR3 vs sir3-4A	OFF	> 0.9999
	ON	> 0.9999
OFF vs ON	SIR3	0.1296
	sir3-4A	0.0481

Tables S2.15 - H3K79me/H3 – 1.0 kb

Table S2.15a One-Way ANOVA summary (analysis of all 7 conditions) for H3K79me/H3 (1.0 kb)

ANOVA table	SS	DF	MS	F (DFn	DFd)	P value
Treatment (between columns)	2.21926	6	0.369877	F (6	23) = 9.59046	P < 0.0001
Residual (within columns)	0.887045	23	0.0385672			
Total	3.10631	29				

Table S2.15b Two-Way ANOVA summary (SIR3-2u and sir3-4A-2u in FOA and –URA only) for H3K79 Me/H3 (1.0 kb)

ANOVA table	SS	DF	MS	F (DFn	DFd)	% of total variation	P value
Interaction	0.0473357	1	0.0473357	F (1	12) = 1.47982	5.00184	0.2472
Row Factor	0.0273325	1	0.0273325	F (1	12) = 0.854475	2.88815	0.3735
Column Factor	0.487849	1	0.487849	F (1	12) = 15.2513	51.5497	0.0021
Residual	0.38385	12	0.0319875				

Table S2.15c Post-hoc comparisons for H3K79me /H3 (1.0 kb)

Post-Hoc Comparison	Bonferroni's multiple comparisons test	Adjusted P value
Sir2 delete H3K79me/H3 vs.	empty	0.0035
	SIR3 OFF	0.0023
	sir3-4A OFF	0.0037
	SIR3 ON	> 0.9999
	sir3-4A ON	0.2966
Sir3 delete H3K79me/H3 vs.	empty	0.0007
	SIR3 OFF	0.0004
	sir3-4A OFF	0.0007
	SIR3 ON	> 0.9999
	sir3-4A ON	0.0631
SIR3 vs sir3-4A	OFF	> 0.9999
	ON	> 0.9999
OFF vs ON	SIR3	0.044
	sir3-4A	> 0.9999

Tables S2.16 - H3K79me/H3 – 5.5 kb

Table S2.16a One-Way ANOVA summary (analysis of all 7 conditions) for H3K79me/H3 (5.5 kb)

ANOVA table	SS	DF	MS	F (DFn	DFd)	P value
Treatment (between columns)	0.390208	6	0.0650346	F (6	16) = 4.49321	P = 0.0075
Residual (within columns)	0.231584	16	0.014474			
Total	0.621791	22				

Table S2.16b Two-Way ANOVA summary (SIR3-2u and sir3-4A-2u in FOA and –URA only) for H3K79 Me/H3 (5.5 kb)

ANOVA table	SS	DF	MS	F (DFn	DFd)	% of total variation	P value
Interaction	0.00334682	1	0.00334682	F (1	8) = 0.233054	1.38788	0.6422
Row Factor	0.00123174	1	0.00123174	F (1	8) = 0.0857713	0.510785	0.7771
Column Factor	0.121682	1	0.121682	F (1	8) = 8.47325	50.4598	0.0196
Residual	0.114886	8	0.0143607				

Table S2.16c Post-hoc comparisons for H3K79me /H3 (5.5 kb)

Post-Hoc Comparison	Bonferroni's multiple comparisons test	Adjusted P value
Sir2 delete H3K79me/H3 vs.	empty	> 0.9999
	SIR3 OFF	0.082
	sir3-4A OFF	0.0607
	SIR3 ON	> 0.9999
	sir3-4A ON	> 0.9999
Sir3 delete H3K79me/H3 vs.	empty	> 0.9999
	SIR3 OFF	0.0194
	sir3-4A OFF	0.0144
	SIR3 ON	0.8281
	sir3-4A ON	> 0.9999
SIR3 vs sir3-4A	OFF	> 0.9999
	ON	> 0.9999
OFF vs ON	SIR3	> 0.9999
	sir3-4A	0.4128

Tables S2.17 - H4K16ac/H3 – 1.0 kb

Table S2.17a One-Way ANOVA summary (analysis of all 7 conditions) for H4K16ac/H3 (1.0 kb)

ANOVA table	SS	DF	MS	F (DFn	DFd)	P value
Treatment (between columns)	0.631504	6	0.105251	F (6	16) = 6.15746	P = 0.0017
Residual (within columns)	0.273491	16	0.0170932			
Total	0.904995	22				

Table S2.17b Two-Way ANOVA summary (SIR3-2u and sir3-4A-2u in FOA and –URA only) for H4K16ac/H3 (1.0 kb)

ANOVA table	SS	DF	MS	F (DFn	DFd)	% of total variation	P value
Interaction	0.0364115	1	0.0364115	F (1	8) = 4.05553	8.34532	0.0788
Row Factor	0.037266	1	0.037266	F (1	8) = 4.15070	8.54116	0.076
Column Factor	0.290808	1	0.290808	F (1	8) = 32.3903	66.6514	0.0005
Residual	0.071826	8	0.00897824				

Table S2.17c Post-hoc comparisons for H4K16ac/H3 (1.0 kb)

Post-Hoc Comparison	Bonferroni's multiple comparisons test	Adjusted P value
Sir2 delete H4K16ac/H3 vs.	empty	0.0692
	SIR3 OFF	0.1142
	sir3-4A OFF	0.1111
	SIR3 ON	> 0.9999
	sir3-4A ON	> 0.9999
Sir3 delete H4K16ac/H3 vs.	empty	0.0484
	SIR3 OFF	0.0799
	sir3-4A OFF	0.0778
	SIR3 ON	> 0.9999
	sir3-4A ON	> 0.9999
SIR3 vs sir3-4A	OFF	> 0.9999
	ON	0.7611
OFF vs ON	SIR3	0.0161
	sir3-4A	> 0.9999

Tables S2.18 - H4K16ac/H3 – 5.5 kb

Table S2.18a One-Way ANOVA summary (analysis of all 7 conditions) for H4K16ac/H3 (5.5 kb)

ANOVA table	SS	DF	MS	F (DFn	DFd)	P value
Treatment (between columns)	0.37774	6	0.0629566	F (6	14) = 5.73798	P = 0.0034
Residual (within columns)	0.153607	14	0.0109719			
Total	0.531346	20				

Table S2.18b Two-Way ANOVA summary (SIR3-2u and sir3-4A-2u in FOA and –URA only) for H4K16ac/H3 (5.5 kb)

ANOVA table	SS	DF	MS	F (DFn	DFd)	% of total variation	P value
Interaction	0.00234673	1	0.00234673	F (1	8) = 0.223217	0.678189	0.6492
Row Factor	0.0125451	1	0.0125451	F (1	8) = 1.19327	3.62545	0.3065
Column Factor	0.247032	1	0.247032	F (1	8) = 23.4972	71.3904	0.0013
Residual	0.0841058	8	0.0105132				

Table S2.18c Post-hoc comparisons for H4K16ac/H3 (5.5 kb)

Post-Hoc Comparison		Adjusted P value
Sir2 delete H4K16ac/H3 vs.	empty	> 0.9999
	SIR3 OFF	> 0.9999
	sir3-4A OFF	> 0.9999
	SIR3 ON	0.0086
	sir3-4A ON	0.0725
Sir3 delete H4K16ac/H3 vs.	empty	> 0.9999
	SIR3 OFF	0.4827
	sir3-4A OFF	0.2101
	SIR3 ON	> 0.9999
	sir3-4A ON	> 0.9999
SIR3 vs sir3-4A	OFF	> 0.9999
	ON	> 0.9999
OFF vs ON	SIR3	0.0345
	sir3-4A	0.1265

Tables S2.19 - Sir3-LexA – *HMR-A* in *sir3 Δ SIR4* strain

Table S2.19a – Levene test for Homogeneity of Variances

Test	Statistic	df1	df2	Sig.
Levene	9.817	2	6	0.01

Table S2.19b One-Way ANOVA summary

ANOVA table	SS	DF	MS	F (DFn	DFd)	P value
Treatment (between columns)	570.761	2	285.381	F (2	6) = 110.328	P = 0.000
Residual (within columns)	15.520	6	2.587			
Total	586.281	8				

Table S2.19c Welch ANOVA summary

ANOVA table	Asymptotically F distributed Statistic	DF1	DF2	Sig.
Welch	64.431	2	3.308	0.002

Table S2.19d Post-Hoc Games Howell comparisons

Post-Hoc Comparison	Significance
Empty-LexA vs. Sir3-LexA	0.011
Empty-LexA vs. Sir3-4A-LexA	0.010
Sir3-LexA vs. Sir3-4A-LexA	0.017

Tables S2.20 - Sir3-LexA –*URA3* in *sir3 Δ SIR4* strain

Table S2.20a – Levene Test for Homogeneity of Variances

Test	Statistic	df1	df2	Sig.
Levene	12.717	2	6	0.007

Table S2.20b One-Way ANOVA summary

ANOVA table	SS	DF	MS	F (DFn	DFd)	P value
Treatment (between columns)	587.043	2	293.522	F (2	6) = 319.188	P = 0.000
Residual (within columns)	5.518	6	0.920			
Total	592.561	8				

Table S2.20c Welch ANOVA summary

ANOVA table	Asymptotically F distributed Statistic	DF1	DF2	Sig.
Welch	160.994	2	3.489	0.000

Table S2.20d Post-Hoc Games Howell comparisons

Post-Hoc Comparison	Significance
Empty-LexA vs. Sir3-LexA	0.005
Empty-LexA vs. Sir3-4A-LexA	0.003
Sir3-LexA vs. Sir3-4A-LexA	0.006

Tables S2.21 - Sir3-LexA – *HMR-A* in *sir3 Δ sir4 Δ* strain

Table S2.21a – Levene Test for Homogeneity of Variances

Test	Statistic	df1	df2	Sig.
Levene	5.191	2	6	0.05

Table S2.21b One-Way ANOVA summary

ANOVA table	SS	DF	MS	F (DFn	DFd)	P value
Treatment (between columns)	10.891	2	5.446	F (2	6) = 13.808	0.006
Residual (within columns)	2.366	6	0.394			
Total	13.257	8				

Table S2.21d Post-Hoc Bonferroni comparisons

Post-Hoc Comparison	Significance
Empty-LexA vs. Sir3-LexA	0.013
Empty-LexA vs. Sir3-4A-LexA	0.010
Sir3-LexA vs. Sir3-4A-LexA	1.000

Tables S2.22 - Sir3-LexA –*URA3* in *sir3 Δ sir4 Δ* strain

Table S2.22a – Levene Test for Homogeneity of Variances

Test	Statistic	df1	df2	Sig.
Levene	4.162	2	6	0.07

Table S2.22b One-Way ANOVA summary

ANOVA table	SS	DF	MS	F (DFn	DFd)	P value
Treatment (between columns)	0.570	2	0.285	F (2	6) = 4.090	0.076
Residual (within columns)	0.418	6	0.070			
Total	0.988	8				

Table S2.22c Post-Hoc Bonferroni comparisons

Post-Hoc Comparison	Significance
Empty-LexA vs. Sir3-LexA	0.087
Empty-LexA vs. Sir3-4A-LexA	0.541
Sir3-LexA vs. Sir3-4A-LexA	0.684

Appendix 3 – Supplementary Figures

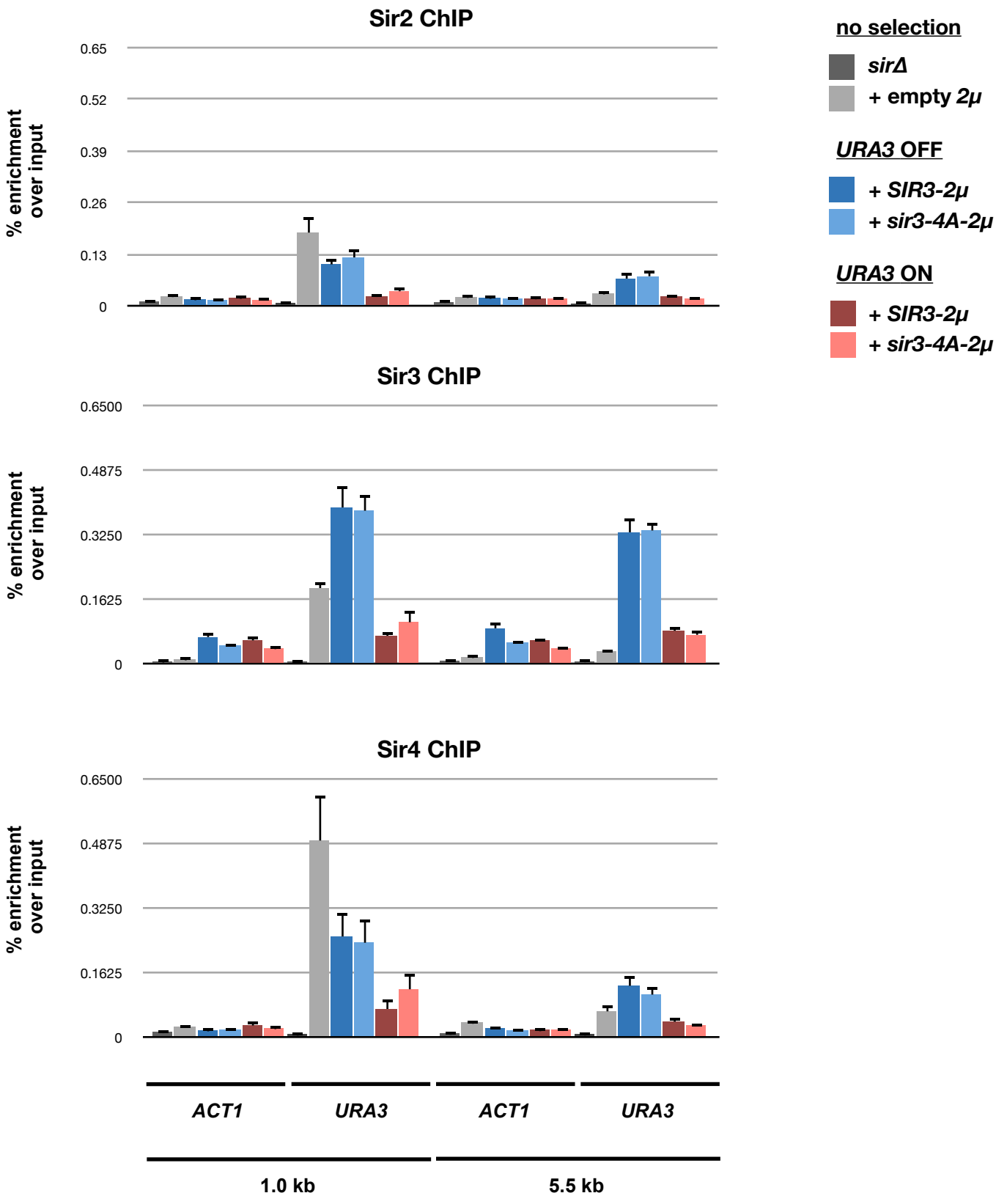
Sir2 ChIP
% enrichment over input
0.65
0.52
0.39
0.26
0.13
0
Sir3 ChIP
% enrichment over input
0.6500
0.4875
0.3250
0.1625
0
Sir4 ChIP
% enrichment over input
0.6500
0.4875
0.3250
0.1625
0
ACT1
URA3
ACT1
URA3
1.0 kb
5.5 kb
no selection
sirΔ
+ empty 2μ
URA3 OFF
+ SIR3-2μ
+ sir3-4A-2μ
URA3 ON
+ SIR3-2μ
+ sir3-4A-2μ

Figure S1. Sir protein enrichments at *ACT1* and at active and at silenced telomeric *URA3* without *ACT1* normalization. The data presented in Figure 14 are displayed here showing enrichments at both *URA3* and *ACT1*. Enrichments are expressed as the percentage of the amount of the DNA originally present in the input sample. Values represent the averages of three or more samples, with error bars representing standard errors of the means.

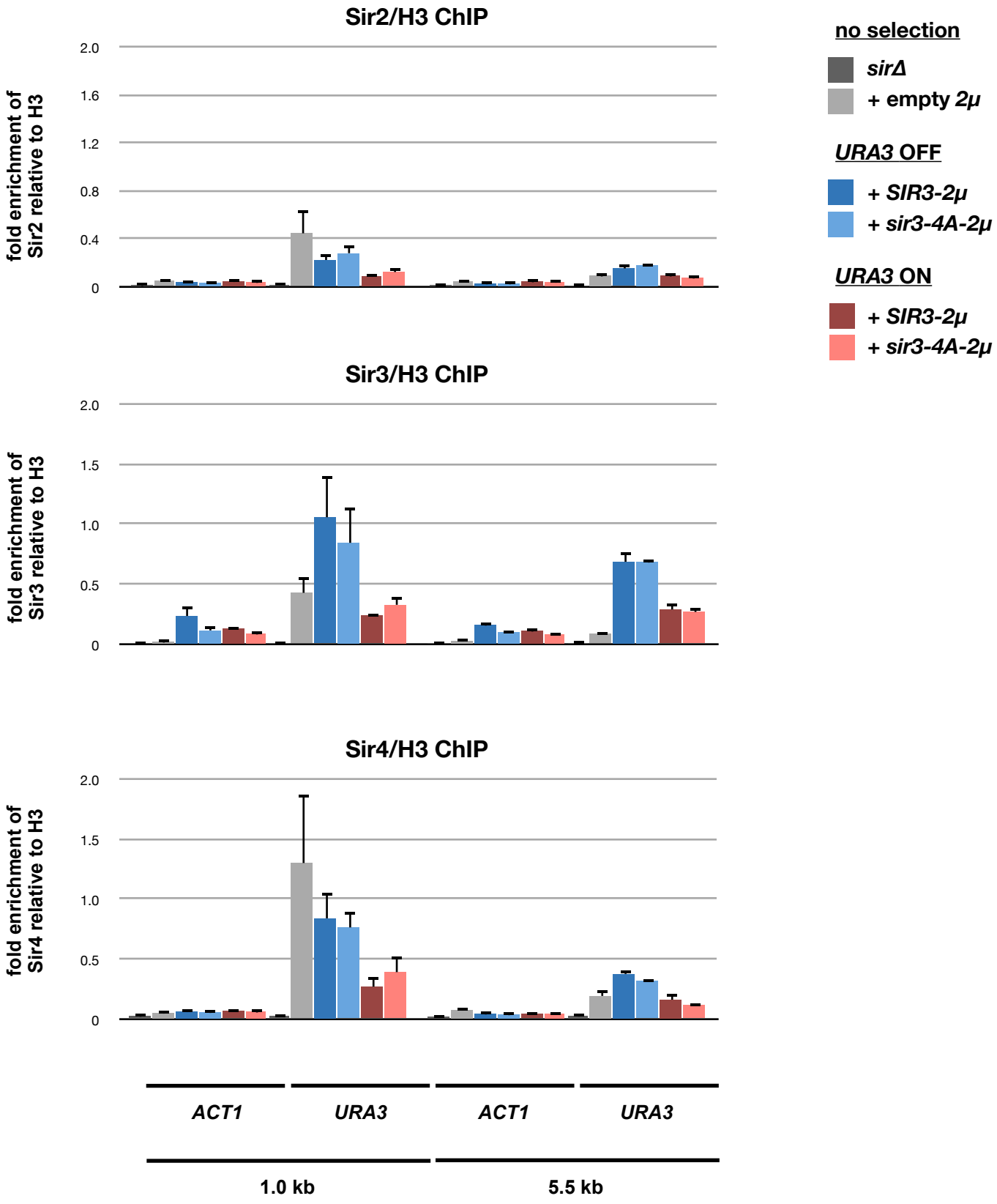
Sir2/H3 ChIP
fold enrichment of Sir2 relative to H3
2.0
1.6
1.2
0.8
0.4
0
Sir3/H3 ChIP
fold enrichment of Sir3 relative to H3
2.0
1.5
1.0
0.5
0
Sir4/H3 ChIP
fold enrichment of Sir4 relative to H3
2.0
1.5
1.0
0.5
0
ACT1
URA3
ACT1
URA3
1.0 kb
5.5 kb
no selection
sirΔ
+ empty 2μ
URA3 OFF
+ SIR3-2μ
+ sir3-4A-2μ
URA3 ON
+ SIR3-2μ
+ sir3-4A-2μ

Figure S2. H3-normalized Sir protein enrichments at *ACT1* and at active and silenced telomeric *URA3* without *ACT1* normalization. The data presented in Figure 16 are displayed here showing enrichments at both *URA3* and *ACT1*. For each sample, the Sir protein enrichment was normalized to that of H3. Values represent the averages of three or more samples, with error bars representing standard errors of the means.

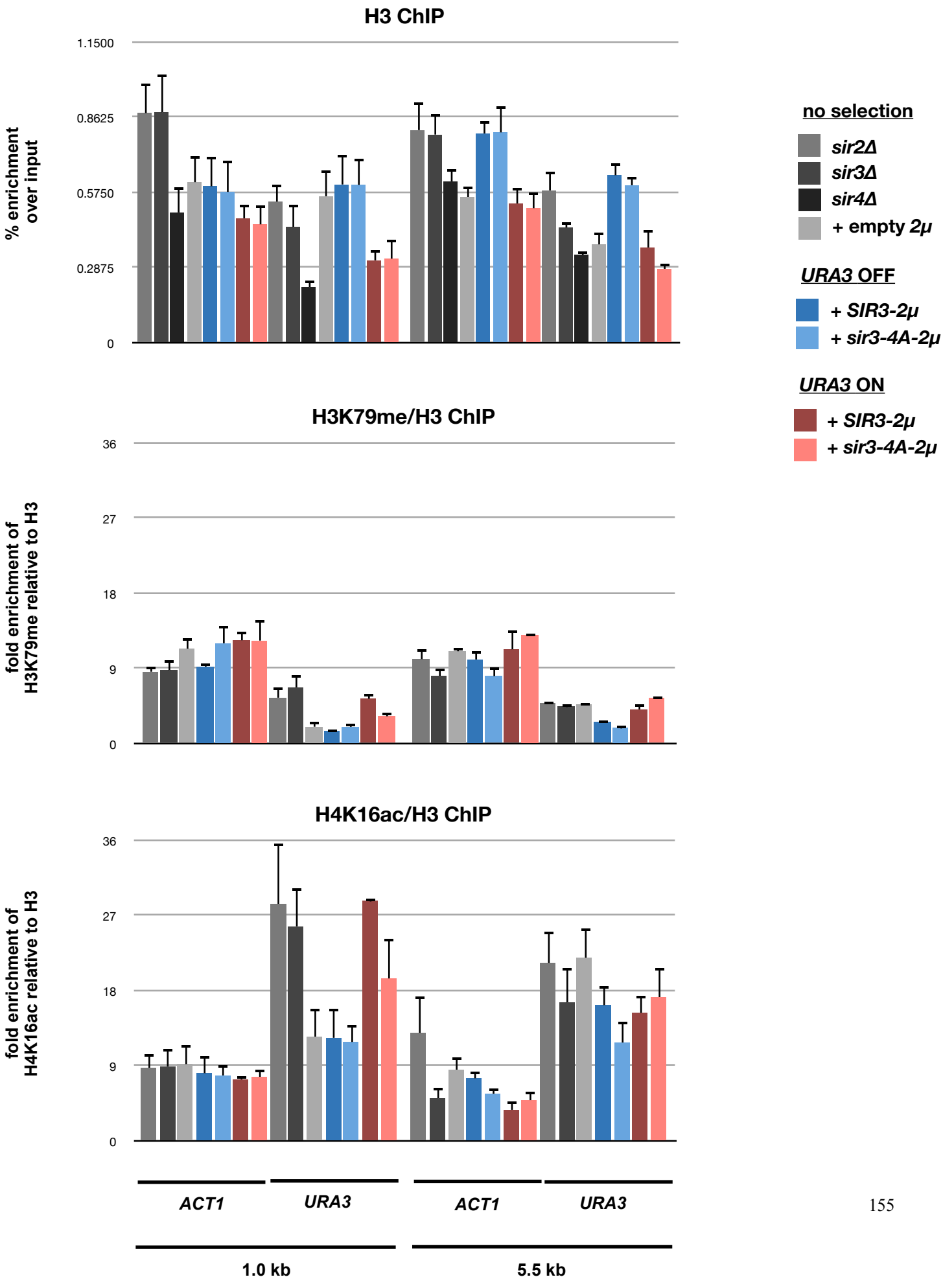
H3 ChIP
% enrichment over input
1.1500
0.8625
0.5750
0.2875
0
H3K79me/H3 ChIP
fold enrichment of H3K79me relative to H3
36
27
18
9
0
H4K16ac/H3 ChIP
fold enrichment of H4K16ac relative to H3
36
27
18
9
0
ACT1
URA3
ACT1
URA3
1.0 kb
5.5 kb
no selection
sir2Δ
sir3Δ
sir4Δ
+ empty 2μ
URA3 OFF
+ SIR3-2μ
+ sir3-4A-2μ
URA3 ON
+ SIR3-2μ
+ sir3-4A-2μ

Figure S3. H3 and H3-normalized H3K79me and H4K16ac enrichments at *ACT1* and at active and silenced telomeric *URA3* without *ACT1* normalization. The data presented in Figures 15 and 17 are displayed here showing enrichments at both *URA3* and *ACT1*. H3 enrichments are expressed as the percentage of the amount of the DNA originally present in the input sample. For each sample, H3K79me or H4K16ac enrichments were normalized to those of H3. Values represent the averages of three or more samples, with error bars representing standard errors of the means.

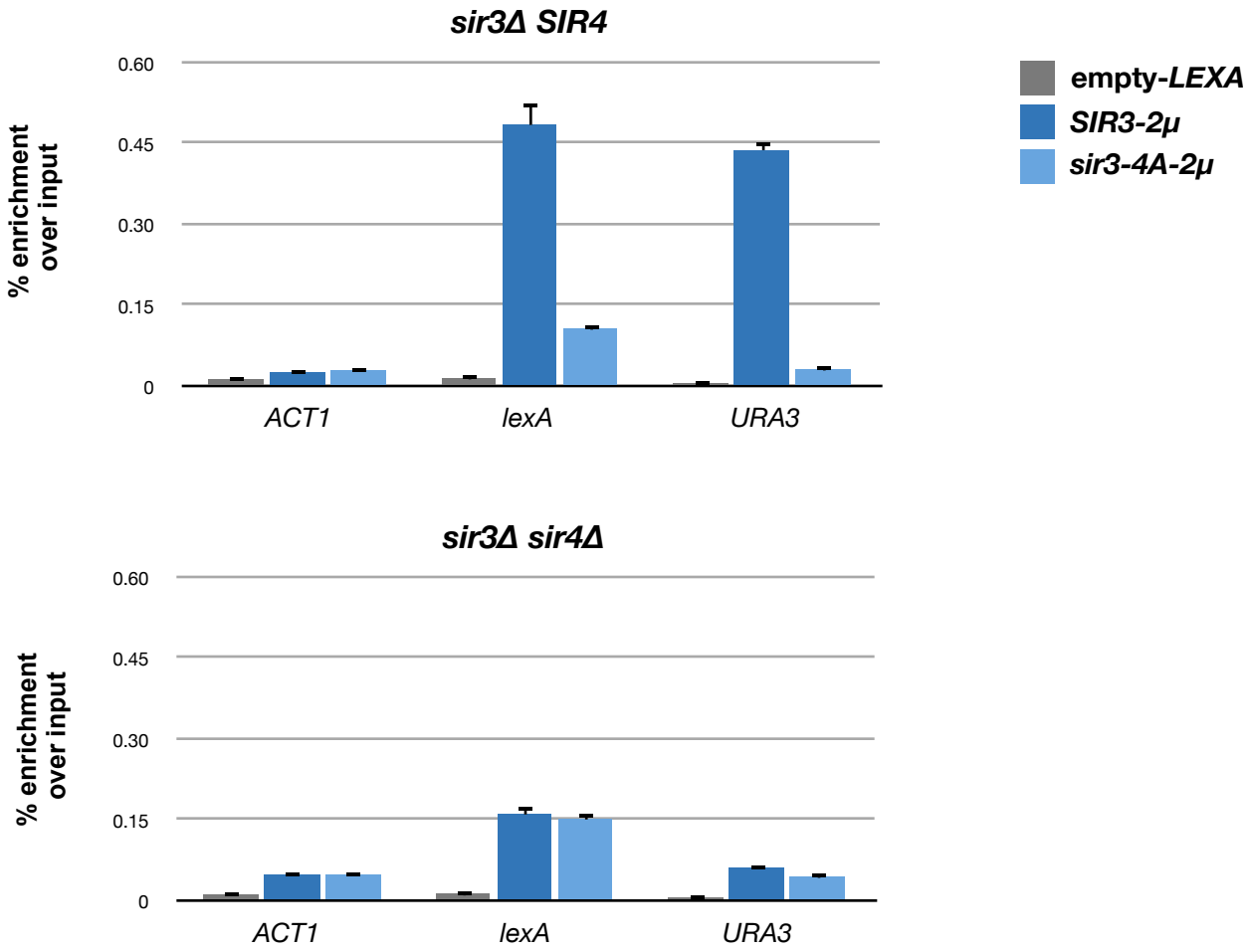
sir3Δ SIR4
% enrichment over input
0.60
0.45
0.30
0.15
0
ACT1
lexA
URA3
empty-LEXA
SIR3-2μ
sir3-4A-2μ
sir3Δ sir4Δ
% enrichment over input
0.60
0.45
0.30
0.15
0
ACT1
lexA
URA3

Figure S4. Sir3-LexA enrichments at *HMR-E::Aeb::4xLexops, HMRa1,a2::KlURA3,* and *ACT1* without *ACT1* normalization. The data presented in Figure 18D are displayed here showing Sir3 enrichment at the A element of *HMR-E* located just upstream of the LexA binding site (*LEXA*), at the *KlURA3* reporter gene (*URA3*), and at the euchromatic *ACT1* locus. Sir3 enrichments are expressed as the percentage of the amount of the DNA originally present in the input sample. Values represent the averages of three or more samples, with error bars representing standard errors of the means.

Curriculum Vitae – Rosalind Gerson

Education

2012 – 2015	**M.Sc. Biochemistry** Department of Biochemistry, Microbiology, and Immunology Faculty of Medicine, University of Ottawa, Ottawa, ON
2008-2012	**B.Sc. Honours Specialization Biochemistry** Faculty of Science, University of Ottawa, Ottawa, ON

Research Experience

2012 – 2015	**Master's Research** Department of Biochemistry, Microbiology, and Immunology Faculty of Medicine, University of Ottawa, Ottawa, ON Supervisor: Dr. Adam Rudner Role of the Sir3-Sir4 interaction in silent chromatin nucleation and spreading in budding yeast
2011 – 2012	**Undergraduate Fourth-Year Honours Research** Department of Biochemistry, Microbiology, and Immunology Faculty of Medicine, University of Ottawa, Ottawa, ON Supervisor: Dr. Adam Rudner Silent chromatin regulation in budding yeast
Summers 2009,2010,2011	**Undergraduate Summer NSERC-USRA Research** Department of Biochemistry, Microbiology, and Immunology Faculty of Medicine, University of Ottawa, Ottawa, ON Supervisor: Dr. Adam Rudner Mapping Sir protein interactions, role of Asf2 in budding yeast silent chromatin spreading
2010	**Undergraduate uOttawa UROP Research** Department of Biochemistry, Microbiology, and Immunology Faculty of Medicine, University of Ottawa, Ottawa, ON Supervisor: Dr. Adam Rudner Mapping Sir3-Asf2 interactions in budding yeast

Awards

2013 – 2014	**Queen Elizabeth II Graduate Scholarship in Science and Technology (QEII-GSST)**
2012 – 2013	**Canadian Institutes of Health Research (CIHR) Master's Award**

Summers 2009,2010,2011	**Natural Sciences and Engineering Research Council of Canada Undergraduate Student Research Award (NSERC-USRA)**
2010	**University of Ottawa Undergraduate Research Opportunity Program (UROP) Award**

Manuscripts in Preparation

Harding, K.*, **Gerson, R.J.***, Dore, C., Rudner, A.D. The interaction between heterochromatin proteins Sir3 and Sir4 is dispensable for silent chromatin spreading in budding yeast, *in preparation.*
* authors contributed equally

Talks

Gerson, R.J., Harding, K., Dore, C., Rudner, A.D. Bypassing the Sir3-Sir4 interaction in silent chromatin spreading. Seminar presented at the University of Ottawa Department of Biochemistry, Microbiology, and Immunology (BMI) Graduate Student Seminar Day, Ottawa, ON, Canada, March 7 2014.

Gerson, R.J.*, Harding, K.*, Dore, C., Rudner, A.D. Bypassing Sir4 in silent chromatin spreading. Talk presented at the 2013 Cold Spring Harbor Cell Biology of Yeasts Meeting, Cold Spring Harbor, New York, USA, November 5 – 9 2013.
* authors contributed equally

Gerson, R.J., Harding, K., Dore, C., Rudner, A.D. Sir3-directed silent chromatin spreads independently of Sir4. Talk presented at the University of Ottawa Cell Dynamics Workshop, Keene, ON, Canada, May 5, 2013.

Gerson, R.J., and Rudner, A.D. Investigating the properties of the heterochromatic protein Asf2 in budding yeast. Seminar presented at the University of Ottawa Faculty of Medicine Summer Student Program (FMSSP) weekly seminar series, Ottawa, ON, Canada, July 12, 2011.

Published Abstracts

Gerson, R.J.*, Harding, K.*, Dore, C., Rudner, A.D. Bypassing Sir4 in silent chromatin spreading. Abstract of talk published at the 2013 Cold Spring Harbor Cell Biology of Yeasts Meeting, Cold Spring Harbor, New York, USA, November 5 – 9 2013.
* authors contributed equally

Harding, K., **Gerson, R.**, Dore, C., Rudner, A. The Role of the Sir3-Sir4 Interactions in the Spreading of Heterochromatin in *Saccharomyces cerevisiae*. Poster abstract published at the 2012 American Society for Cell Biology (ASCB) Annual meeting, San Francisco, California, USA, December 15-19 2012.

Pilon, S.D., **Gerson, R.**, Harding, K., Kettenbach, A.N., Gerber, S.A., Rudner, A.D. Conservation of the SIR complex in fission yeast. Poster abstract published at the 2011 American Society for Cell Biology (ASCB) Annual meeting, Denver, Colorado, USA, December 3-7, 2011.

Posters

Gerson, R.J., Harding, K., Dore, C., Rudner, A.D. Sir3 directs spreading of silent chromatin in budding yeast. Poster presented at the Ottawa Institute of Systems Biology (OISB) 2013 Meeting, Mont Tremblant, QC, Canada, June 11 2013, and at the University of Ottawa Department of Biochemistry, Microbiology, and Immunology (BMI) Poster Day, Ottawa, ON, Canada, May 16 2013.

Gerson, R.J., Dore, C., Rudner, A.D. Sir3-Sir3 interactions mediate heterochromatin spreading in *Saccharomyces cerevisiae*. Poster presented at the Ottawa Carleton Institute of Biology (OCIB) symposium, Ottawa, ON, Canada, April 26, 2012, and at the University of Ottawa Biochemistry Honours Students Poster Day April 10, 2012.

Gerson, R.J., and Rudner, A.D. Mapping interactions between the heterochromatic proteins Asf2 and Sir3 in budding yeast. Poster presented at the Ottawa Institute of Systems Biology (OISB) 2011 Meeting, Montebello, QC, Canada, June 8 2011, and at the University of Ottawa Undergraduate Research Opportunity Program (UROP) Symposium, Ottawa, ON, Canada, March 29, 2011